Titre: Title:	Assessment of the biocompatibility of nanostructured polymeric fibers
Auteur: Author:	Sashka Dimitrievska
Date:	2007
Type:	Mémoire ou thèse / Dissertation or Thesis
Référence: Citation:	Dimitrievska, S. (2007). Assessment of the biocompatibility of nanostructured polymeric fibers [Mémoire de maîtrise, École Polytechnique de Montréal]. PolyPublie. https://publications.polymtl.ca/7973/

UNIVERSITÉ DE MONTRÉAL

ASSESSMENT OF THE BIOCOMPATIBILITY OF NANOSTRUCTURED POLYMERIC FIBERS

SASHKA DIMITRIEVSKA
INSTITUT DE GÉNIE BIOMÉDICAL
ÉCOLE POLYTECHNIQUE DE MONTRÉAL

MÉMOIRE PRÉSENTÉ EN VUE DE L'OBTENTION
DU DIPLÔME DE MAÎTRISE ÈS SCIENCES APPLIQUÉES
(GÉNIE BIOMÉDICAL)
AVRIL 2007

Your file Votre référence
ISBN: 978-0-494-29228-0
Our file Notre référence
ISBN: 978-0-494-29228-0

UNIVERSITÉ DE MONTRÉAL

ÉCOLE POLYTECHNIQUE DE MONTRÉAL

Ce mémoire intitulé :

ASSESSMENT OF THE BIOCOMPATIBILITY OF NANOSTRUCTURED POLYMERIC FIBERS

Présenté par : DIMITRIEVSKA Sashka

en vue de l'obtention du diplôme de : Maîtrise ès sciences appliquées
a été dûment accepté par le jury d'examen constitué de :

M. DE CRESECENZO Gregory , Ph.D., président
M. YAHIA L'Hocine, Ph.D., membre et directeur de recherche
M. BUREAU Martin N., Ing., membre et codirecteur de recherche
M. AJJI Abdellah, M.Sc.A., membre et codirecteur de recherche
M. BEAULÉ Paul E., M.D., membre

Mama, kolku i da se lutish pak e za tebe!

Acknowledgments

Naturally, I would like to start by thanking my research director *Dr. L'Hocine Yahia* for granting me the financial aid, freedom and flexibility.

I would especially like to thank my co-director *Dr. Martin. N. Bureau* His contagious motivation, quick orientation, graceful guidance, endless understanding and stubborn support were essential during the course of this work. I have never met anybody with more broad-ranging knowledge, interests and passions. This colorfulness adds to his charismatic character an enthusiastic approach to difficulties making you believe it is possible to do everything you want to do, you just have to try! He has humorously become the core for us students at Boucherville by artfully keeping us all inspired.

My gratefulness also goes to *Dr. Abdellah Ajji,* who as a co-director and inventor of the fibers this research is based on, always left his door open to all questions I may have had.

Dr. Alain Petit, with one *l*, who unofficially became a co-director of this research, I would like to thank for generously offering his time and scientific cues towards the insights of biocompatibility. Without his insightful cellular mechanisms comprehension this research would have not been up-to-par.

Dr. Gregory DeCrescenzo, thank you not only for taking the time to act as a president of this thesis committee but also for your raw but always well intended peers views of the scientific and non-scientific world.

I would like to thank *Dr. Paul Beaulé* for accepting the role of external member, which in this case given the physical distance is even more time consuming than customary.

I would like to thank *Dr. Merhi* from the Montreal Hearth Institute for warmly opening the doors of his laboratory; and his team: *J.F., Daniel* and *Haisam* for accepting me in their thigh knitted squad.

Antoine, for all your help with the tedious thesis formatting, graph plotting and endless tolerance, thank you.

Caroline, who left a mark on all of us at LIAB with her precise chemical views, strong ethics and easy friendship; for her patient listening, understanding and guidance through the loop-holes of the last few years, many thanks.

Laura for your patience, admirable cellular culture techniques initiation and late night exchanges about common road-blocks, thank you.

Dr Yang, for offering your expertise in the complex chemical surface analysis interpretation when everyone else gave up, thank you.

I would like to acknowledge the contributions from: IMI-CNRC *Karine Theberge* for FEG-SEM and *Dominique Desganes* for FTIR analysis, *Dr. Bashir, Karim and Edu* from the Physics department for their accommodating Plasma sterilizations.

My most tender gratitude goes to *my parents* and *Ryan* for courageously embracing my collapses and triumphs with love, support and encouragement.

Résumé

Afin de satisfaire une portion croissante de la population qui utilise des prothèses pour le remplacement d'os porteurs pour des périodes pouvant dépasser trente ans, un changement de concept est proposé, en mettant l'accent sur la régénération des tissus plutôt que le remplacement. En se basant sur la bioactivité de l'hydroxyapatite (HA) et les excellentes propriétés mécaniques et biologiques du polyéthylène téréphtalate (PET), un composite de PET, chargé avec des nanoparticules de HA, a été fabriqué. Le nanocomposite PET/HA a été fabriqué pour imiter la structure de l'os naturel qui est un composite de nano-cristaux de HA et d'un polymère naturel. La deuxième étape du travail consistait à évaluer la composition chimique de surface des nanocomposites de PET/HA par la technique de spectrométrie photoélectronique X (XPS), afin que l'effet de l'ajout de HA puisse être analysé. Il s'agissait aussi de comparer, toujours par XPS et par des mesures de cytotoxicité in vitro, les effets sur la composition chimique des composites suite à la stérilisation par deux méthodes distinctes, soit l'utilisation de l'oxyde d'éthylène (EtO) et du plasma à basse température (LTP).

Plus précisément, pour l'évaluation de la biocompatibilité in vitro des diverses fibres de nanocomposites de PET/HA, nous avons évalué les effets des nanocomposites de PET/HA sur la prolifération, la morphologie et la viabilité des cellules fibroblastiques L929. De plus la lignée cellulaire de macrophages Raw 264.7 est utilisée pour déterminer les réactions inflammatoires en mesurant la sécrétion de cytokines, telles que le facteur α nécrosant des tumeurs (TNF-α). Toutes ces études ont été faites en parallèle

avec de extraits des nanocomposites ainsi que des fibres de nanocomposites, dans une matrice 3D. Ceci a été réalisé par des tests de MTT sur les fibres de composites, dans le but d'évaluer les effets à court termes des produits de la dégradation. La morphologie cellulaire des fibroblastes L929 a été analysée après le contact direct de la matrice 3D de fibres pour des périodes de temps différentes et la viabilité cellulaire a aussi été évaluée par le test de bleu d'Alamar. La mesure de la réponse inflammatoire est alors obtenue en analysant la présence de cytokine TNT-α provenant des macrophages Raw 264.7 en présence des extraits de fibre. La composition chimique des fibres de nanocomposites de PET/HA, avec une proportion croissante de nanoparticules de HA, a été analysée par XPS afin d'établir quels sont les effets de l'ajout de HA sur la chimie de surface des nanofibres de PET/HA. Les modifications de la surface des fibres de nanocomposites de PET/HA suite à la stérilisation par le LTP et l'EtO ont été analysées par XPS. La biocompatibilité a été analysée de nouveau suite à la stérilisation pour en déterminer les effets.

Cette étude a démontré, suite aux tests MTT, que des extraits provenant de fibres de nanocomposites de PET/HA avec différentes concentrations de HA n'avaient pas d'effet sur la viabilité des fibroblastes L929. Il est toutefois possible que les conditions étaient insuffisantes pour générer le même niveau de dégradation ou de particules dégradables que dans l'environnement in vivo, avec les contraintes mécaniques. Les tests de cytotoxicité par contact indirect ont été accompagnés de test par contact direct dans lesquels les fibroblastes ont été cultivés sur des matrices 3D faites de fibres de nanocomposites de PET/HA. Comme il a été observé par FEG-SEM, les fibroblastes

cultivés sur des matrices 3D de PET10 ont presque complètement couvert les pores interconnectant entre les fibres en formant des couches semblables à la matrice extracellulaire, en plus d'avoir une apparence multicouche. Bien que des études plus approfondies soient nécessaires pour la caractérisation de la couche semblable à la matrice extracellulaire, les résultats suggèrent que le composite PET10 permettra la croissance de structures tissulaires organisées capables d'entraîner la prolifération 3D. Étant donné que l'utilisation ultime de ces fibres serait la fabrication d'un recouvrement pour une prothèse de hanche, la réponse inflammatoire due aux produits de dégradation a été quantifiée en observant la libération de TNT-α par les macrophages RAW 264.7. L'expérience présente a démontré que les macrophages cultivés avec des extraits de fibres de composites de PET/HA libéraient plus de TNF-α que les cellules du contrôle négatif. Finalement, le niveau de libération de TNF-α suivant la culture de macrophages en contact direct avec la matrice 3D de PET10 n'a pas été significativement plus grande que celui du contrôle et a été notablement inférieur que les niveaux libérés suite à l'incubation avec la matrice 3D de PET0. Ceci indique que la réponse inflammatoire diminue avec l'ajout de HA dans les fibres de nanocomposites PET/HA.

La relation de dépendance observée entre la dose puis la réponse favorable des cellules et l'accroissement du dosage de HA aux fibres a motivé l'analyse de surface par XPS des fibres de nanocomposites. L'analyse par XPS des fibres de nanocomposites de PET/HA non traitées a démontré que le HA n'est pas détecté en surface. Toutefois, la concentration en oxygène de la couche de surface augmente avec la charge en HA dans les fibres. L'analyse XPS suite à la stérilisation par LTP ou EtO a révélé des

modifications chimiques de la surface des fibres. Il reste que suite à ces traitements, une réévaluation de la cytotoxicité a démontré des réponses similaires par les deux traitements de stérilisation.

En conclusion, la capacité des matrices de fibre de supporter l'attachement, l'étalement et la croissance in vitro des cellules L929, combinée avec les extraits compatibles en dégradation et le faible potentiel d'inflammation des fibres et des extraits, suggère la possible utilisation de ces composites comme biomatériaux pour les os supportant les charges. Dans le but d'expliquer la réponse biologique favorable pour des concentrations plus élevées de HA, il a été observé que le chargement en HA des fibres augmente le contenu global en oxygène des composites alors que le HA demeure non détecté par le XPS. Finalement, les deux traitements de stérilisation semblent acceptables.

Abstract

It is proposed that to satisfy a growing percentage of the population that requires greater than thirty-year survivability of load-bearing bone replacement devices, a concept shift, from emphasis on replacement of tissues to regeneration of tissues, is required. Based on the bioactivity of hydroxyapatite (HA) and the excellent mechanical and biocompatible performance of polyethylene terephthalate (PET), a composite of PET filled with nanograde HA was designed and fabricated to mimic the structure of biological bone which exhibits a composite of nanograde apatite crystals and natural polymer. The PET/HA nanocomposite was fabricated by compounding, and spun into fiber form so that the mechanical properties of a given structure can be custom tailored by changing the final 3D orientation of the fibers. This study primarily focused on the *in vitro* biocompatibility evaluation of the novel PET/HA nanocomposite as potential biomaterials. In a second place, this work evaluated the HA nanoparticles effects on the polymeric fibers surface chemistry by XPS analysis, and compared the effects induced by ethylene oxide (EtO) and low temperature plasma (LTP) sterilization on the composites chemical composition by XPS and *in vitro* cytotoxicity.

More precisely, to asses the *in vitro* biocompatibility of the various PET/HA nanocomposite fibers we investigated the *in vitro* proliferation, morphology, and viability of L929 fibroblast cell line, as well as the inflammation potential of RAW 264.7 macrophages cultured on the fibers scaffolds and extracts. This was done through the MTT assay with the extracts of the composite fibers in order to evaluate the short-

term effects of the degradation products. The cell morphology of L929 fibroblasts was analyzed after direct contact with the 3D fibers scaffolds for different time periods and the cell viability was also analyzed by the Alamar Blue assay. The release of the inflammatory cytokine, TNF-α from RAW 264.7 macrophages in the presence of fibers extracts and fibers was used as a measure of the inflammatory response. The PET/HA nanocomposite fibers (made by twin screw compounding and melt blowing) chemical composition with increasing amounts of HA nanoparticles was analyzed by XPS, so that the effects of the HA addition can be elucidated onto the PET/HA nanofibers surface chemistry. The surface modifications on the PET/HA nanocomposite fibers after LTP and EtO sterilization, were assessed by XPS. The biocompatibility was reassessed as previously described with LTP- and EtO- treated fibers as a measure of the sterilization method on the PET/HA fibers biocompatibility.

The present study showed that extracts from the PET/HA nanocomposite fibers with different HA concentrations had no effect on the viability of L929 fibroblasts as seen by the MTT assay. However, it is possible that the conditions were insufficient to generate the same levels of degradation or leachables products than in an *in vivo* environment with mechanical constraint. The indirect cytotoxicity contact tests were complemented with direct contact tests, where L929 fibroblasts were cultured on 3D scaffolds constructed from the PET/HA nanocomposite fibers. The direct contact tests showed that the metabolic activity, associated with cell number, increased proportionally with the amount of HA present in the PET/HA nanocomposite fibers. Further, as seen by FEG-SEM fibroblasts cultured on the PET10 3D scaffolds (scaffolds constructed from

the PET/HA nanocomposite fibers with the highest percentage of HA: 10% HA) almost fully covered the interconnecting pores between the fibers by forming extracellular matrix-like layers in addition to their multilayer appearance. Although more conclusive studies are needed to characterize the extracellular-like matrix formed, the results suggest that the novel PET10 composites would lead to well-organized tissue structures able to promote three-dimensional proliferation. As the ultimate application of the fibers would be a hip prosthesis, the inflammatory responses due to degradation products was quantified by looking at the release of TNF-α by RAW 264.7 macrophages. The present experiments demonstrated that macrophages cultured with PET/HA composite fibers extracts released more TNF-α than the negative control cells. Lastly, the level of release of TNF-α following culture of macrophages in direct contact with PET10 3D scaffolds was not significantly greater than the control, and was notably lower than the levels released following incubation with PET0 3D scaffolds; indicating that the addition of HA into the PET/HA nanocomposite fibers lowers the inflammatory response.

The dose-dependant relationship of the favorable cellular response and increasing HA dosage inspired the XPS surface analysis of the PET/HA nanocomposite fibers. The XPS analysis of the untreated PET/HA nanocomposite fibers revealed that HA is undetected at the surface. However, the surface layer of the fibers increased in O concentration with increasing loading of HA (for a maximum of 12% O increase at 10% HA), mainly due to the O-C=O/C-OH bond increase. XPS analysis after LTP and EtO sterilization revealed the following chemical modifications onto the PET/HA nanocomposite fibers: EtO treatment induced alkylation, as seen in the increase on the

C-O peak despite the constant overall O %; LTP treatment induced some etching and an increase in the C-O/C-OH bonds and overall O% increase, which lead to a better biologic response as seen with the TNF-α release.

The *in vitro* cytotoxicity was re-evaluated after the LTP and EtO treatments. Despite the resulting surface modifications, the cell viability of both LTP and EtO-treated fibers remained similar. Following macrophages incubation with the fibers, a trend of higher TNF-α release by the EtO-treated polymer, as compared to the LTP sterilized ones, was observed. This trend suggests a higher inflammatory potential for the EtO sterilized fibers.

In conclusion, the ability of the fiber matrices to support L929 attachment, spreading and growth *in vitro*, combined with the compatible degradation extracts and low inflammation potential of the fibers and extracts, suggests potential use of these composites as load- bearing bone biomaterials. In an attempt to elucidate the favorable biological response at higher HA concentrations it was seen that HA loading of fibers increases the overall O content of composites while HA remains undetected by XPS. Both sterilization treatments seem acceptable, but LTP demonstrated an additional advantage by the beneficial hydroxyl functional groups additions onto the PET/HA nanocomposite fibers surface leading to better biologic response as seen by the inflammation potential decrease.

Condensé

Afin de satisfaire une portion croissante de la population qui utilise des prothèses pour le remplacement d'os porteurs pour des périodes pouvant dépasser trente ans, un changement de concept est proposé, en mettant l'accent sur la régénération des tissus plutôt que leur remplacement. Le concept de polymères composites renforcés par des particules bioactives semblables aux os a d'abord été introduit au début des années 1980 par Bonfield *et al.* avec le développement de l' HAPEX™, un composite de polyéthylène haute densité (PEHD) renforcé d'hydroxyapatite (HA), servant à la fabrication en gros de produits 3D isotropes. Ce travail de pionnier a ensuite inspiré la création de plusieurs composites bioactifs, faits d'un polymère et d'HA, qui visait à correspondre aux propriétés et à la structure de l'os pour des applications orthopédiques avancées. Toutefois, ces composites particulaires n'atteignent pas les propriétés mécaniques, particulièrement la rigidité, de l'os cortical, ce qui limite leur application pour le remplacement d'os porteurs. En se basant sur la bioactivité de l'hydroxyapatite (HA) et les excellentes propriétés mécaniques et biologiques du polyéthylène téréphthalate (PET), un composite de PET, chargé avec des nanoparticules de HA, a été fabriqué. Les microfibres du nanocomposite de PET/HA sont un biocomposite prometteur qui peut être moulé en des structures 3D anisotropes dont les propriétés peuvent être ajustées en contrôlant l'orientation 3D des microfibres. Une application intéressante des microfibres non résorbables est un revêtement de composite pour les

prothèses de remplacement total de la hanche ou d'autres biomatériaux porteur dans leur but d'accroître leur ostéointégration.

Le nanocomposite PET/HA a été fabriqué pour imiter la structure de l'os naturel qui est un composite de nano-cristaux de HA et d'un polymère naturel. Un des premiers stades dans le développement des microfibres de nanocomposite de PET/HA est l'évaluation de leur cytotoxicité. Il est souhaitable que ces microfibres de nanocomposite possèdent une réponse cytotoxique minimale et facilitent l'attachement cellulaire dans le but d'être utilisées comme matrice pour l'ingénierie tissulaire. L'évaluation de la cytotoxicité *in vitro* est une méthode pratique et efficace pour déterminer la réponse biologique à un biomatériau. Cette évaluation servira aussi comme procédé de sélection de départ pour des études *in vivo* futures. La deuxième étape du travail consistait à évaluer la composition chimique de surface des nanocomposites de PET/HA par la technique de spectrométrie photoélectronique X (XPS), afin que l'effet de l'ajout de HA puisse être analysé. Il s'agissait aussi de comparer, toujours par XPS et par des mesures de cytotoxicité *in vitro*, les effets sur la composition chimique des composites suite à la stérilisation par deux méthodes distinctes, soit l'utilisation de l'oxyde d'éthylène (EtO) et du plasma à basse température (LTP).

L'étape initiale d'une étude de biocompatibilité *in vitro* est l'évaluation de la cytotoxicité *in vitro* d'un biomatériau basée sur l'examen morphologique de l'endommagement et de la croissance cellulaire en contact direct ou indirect avec le matériau. La toxicité des biomatériaux proposés implique la perturbation de l'homéostasie cellulaire entraînant une multitude de changements biochimiques. Une

importance accrue est attribuée à la mort cellulaire, à la prolifération cellulaire et à l'adhésion cellulaire, qui sont tous des paramètres associés directement à toxicité *in vitro*. De plus, la réponse inflammatoire est un élément significatif de la réponse de l'hôte aux biomatériaux car elle contribue aussi au phénomène de descellement aseptique des prothèses orthopédiques, ce qui entraîne son utilisation comme critère de biocompatibilité. Les macrophages Raw 264.7 ont été cultivés *in vitro* pour déterminer l'effet direct et indirect des composites de PET/HA sur la production et le relâchement du facteur α de nécrose des tumeurs (TNF-α). Le TNF-α a été sélectionné pour son contrôle bien connu des inflammations locales, de l'activation cellulaire et de la chimiotaxie ainsi que pour son rôle établi comme stimulateur efficace de la résorption de l'os par son effet inhibitoire sur les ostéoblastes, et son habilité à activer les ostéoclastes. De plus, l'ajout d'un renforcement d'HA entraîne des résultats contradictoires car certains auteurs rapportent l'amélioration des performances des implants renforcés d'HA, alors que d'autres rapportent que des revêtements de céramiques peuvent produire des débris d'usure particulaires, l'accroissement de la production de cytokines en plus d'induire l'ostéolyse.

Des expériences *in vitro* peuvent être particulièrement bénéfiques pour des composites de polymère/céramique car elles peuvent tester individuellement les trois phases qui ont lieu dans le cycle de vie d'un matériau durant son implantation, soit des macromères n'ayant pas réagi (s'il y en a), des réseaux inter-reliés et des possibles produits de désintégration. Dans la présente étude, nous avons évalué la cytotoxicité de ces trois phases pour les nouveaux nanocomposites de fibres de PET/HA. Nous avons

supposé que les nanocomposites de PET/HA comportant 10% de HA allaient démontrer une biocompatibilité *in vitro* acceptable et des propriétés de surface supérieures pour la prolifération cellulaire.

Plus précisément, pour l'évaluation de la biocompatibilité *in vitro* des diverses fibres de nanocomposites de PET/HA, nous avons évalué les effets des nanocomposites de PET/HA sur la prolifération, la morphologie et la viabilité des cellules fibroblastiques L929. De plus la lignée cellulaire de macrophages Raw 264.7 est utilisée pour déterminer les réactions inflammatoires en mesurant la sécrétion de cytokines, telles que le facteur α nécrosant des tumeurs (TNF-α). Toutes ces études ont été faites en parallèle avec de extraits des nanocomposites ainsi que des fibres de nanocomposites, dans une matrice 3D. Ceci a été réalisé par des essais de MTT (Methyl Tetrazolium) sur les fibres de composites, dans le but d'évaluer les effets à court terme des produits de la dégradation. La morphologie cellulaire des fibroblastes L929 a été analysée après le contact direct de la matrice 3D de fibres pour des périodes de temps différentes et la viabilité cellulaire a aussi été évaluée par l'essai de bleu d'Alamar. La mesure de la réponse inflammatoire est alors obtenue en analysant la présence de cytokine TNT-α provenant des macrophages Raw 264.7 en présence des extraits de fibres. La composition chimique des fibres de nanocomposites de PET/HA, avec une proportion croissante de nanoparticules de HA, a été analysée par XPS afin d'établir quels sont les effets de l'ajout de HA sur la chimie de surface des nanofibres de PET/HA. Les modifications de la surface des fibres de nanocomposites de PET/HA suite à la

stérilisation par le LTP et l'EtO ont été analysées par XPS. La biocompatibilité a été analysée de nouveau suite à la stérilisation pour en déterminer les effets.

Cette étude a démontré, suite aux essais MTT, que des extraits provenant de fibres de nanocomposites de PET/HA avec différentes concentrations de HA n'avaient pas d'effet sur la viabilité des fibroblastes L929. Il est toutefois possible que les conditions étaient insuffisantes pour générer le même niveau de dégradation ou de particules dégradables que l'on retrouve dans l'environnement *in vivo*, avec les contraintes mécaniques. Les essais de cytotoxicité par contact indirect ont été accompagnés d'essais par contact direct dans lesquels les fibroblastes ont été cultivés sur des matrices 3D faites de fibres de nanocomposites de PET/HA. Comme il a été observé par FEG-SEM, les fibroblastes cultivés sur des matrices 3D de PET10 ont presque complètement couvert les pores interconnectant entre les fibres en formant des couches semblables à la matrice extracellulaire, en plus d'avoir une apparence multicouche. Bien que des études plus approfondies soient nécessaires pour la caractérisation de la couche semblable à la matrice extracellulaire, les résultats suggèrent que le composite PET10 permettra la croissance de structures tissulaires organisées capables d'entraîner la prolifération 3D. Étant donné que l'utilisation ultime de ces fibres serait la fabrication d'un revêtement pour une prothèse de hanche, la réponse inflammatoire due aux produits de dégradation a été quantifiée en observant la libération de TNT-α par les macrophages Raw 264.7. L'expérience présente a démontré que les macrophages cultivés avec des extraits de fibres de composites de PET/HA libéraient plus de TNF-α que les cellules du contrôle négatif. Finalement, le niveau de libération de TNF-α suivant la culture de

macrophages en contact direct avec la matrice 3D de PET10 n'a pas été significativement plus grande que celui du contrôle et a été notablement inférieur que les niveaux libérés suite à l'incubation avec la matrice 3D de PET0. Ceci indique que la réponse inflammatoire diminue avec l'ajout de HA dans les fibres de nanocomposites PET/HA.

La relation de dépendance observée entre la dose puis la réponse favorable des cellules et l'accroissement du dosage de HA aux fibres a motivé l'analyse de surface par XPS des fibres de nanocomposites. L'analyse par XPS des fibres de nanocomposites de PET/HA non traitées a démontré que le HA n'est pas détecté en surface. Toutefois, la concentration en oxygène de la couche de surface augmente avec la charge en HA dans les fibres.

En termes des modifications de surface induites sur les fibres de nanocomposite de PET/HA par l'ajout d'HA, la réduction du contenu global de carbone de surface en faveur de l'accroissement du contenu d'oxygène par l'intermédiaire de la formation de nouveaux groupes d'hydroxyle est la plus importante. La formation de groupe d'hydroxyle est plausiblement causée pendant le traitement des fibres par l'intermédiaire de la réaction de l'hydroxyapatite libre avec les groupements OH avec le polymère PET; par exemple, la matrice du PET a réagi avec les nanoparticles d'HA ajoutées par les liens faibles d'hydrogène, encapsulant des nanoparticles d'HA et exposant les groupements-CH/COH/-COOH à l'intérieur d'une couche de 10 nm d'épaisseur. Cette encapsulation sous des températures plus élevées, telles que 280°C utilisée dans le traitement des fibres, renforce les liens faibles laissant les groupements hydroxyles

nouvellement formés exposés à la surface. La couche hydratée encapsulant les nanoparticles est ce qui empêche finalement la détection des éléments principaux d'HA : P et Ca par des balayages au XPS. Comme il est maintenant expliqué par les analyses de XPS, la réponse cellulaire accrue sur PET10 est due à l'augmentation des groupements hydroxyles (et du contenu d'oxygène en général), reconnue pour favoriser l'attachement de cellules et leur croissance. En plus, la caractérisation SEM-EDX a permis de détecter certaines nano- et microparticules d'HA exposées à la surface. Comme l'HA n'est pas détectée par XPS, la concentration de surface des particules doit être inférieure à 3%, soit la limite de détection du XPS. En plus, tel qu'observé par SEM, la rugosité accrue pour des pourcentages plus élevés d'HA, induits par de gros agrégats d'HA, influence la réponse cellulaire. Il apparaît ainsi que les réponses biologiques améliorées précédemment observées à des pourcentages plus élevés d'HA étaient probablement dues à la rugosité accrue des fibres, en combinaison avec la chimie oxydée de surface, et non l'HA exposée en surface, comme on le supposait au départ.

Comme tous les biomatériaux novateurs, les fibres de nanocomposite de PET/HA présentées doivent être efficacement stérilisées avant d'être utilisées comme matériaux biologiques. Puisqu'on l'accepte généralement que les processus de stérilisation utilisés modifient les caractéristiques physiques et chimiques des matériaux polymériques, la méthode de stérilisation doit être soigneusement choisie. Cependant, la littérature semble présenter des résultats contradictoires au sujet des effets du procédé de stérilisation sur la réponse biologique, car plusieurs études ont prouvé que la stérilisation peut changer la réponse biologique tandis que d'autres investigateurs ont constaté que les

différents protocoles de stérilisation n'ont pas d'effet significatif sur la réponse biologique aux polymères spécifiques. De là découle la nécessité continue d'examiner les effets des protocoles de stérilisation relatifs à l'implantation de matériaux novateur. L'analyse XPS suite à la stérilisation par LTP ou EtO a révélé des modifications chimiques de la surface des fibres. Des changements observés peuvent être expliqués par la nature de l'agent de stérilisation puisque des modifications de plasma se produisent dans un mécanisme spécifique à chacun des gaz utilisés. La technique de LTP utilisée combine l'utilisation d'un agent chimique fortement oxydant, de l'oxygène (O_2) et de l'azote inerte (N_2), vaporisé et laissé pour diffuser dans la chambre, alternativement avec le plasma. Bien que la phase chimique soit employée pour son efficacité de bactéricide dans la technique LTP, elle est responsable de l`addition de groupes fonctionnelles de COOH. La déconvolution de la région de C1s a indiqué la formation du carbone fortement oxygéné, soutenant l'idée que des emplacements ont au moins partiellement réagi avec de l'eau l'oxygène et d'air afin de constituer les groupes de C-OH, augmentant le contenu d'oxygène global dans la surface de fibres traites par LTP. D'une part, bien que les résultats qualitatifs d'EtO suggèrent une augmentation des groupes fonctionnels oxygénés, la forme globale de C 1s suggère une simple d'alkylation. L'alkylation a été prévue car l'alkylation est le mécanisme d`action de l'EtO.

Afin d'évaluer les effets des méthodes de stérilisation sur la biocompatibilité *in vitro* de fibres nanocomposite PET/HA, quatre méthodes ont été employées : (1) l'évaluation de la viabilité du fibroblaste L929 en utilisant des médias d'extrait obtenus à partir des fibres différemment stérilisées, (2) l`évaluation de viabilité des

fibroblastes L929 en contact direct avec les matrices fibreuse 3D différemment stérilises, (3) l'évaluation du relargage de TNF-α par les Raw 264.7 macrophages suivant l'incubation avec des médias d'extrait obtenus des fibres différemment stérilisées, et (4) l'évaluation du relargage de TNF-α par les Raw 264.7 macrophages suivant l'incubation en contact l'incubation de macrophages avec les fibres différemment stérilisés. Les résultats ont prouvé que le traitement à l'LTP et l'EtO extraits des fibres n'ont eu aucun effet sur la viabilité de cellules, ce qui suggère la biocompatibilité des extraits. Les essais de contact indirects ont été complétés avec des essais de contact direct pour évaluer les effets de modifications chimiques suite à la stérilisation sur le comportement cellulaire. Étonnamment, la viabilité de fibroblastes suivant l'incubation de contact direct avec les échantillons stérilisés était inchangée par le type de stérilisation utilisé. Les réponses inflammatoires dues aux produits de dégradation ont été également mesurées en regardant le dégagement de TNF-α par les 264.7 macrophages. Les expériences actuelles ont démontré une tendance de dégagement sensiblement plus élevé de TNF-α suite a l incubation avec les extraits et fibres stérilisés par EtO.

En conclusion, la capacité des matrices de fibres de supporter l'attachement, l'étalement et la croissance *in vitro* des cellules L929, combinée avec les extraits compatibles en dégradation et le faible potentiel d'inflammation des fibres et des extraits, suggère la possible utilisation de ces composites comme biomatériaux pour les os supportant les charges. Dans le but d'expliquer la réponse biologique favorable pour des concentrations plus élevées de HA, il a été observé que le chargement en HA des

fibres augmente le contenu global en oxygène des composites alors que le HA demeure non détecté par le XPS. Finalement, les deux traitements de stérilisation semblent acceptables.

Toutefois, en termes d'évaluation biologique de structures 3D pour le remplacement d'os, les implications à court terme sont évidentes. Principalement, la biocompatibilité spécifique des matrices 3D de fibres doit être évaluée en utilisant une lignée cellulaire d'ostéoblastes. De plus, leur capacité à supporter la différentiation des ostéoblastes et la formation de matrice extracellulaire pourrait aussi être un facteur important à déterminer. Tel que mentionné dans l'introduction, les matrices 3D doivent aussi permettre la migration cellulaire dans la structure pour la régénération de l'os. L'infiltration cellulaire, la viabilité et la prolifération à l'intérieur de la matrice devraient aussi être évaluées. Finalement, en termes de la perspective biologique, si les matrices 3D présentent toujours des résultats *in vitro* intéressants comparativement à ce qui est présenté dans la littérature pertinente, elles devraient alors être évaluées *in vivo* dans un modèle animal révélateur. Évidemment, la caractérisation complète de la biocompatibilité et de la bioactivité des nanocomposites novateurs n'a pas été réalisée dans cette recherche car elle avait été orientée vers l'éclaircissement de la biocompatibilité générale des fibres de nanocomposites de PET/HA pour des expériences *in vitro* et *in vivo* futures[4].

Le second aspect qui doit clairement être optimisé dans cette recherche est la conformation des matrices 3D elles-mêmes. Elles ont été fabriquées pour posséder des pores de grande dimension et une porosité de 90%, comme celle des os. Toutefois, la

taille idéale des pores de 100 à 350 µm n'a pas été optimisée pour permettre la croissance maximale de tissus et devrait être considérée comme un paramètre fondamental pour l'utilisation future des matrices.

Table of content

List of figures

List of tables

List of abbreviations

3D	Three dimensions
°C	Degree Celsius
ε_{ox}	Molar extinction coefficient of Alamar Blue oxidized form
ε_{red}	Molar extinction coefficient of Alamar Blue reduced form
λ_1 and λ_2	Wavelenghts
µg	Microgram
Ml	Microlitre
A	Absorbance of test wells
A'	Absorbance of negative control well
AAMI	Association for the Advancement of Medical Instrumentation
Al	Aluminium
C	Carbon
Ca	Calcium
Cm	Centimetre
CNRC	Conseil national de recherche du Canada
Ctl	Control
Dl	Decilitre
DMEM	Dulbecco modified Eagle Medium
DNA	Deoxyribonucleic acid
E	Young Modulus
ECM	Extra-cellular Matrix
EDX	Energy dispersive X-ray spectroscopy
ELISA	Enzyme-linked immunosorbent assay
EtO	Ethylene oxide sterilization
eV	Electron Volt
FBS	Fetal Bovine Serum
FDA	Food and Drug Administration
FEG-SEM	Field Emission Gun Scanning Electron Microscope
FTIR	Fourier-transformed infrared
G	Gram
H	Hour
H	Hydrogen
h_v	Radiation energy
HA	Hydroxyapatite $(Ca)^{10}(PO4)^{6}(OH)^{2}$
HDPE	High density polyethylene

K	Kinetic energy
keV	Kilo Electron Volt
kV	Kilovolt
IMI	Industrial Materials Institute
L	Litre
L929	Murine L929 fibroblast cell line clone from conjunctive mouse tissue
LPS	Lipopolysaccharide
LTP	Low temperature Plasma Sterilization
M	Metre
Mg	Magnesium
min	Minutes
ml	Millilitre
mm	Millimetre
MTT	Methyl tetrazolium
N	Newton
nm	Nanometre
NSERC	Natural Sciences and Engineering Research Council of Canada
O	Oxygen
P	Phosphate
PA66	Polyamide (Nylon) 66
PBS	Phosphate buffered saline
PE	Polyethylene
PET	Polyethylene teraphthalate
PETX	X (0, 2, 4, 6, 8, 10): Weight percentage of HA in the PET fibers
pg	Picogram
PGA	Polyglycolic acid
PLA	Polylactic acid
PLGA	Poly(lactic-co-glycolic acid)
ppm	Part per million
Raw264.7	Adherent mouse macrophage cell line
RNA	Ribonucleic acid
rpm	Rotations per minute
SEM	Scanning electron microscopy
TCP	Tissue culture plate
TNF-α	Tumor necrosis factor-α
TSE	Twin-screw
UHV	Ultra-high vacuum

W	Watt
Wt	Weight
XPS	X-ray Photoelectron Spectroscopy

Chapter 1 : Introduction

The World Health Organization declared the years of 2002-2010 as the Bone and Joint decade. In the United States alone bone related procedures cost an estimated 300 billion dollars a year. Although allografts (bone graft from donor) remains the gold standard in bone related treatments, the limited supply and risks associated to pathogen transfer (prions, viruses, etc.) require a more versatile solution.

An ideal bone substitute should be tolerated by the host tissue without any adverse reaction; it should promote bone formation, have appropriate mechanical strength and be malleable. For load bearing bone implants titanium and its alloys have been widely used due to their high strength to weight ratio, toughness and bioinertness. Despite their wide-spread success, challenges remain for Titinanium based biomaterials. Mainly Titanium high stiffness (110 GPa) compared to bone (10-15 GPa) commonly leads to problems such as stress shielding, bone resorption and implant loosening. It is postulated that the preferred type of high performance load bearing bone implant is inspired from nature. Bone is a hierarchically structured composite material formed of nanofibers containing a polymer phase (collagen type I) and a mineral phase, (crystalline apatite nanoparticles) organized in a complex 3D structure. An ideal biomimetic (*i.e.*, imitating natural tissues) bone load bearing biomaterial should be physically, structurally and mechanically similar to bones, in addition to the conventional long-term stability, biocompatibility, and mechanical reliability.

The experimental part of this thesis evaluates the biocompatibility, surface chemistry and sterilization method of newly developed biomimetic nanocomposite fibers fabricated form a polymeric matrix and charged with hydroxyapatite nanoparticles as an ultimate load bearing bone replacement.

Chapter 2 : Literature Review

2.1 General concepts about biocompatibility

The notion of biocompatibility has evolved with the development of materials used in medical devices. Originally, a biocompatible material was defined as a material that would do no harm to the surrounding environment. The principle was based on inertness as reflected by the definition of biocompatibility initially employed: "the quality of not having toxic or injurious effects on biological systems"[1]. Nevertheless increasing demand for accelerated healing of tissues lead to the development of devices with materials that were more responsive to local biological conditions, where interactivity became the central principle. Naturally, the official definition of biocompatibility evolved to: "the ability of a material to perform with an appropriate host response in a specific application". Unfortunately the definition remained vague and *an appropriate host response* is difficult to determine. Through recent remarkable advances in biological surface sciences, the current definition of biomaterial evolved to "a material intended to interface with biological systems to evaluate, treat, augment, or replace any tissue, organ, or function of the body". It is now accepted that biocompatibility of medical implants is influenced by different factors, such as the toxicity of the material used, the form and design of the implant, the resistance of the device to chemical or structural degradation, the dynamics or movement of the device *in situ*, and the nature of the reactions occurring at the biological interface.

Naturally these factors vary with the implantation area, *i.e.,* in soft or hard tissues, or in the cardiovascular system. As the biomaterials developed in this thesis are intended for hard tissue replacements exclusively, the following literature review is axed around bone and hard tissue biomaterials and biocompatibility.

Currently, *in vitro* biocompatibility of novel biomaterials testing is performed as a prerequisite to *in vivo* evaluation. The *in vitro* techniques currently employed evaluate the *in vitro* cytotoxicity of a biomaterial based on the morphological examination of cell damage and growth when in direct or indirect contact with the materials. The importance of cell-biomaterial interaction comes from the cellular *in vitro* sensitivity, reactivity and ease of evaluation. Although not yet well understood, it is presumed that cells are responsive to changes in their homeostasis due to their complexity. Briefly, cells are highly organized structures composed by organelles that perform very specialized functions (*e.g.,* production of glyco- and lipoproteins, DNA synthesis and production of proteolytic enzymes). The remainder comprises the cytoplasm and the cellular membrane, which surrounds both the organelles and cytoplasm. Different regions of the cellular membrane correspond to different functions, such as mechanical attachment, adsorption, secretion and communication with other cells[2,3].

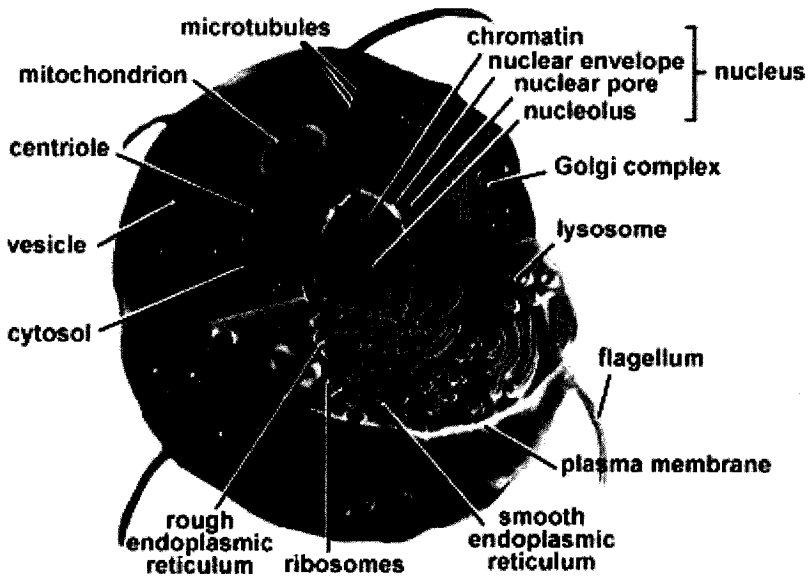

Figure 2.1 Schematic representation of eukaryotic cell and its organelles. (picture taken from http://www.estrellamountain.edu/faculty/farabee/biobk/biobooktoc.html)

Disturbance of the above described cellular homeostasis leads to a cascade multiplicity of biochemical changes. This disturbance of the cellular homeostasis is what is commonly described as toxicity of the proposed biomaterials. In terms of *in vitro* toxicity[4] of biomaterials, high importance is given to the following cellular parameters:

- cell death,
- cell proliferation,
- cell morphology,
- cell adhesion.

Disruption of cellular proliferation and morphology leading to cell death by a biomaterial understandably classifies it as incompatible and cytotoxic. However cellular adhesion is a less straightforward parameter of equal importance and a short description was deemed necessary.

2.1.1 Cellular adhesion and biomaterial surface

Tissues are not made up solely of cells. A substantial part of their volume is *extracellular space*, which is largely filled by an intricate network of macromolecules constituting the extracellular matrix (ECM). The ECM helps to hold cells and tissues together, and provides an organized lattice within which cells can migrate and interact with each other (paracrine cell signaling)[3]. ECM occurs in two forms: interstitial matrix (*i.e.,* connective tissue) and basement membrane (*i.e.,* epithelium)[2]. Besides providing mechanical support for cellular anchorage, the diverse functions of ECM include: control of cell growth, determination of cell orientation, support for cell proliferation and tissue renewal, maintenance of cell differentiation, etc.

The importance of the cellular adhesion and spreading to a biomaterial in an appropriate ECM-like fashion comes from the fact that most cell types undergo apoptosis (cell death) when deprived of adhesion to ECM[5]. Hence, cell adhesion is generally regarded as a crucial survival factor for cells. In terms of biocompatibility, cellular adhesion evaluation becomes an important *in vitro* aspect as the biomaterial can potentially support certain adhesive sites but not others. It gets even more complex as in a physiological environment protein adsorption onto biomaterials always precedes cellular adhesion. The strength and type of the biomaterial-cell adhesive sites are actually governed by the pre-adsorbed proteins in combination with proteins produced by the cell, and the biomaterial characteristics. There are three important types of adhesive sites between cells and biomaterials for proper biomaterial integration[6]:

1) focal adhesion: a very strong adhesion that involves binding to fibronectin, corresponding to a 10-20 nm gap normally observed at the cell boundaries;
2) close contact, generally surrounds the focal adhesions by a 30-50 nm gap;
3) extracellular matrix contacts, formed by strands and fibers of ECM material that connect the ventral cell wall with the underlying substratum, corresponding to a large gap around 100 nm.

As mentioned before, cells can also adhere to ECM or to other cells. The contacts formed in cells-ECM interactions differ significantly from those found in cell-surface interactions, and are characterized by the following four adhesive sites: gap junction (nexus), desmosome, hemidesmosome and tight junction.

The cascade of cell-surface interaction to cell-surface spreading is a result of the combined process of continuing adhesion and cytoplasmic contractile meshwork activity. The generation of cytoskeleton development is also induced by the stress promoted with the spreading. Cell adhesion and spreading are directly influenced by the physico-chemical characteristics of the underlying biomaterial solid surface. As it is hard to predict the cellular response elicited by novel biomaterials, biomaterial-cell interactions and resulting ECM are routinely analyzed by *in vitro* biocompatibility studies. Consequently, biomaterial surface properties impact in its resulting biocompatibility is obvious. However, a generally overlooked aspect of a biomaterial surface is its potential bioactivity also acquired through the surface interaction with the surrounding cells. In other words, synthetic foreign materials acquire bioreactivity by properly interacting with dissolved proteins. Adsorbed proteins transform an inert, non-

thrombogenic material into a biologically active surface that can modulate cell adhesion, spreading, and function. It is thought that the particular properties of surfaces, as well as the specific properties of individual proteins, together determine the organization of the adsorbed protein layer, and that the nature of this layer determines the cellular response to the adsorbed surfaces. In fact it is easy to grasp how the *biomaterials surface* that modulates the *protein-biomaterial interactions* that modulates the *cell-biomaterials interactions* is the foundation of its *biocompatibility*. In a nutshell, cell adhesion is the pre-requisite for further cellular functions, such as spreading, proliferation, migration and biosynthetic activity.

It is easy to see how the raw material describing its surface in terms of chemistry, topography and hydrophobicity become essential aspects for its biocompatibility. Consequently, in the primary stage of building a 3D scaffold, the selection of the most adequate raw material is a crucial consideration. The raw material has to be engineered in a suitable 3D scaffold as the successful regeneration of tissues from matrix-producing connective tissue cells or anchorage-dependent cells (*e.g.*, osteoblasts) relies on the use of a suitable 3D scaffold. Therefore, the design and production of an appropriate 3D scaffold material is the second most important stage in tissue engineering strategies.

2.1.2 Scaffold requirements

The requirements for a scaffold material to be considered suitable for tissue engineering applications are complex. Also, no consensus exists among the biomaterials research community about the specific demands that are required for a particular application. These requirements depend mainly on the tissue to be restored and on the

size of the defect to be treated. Nevertheless, there are some general key characteristics that a bone scaffold must possess:

1) **Biocompatibility**, as previously described remains a fundamental issue[7-9].

2) **Appropriate surface chemistry**[8-11], as most bone cell types are anchorage-dependent, they require a suitable substrate to retain their ability to adhere, proliferate and differentiate. Therefore, as extensively reviewed in the literature, the surface topology and chemistry of biomaterials , are fundamental in cell adhesion and biomaterial incorporation[12-14]. However, it is very rare that any biomaterial with good bulk properties for a specific use in the biomedical field also possesses the required surface characteristics[15,16] for that application. It follows that most of the biomaterials need surface modification to acquire surface characteristics that allow for adequate cell adhesion[15,16]. These surface modifications include, for example, roughening, coating, blending and grafting[15,16].

3) **Appropriate mechanical properties**[17-20], it is necessary to build the scaffolds that mimic the mechanical properties of the native tissue as they provide the basic 3D mechanical framework for the cells to attach and proliferate before they can differentiate into a tissue. Not only the mechanical properties but also the geometry of the tissue plays a major role in engineering the design for scaffolds.

4) **Appropriate pore size and fiber diameter**[7-9,18], are important factors that are associated with cellular adhesion and nutrient supply to regenerated cells. There

is a lack of consensus among the scientific community about the ideal scaffold pore size and fiber diameter and this issue is discussed more in depth in the following section.

5) **Easily processed into 3D shapes**[8,18,21] that can be maintained after implantation as the regenerated tissue is expected to take the shape of the scaffold.

6) **Easily sterilized**[9,22], either by exposure to high temperatures, ethylene oxide (EtO), or low temperature sterilization techniques, while remaining unaffected by one of these techniques. As the sterilization of biomaterials remains a controversial topic it is explained in more depth in Chapter 6, in the second article of the thesis.

A quick analysis of the required bulk and specific requirement of scaffolds reveals quickly the shortcomings of the 1980s adapted approaches to implant design. During the 1980s, the implant design surfaces were based on mechanical retention optimization and nature imitation. As the interactions with the body were not understood, these solutions illustrate the principle that "existing biomaterials, although demonstrating generally acceptable clinical success, look like dinosaurs poised for extinction in light of the winds of change blowing through the biomedical, biotechnological and physical science" enunciated by Ratner in 1993[23]. The synthesis of cell adhesion-specific materials to produce 3D synthetic scaffolds with tailored properties such as porosity, mechanical and surface chemistry only became a reality with the engineering advances.

2.1.3 Micro- and nanofibrous scaffolds

Scientists around the globe have tried to address these issues by fabricating a 3D surface having the properties equivalent to the replacing tissue. These artificial 3D matrices, called scaffolds, provide the structural integrity similar to the natural ECM in the body. The scaffold can then be seeded with cells taken from the patient's normal tissue or from the donor. The biochemical and/or mechanical signals are then provided for the differentiation of the cells into tissues.

Nanoscale fibrous materials are the fundamental building blocks of living systems and are predominantly found in the ECM of tissues and organs. Nanoscale fibrous structures not only replicate the morphology of natural tissues building blocks but they are also known for high surface area to volume ratio. This has inspired an important wave in the biomedical/biomaterials field in the fabrication of nanoscale fibrous structures by various process, in particular electrospinning. Many studies have been proposing electrospun nanofibrous structures with diameters as small as 3 nm as attractive biomaterial platform for tissue regeneration.

However the nanofibrous polymeric mats for tissue engineering have a major limitation for 3D applications due to their pore size, which is smaller than a cellular diameter (typically 10 μm) and can not allow cell migration within the structure. It is generally accepted that the optimal pore size for cell growth depends on the tissue that is intended to restore. In the case of bone regeneration authors defend that a maximal tissue ingrowth is attained with a pore size ranging from 200 to 400 μm[18], and others claim it should be from 100 to 150 μm[8], or from 100 to 350 μm[24]. Despite the lack of consensus

regarding the optimal pore size it is clear that nanoscale polymeric mats no longer appear as the ideal candidates due to their nano-sized pores.

Furthermore, the small size of the nano-fibers tends not to maximize the points of cell attachment, which is a negative effect on the expression of several factors and on cell spreading and differentiation[25]. As shown by Li *et al* with poly(L-lactide) micro- and nanofibers scaffolds, chondrocyte cells grew in a well-spread morphology and organized cytoskeleton on microfibers, in contrast to rounded morphology and disorganized actin cytoskeletal structure on the nanofibrous scaffold[26].

As other researches[25-27], we have developed in the present thesis a novel structure engineered from micro-fibers that is aimed to serve as a scaffold and mimic the physical structure of ECM for bone tissue regeneration, in addition to simultaneously providing the macro-support that cells require. Additionally the micro-fibrous mat allows an interconnected pore network structure that enhances the diffusion rates to and from the centre of the scaffold and facilitates vascularisation[7-9], thus improving oxygen and nutrient supply and waste removal. Before describing in length the 3D scaffold that we have developed, a quick overview of bone remodeling is presented so that the motivation behind the new material engineering can be understood.

2.2 Bone reparation mechanism

Osseointegration, process in which implants are clinically and rigidly fixed to surrounding bone, is achieved by constant functional loading[28]. Although the clinically

observable symptoms of implant stability are easily understood by this definition, the biologic processes controlling bone formation and bone maintenance at the implant to bone interface remain obscure. A short review of osseointegration biological perspective is thereby presented for a clearer understanding of the requirements on novel 3D bone scaffolds.

A complex cascade of cellular and molecular events is triggered by the site preparation and subsequent placement of the implant. The often overlooked surgically-prepared bone site fills with blood as a result of the hemorrhage caused by the implantation trauma. The initial blood-implant contact allows blood proteins and platelets to adsorb onto the surface of the implant[29]. Most importantly this blood-implant contact allows fibrin fibers to contact both bone and implant. The importance of the fibrin fibers covering the implant comes from their usage as bridges for osteogenic cells from the marrow to migrate towards the implant and differentiate into mature osteoblasts during this migration. Osborn and Newesley [30] hypothesis that two processes of endosseus (implants embedded into bone) healing occur is a now well accepted one. More specifically around endosseous implants as shown in Figure 2.2, osteoblasts may lay down bone on the old bone surface *distance osseogenesis* or on the implant surface itself *contact osseogenesis*.

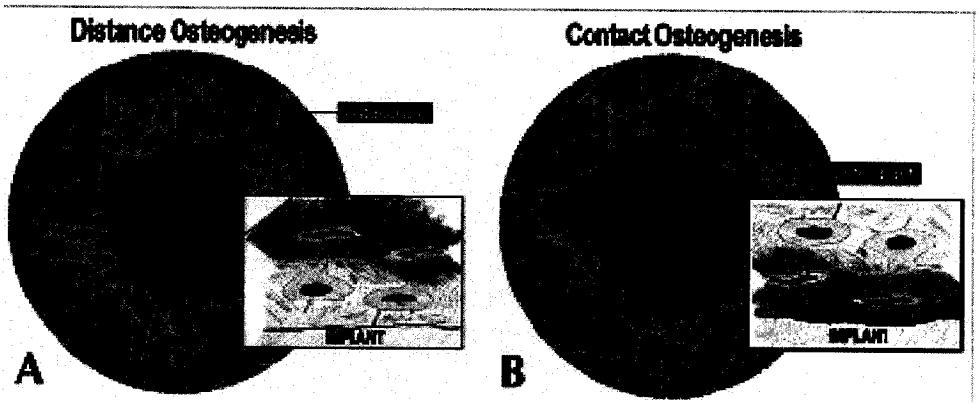

Figure 2.2 : Initiation of *distance osteogenesis* (A) and *contact osteogenesis* (B) where osteogenic cells line the old bone or implant surface, respectively. (Figure taken from [31])

As shown in Figure 2.2, during distance osseogenesis the new bone grows toward the implant with the existing bone providing the osteogenic cells that lay down new matrix. The shortcoming of distance osseogenesis is very obviously that bone does not form on the implant itself but rather surrounds the implant. As bone then surrounds the implant rather than directly bonding to it, an unstable interface of connective ECM tissue surrounds the implant and stable bone bonding, osteointegration is not possible. On the other hand, contact osseogenesis means that a population of osteogenic cells have migrated to the implant surface and colonized it before they start bone matrix formation. Consequently, bone grows directly on the implant surface, fusing with native bone and forming a stable connection allowing a stable implant upon mechanical loading.

As previously mentioned during contact osseogenesis the osteoblasts migration to the implant surface is dependant upon fibrin anchorage onto the implant. The structure and composition of the implant interface determine the fibrin anchorage strength, and consequently osteoblasts migration onto the implant surface. In other

words if the implant surface is smooth, adsorbed fibrin will detach from the implant during the migration of the osteogenic cells through the fibrin matrix, due to lack of fibrin anchorage to the substrate. Consequently the migrated osteogenic cells and the secreted matrix will not be in contact with the implant surface similarly to the resulting matrix in distance osteogenesis. On the other hand, when the implant surface has the correct micro-roughness, fibrin anchorage endures the osteogenic cells migration induced contraction. In other words, the differentiating osteogenic cells are able to reach the implant surface before secreting bone matrix. The concept is illustrated in Figure 2.3 below where

a) the rougher micro-topography implant surface supports fibrin attachment despite the cell induced stress and

b) fibrin detaches as the osteogenic cells migrate due to the smooth implant surface.

Therefore the structure of the implant surface is essential for an optimal implant bone anchorage with regard to the attachment of fibrin.

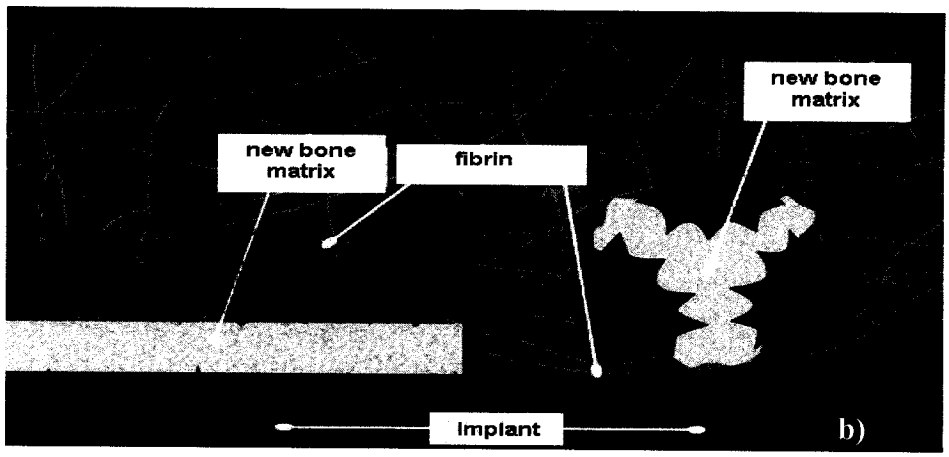

Figure 2.3 Migration of osteogenic cells through the transitory fibrin matrix of the blood clot toward the implant surface. In a) the strength of fibrin attachment is sufficient to withstand the contractile forces imposed on the fibrin by the active migration of osteogenic cells and in b) the smooth surface of the implant doesn't support a sufficiently strong implant-fibrin bond to support the tractional forces can. (These drawings have been adapted as still images from computer animations at www.ecf.utoronto.ca/~bonehead)

In vitro and *in vivo* experiments have confirmed that *de novo* formation (new bone formation) on implant surfaces and natural bone remodeling are different processes. A common linking factor to *de novo* formation and osteointegration is when bone is formed for the first time at the appropriate site by differentiating osteogenic cells, as in contact osteogenesis. Although it is inevitable that both distance and contact osteogenesis occur in every endosseous healing site, the biological significance of these different healing reactions is of critical importance in both attempting to unravel the role of implant design in endosseous integration and elucidating the differences in structure and composition of the bone/implant interface.[31]

2.3 Polymer/ceramics composites for biomedical applications

Orthopedic biomaterials can be implanted into or near a bone fracture to facilitate healing or to compensate for a lack or loss of bone tissue. The materials used in

orthopedic surgery include ceramics, polymers, metals and resorbable materials, such as bioglass, and various modifications of hydroxyapatite. However, no single material possesses all the above enumerated characteristics needed for a successful synthetic bone replacement manufacturing. Hence the trend of combining two materials to produce a tailor fitted composite drawing on the advantages of each to make a superior composite has become a very popular alternative. The main inspiration in the choice of the primary materials used for the tailor composite has been bone. At the ultra-structural level bone is an apatite–collagen composite material as shown in Figure 2.4.

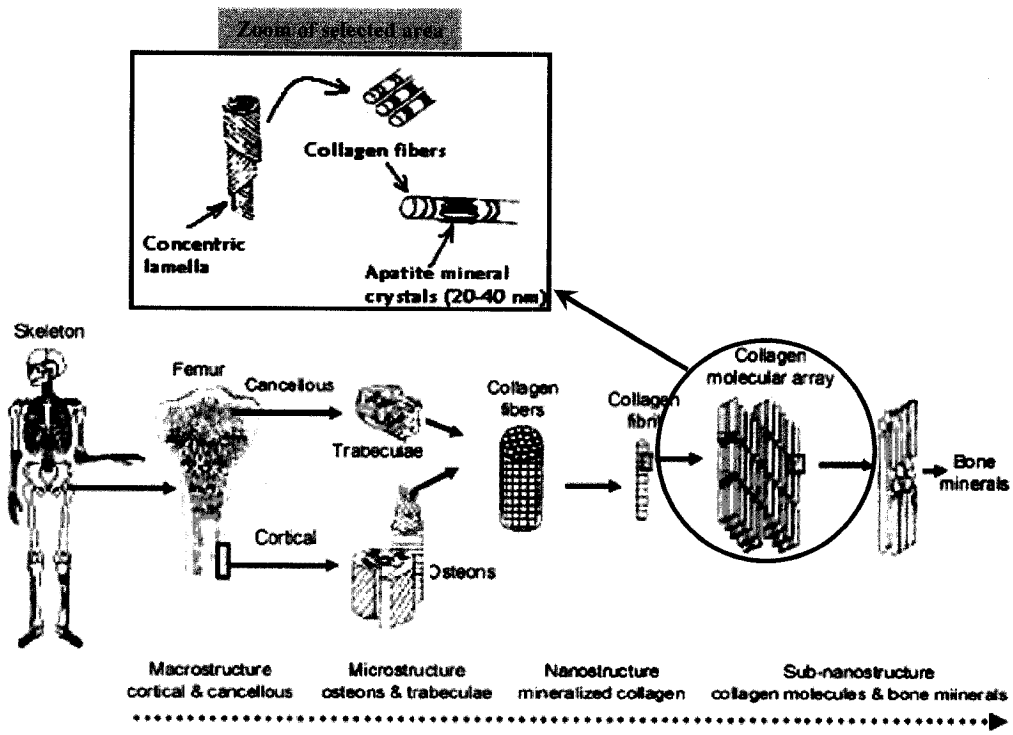

Figure 2.4 The hierarchical structure of bone, from macro- to nano-assembly. (Figure adapted from [32])

Replacing bone by a polymer matrix composite containing a particulate, bioactive component appears as a natural choice for substituting cortical bone[32].

2.3.1 Hydroxyapatite

As there are few materials capable of inducing bone growth, bone regeneration is the most limiting factor in materials selection. One of the most studied materials is hydroxyapatite (HA), possessing the $Ca_5(PO_4)_3(OH)$ chemical formula. As natural apatite is the primary inorganic component of all calcified tissues in the human body[33], synthetic apatite, or HA, has been proven bioactive and suitable for bone replacement. HA is versatile in preparation by a number of different ways rendering it highly accessible. Processes like sol-gel[34], precipitation[35], and solid-state reactions[34] have all been used to successfully produce HA powder. In fact HA powder fabrication is such a common process that HA is readily available from a number of commercial companies. Unfortunately, HA on its own has mechanical properties inferior to the necessary properties to sustain load-bearing applications in the body.

2.3.2 HA-Polymer Composites

The rationale for HA-reinforced polymer composites is based on mimicking the mechanical and biological properties of bone tissue. HA-reinforced polymer composites can provide tailored mechanical properties that could possibly be used to alleviate mechanical mismatch problems between bone the host tissue and substitutes or implants.

Due to the concept popularity, HA composites have been widely produced and investigated. For instance, HA has been formed into a composite with metal such as titanium, zirconia, and alumina[34]; and reinforced through the addition of particles[36], whiskers and fibers[34]. All of these materials have significant limitations in terms of the resulting modulus mismatch with bone. Undoubtedly, these materials will need to be further refined for use as a hard tissue replacement.

Polymers, on the other hand, are the only other materials incorporated with HA to form composite materials with modulus and toughness values similar to bone. This has inspired a new trend of polymer composite blending in which the category of biodegradable polymers has become a popular venue. The reasons behind this motivation are simple: ideally a scaffold would degrade on the same time scale that the cells can produce the natural ECM, leaving only native ECM and cells behind. As a result the immune response to the polymer composite would cease. Although many authors note that the breakdown products of PLA, PGA, and PLGA (degradable polymers used for polymer/HA composites) are water and CO_2 and are well accepted by the body, one must take into consideration the complete degradation process whereby the polymer is first broken down into its repeat units: lactic and glycolic acid. The release of lactic and glycolic acid causes a local decrease in pH, which many expect it to create a harsh environment for the cells. In addition, many degradable polymers used for tissue engineering scaffolds do not have a linear rate of degradation and often lose mechanical integrity long before natural ECM can be formed. Hence the open and literature debate of the advantages of degradable versus non-degradable polymer matrix

in the fabrication of biomedical composites remains very modern. At the present time only non-biodegradable polymers can withstand high mechanical stresses experienced with articulating joints or load bearing bones such as femur. In this respect the biomaterial replaces the lacking or damaged tissues and supports the remaining healthy tissue. As this is the ultimate aim of the presently designed fibers, the following literature review is axed around non-degradable polymer-HA composites.

The concept of bioactive particulate reinforced polymer composite as bone analogue was first productively introduced in the early 1980's by Bonfield *et al.*[37]. Bonfield's group also developed the earliest bioactive reinforced polymer composite, as the commercially successful composite HAPEX™, by reinforcing polyethylene (PE) with HA. HAPEX™ is now an FDA approved composite widely used for ear defects and it is shown below in Figure 2.5.

Figure 2.5 Middle ear implants with hydroxyapatite heads and HAPEX™ shafts developed by Bonfield *et al.* (picture taken from[38])

This pioneering work inspired many other bioactive polymer/HA composites, designed in an attempt to match the properties and structure of those of bone for ultimate orthopedic applications. Among others, the following non-resorbable matrix polymers

have been filled with synthetic HA as potentially attractive biomaterials: polyethylenes[37,39-41], PA66[42],polysulfone[2], polyacrylics[43-47] and polyetheretherketones[48-51].

2.3.3 Polyethylene Terephthalate

Polyethylene terephthalate (PET) is a linear, aromatic polyester first manufactured by Dupont in the late 1940s. The chemical structure of PET is shown in Figure 2.6.

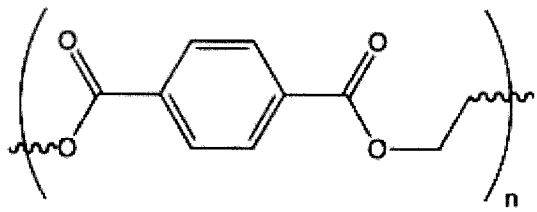

Figure 2.6 : Chemical structure of PET repeat unit (molecular weigh 192). (Figure taken from [52])

Since its conception PET has been mainly trademarked by Dacron, particularly for fibers so this nomenclature is commonly used when referring to PET. As illustrated in Figure 2.5, PET has been successful for cardiovascular grafts since the 1950's in critical procedures where high strength and predictable long-term performance is needed[52].

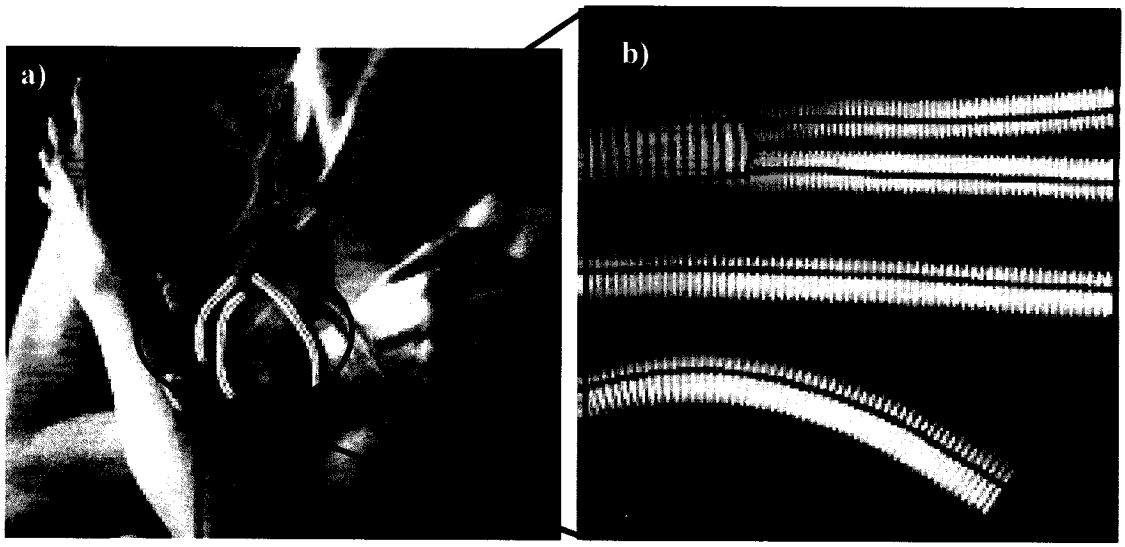

Figure 2.7 : a) Dacron positioning following surgery and b) Dacron. (Picture adapted from[52])

This long standing success story is mainly due to PET chemical structure which promotes resistance to hydrolysis due to its hydrophobic aromatic groups and high crystallinity[52]. Current medical applications of PET encompass critical procedures where high strength and predictable long-term performance is emphasized; such as in implantable sutures[53], surgical mesh[54], vascular grafts[55], sewing cuffs for heart valves[56].

Furthermore the synthetic graft market in vascular applications is currently dominated by PET or otherwise known Dacron. Therefore, through the widespread and successful usage of PET, it has been demonstrated as a biomaterial, chemically stable and resistant to degradation and to toxic or inflammatory by products. Paradoxically, the same characteristics that allow PET its long history in vascular related human implantation renders it bio-inert in terms of bone related functions. It is anticipated that by charging oriented PET fibers with variable amounts of bioactive inorganic HA particles the composite becomes a theoretically successfully functionalized bioactive

material able to sustain physiological loads necessary for success as a load-bearing bone replacement. Furthermore the PET/HA fibers are to have a final diameter in the micron range as this seems to be the preferred structure for cellular migration. The fibers ultimate 3D scaffold structure has not been fully exploited yet, as the aim of the thesis was mainly the potential of fibers themselves.

Lastly, for a complete literature review on the topics exploited in this thesis the reader must refer to the two articles incorporated in the thesis body, as repetition was avoided by exploiting uncovered topics by the articles.

2.4 Aims of the present study

The experiments described here were designed to investigate the *in vitro* biocompatibility of the novel PET/HA composite and their capacity to serve as bone substitutes. The specific aims were:

- To examine the *in vitro* cytotoxicity of both phases that would occur during the implantation life cycle of the nanocomposites, namely: the cross-linked network surface and its possible eventual degradation products. (Manuscript 1)
- To elucidate the effects of the ceramic nano-fillers, HA, on the *in vitro* cellular viability, attachment, proliferation and cytokines production; as we hypothesized that the nanocomposites with highest (10%) HA addition would demonstrate superior surface properties for biocompatibility. (Manuscript 1)

- To evaluate the HA nanoparticles effects on the polymeric fibers surface chemistry by X-ray photoelectron spectroscopy (XPS) and Scanning electron microscopy in combination with energy dispersive X-ray analysis (SEM-EDX analysis. (Manuscript 2)
- To examine the effects induced by ethylene oxide (EtO) and low temperature plasma (LTP) sterilization processes on the composites chemical composition by XPS, and *in vitro* cytotoxicity. (Manuscript 2)

Chapter 3 : Materials and Methods

This chapter presents the materials and methods used to evaluate the effects of the HA nanoparticles on the novel nanocomposites biocompatibility, surface chemistry as well as the effects of various sterilization treatments on the novel nanocomposites biocompatibility and surface chemistry. As such the chapter is subdivided in two parts based on the two publications concerning this work. The methods employed were chosen from (1) the review of the methods used by other researchers and (2) the regulations of the AAMI 10993, Biological Evaluation of Medical Devices Series, Part 5:1999.

3.1 Novel nanocomposite fibers and 3D fiber scaffolds

3.1.1 PET/HA nanocomposite fibers fabrication

A master batch from the commercially available PET (M&G Polymers) was prepared by compounding it with HA nanoparticles in the form of pellets using a twin screw extruder (shown in Figure 3.1) at 280°C. The fiber spinning line consisted in a single screw extruder equipped with a 15 cm linear die with 150 holes of 380 microns each. The fibers were drawn from the die using a roller positioned at about 2 m from the die exit. The pellets were then diluted by dry blending prior to feeding in a fiber spinning line to prepare PET fibers with 0, 2, 4, 6, 8 and 10 wt% HA, respectively designated as PET0, PET2, ..., PET10. Although the main candidates for orthopaedic surgery are the fibers produced with the highest amount of HA (i.e. 10% HA or PET10),

all six samples were studied to evaluate the various effects of HA nanoparticles on the nanocomposite fibers. The final diameter of the fibers was in the range of 25 to 50 microns and the general trend was a smaller fiber diameter as the added HA increased.

The PET fibers were charged with a maximum of 10 wt% HA proportion as higher HA fills induced fiber breakage during the manufacturing process.

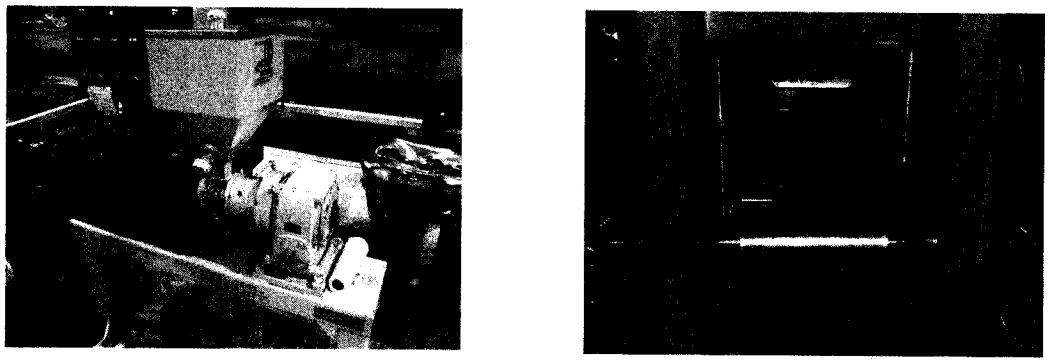

a) b)

Figure 3.1 : Twin screw extruder used to prepare PET/HA fibers a) extruder funnel where mix is added b) pick up roll.

3.1.2 Fiber matrix 3D preparation

For all direct contact *in vitro* assays, samples of 3D fiber scaffolds were prepared by compression moulding 2 g of fibers of the sample of interest on a Carver press (Figure 3.2a). In the current work, the fiber scaffolds were not optimized for implantation as this was a preliminary evaluation of their biological pertinence. As a potential material for bone grafts, the materials were used with highest porosity possible (approximately 90% in each fiber scaffold) to mimic the porosity of spongy (trabecular)

bone. The materials used thus appear as a bundle of fibers forming a 3D matrix with approx. 90% porosity.

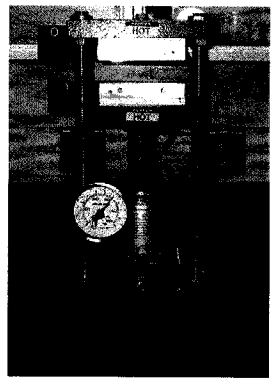

a)

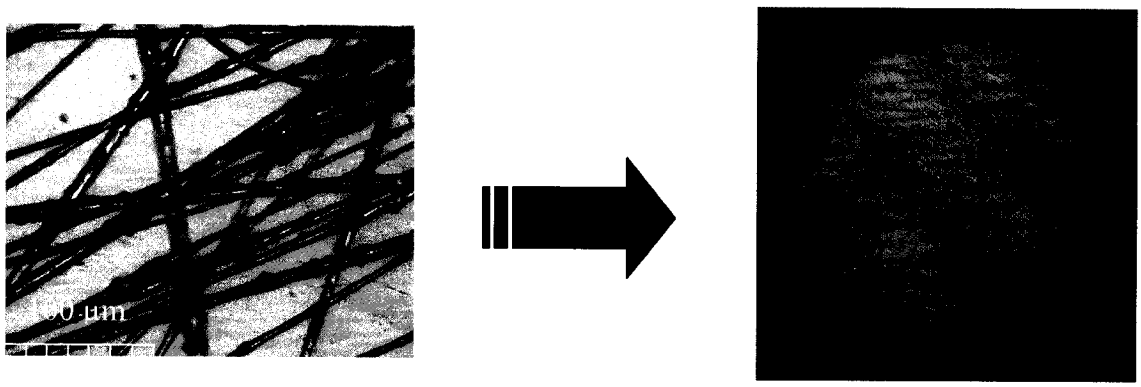

b)

Figure 3.2 : a) Picture of Carver press used, available at IMI-CNRC and b) scaffolds morphology as fabricated on the Carver press.

3.2 Materials used for *in vitro* study

3.2.1 Samples used for in vitro studies

The samples used for the *in vitro* studies can be divided by the type of study performed: indirect contact or direct contact tests. For the indirect contact tests, 2 g of PET/HA fibers (prepared as presented in paragraph 3.1.1) were used to generate the extraction medium. For the direct contact tests, 2 g of PET/HA 3D fiber matrix samples (prepared as presented in par, 3.1.2) were used per assay run.

Prior to sterilization all samples were cleaned by a 2-step ultrasonification procedure as the samples were prepared in non-clean room environment not suitable for clean biological mass production.

3.2.2 Cell cultures

Two cell lines were used to evaluate the *in vitro* biocompatibility of the fiber nanocomposites degradative particles and the 3D fiber scaffolds:

- Murine L929 fibroblast cell line (ATCC, Rockville, MD, USA), used for cytotoxicity determination
- Raw 264.7 macrophage cell line (ATCC, Rockville, MD, USA), used for the potential inflammation assessment.

Both cells lines were grown at 37°C in a 5% CO_2 humidified atmosphere. The cell medium was changed every 2 to 3 days, whenever cells reached 80% confluence.

3.2.3 Selection of cell lines

As this study is the first one looking at the biocompatibility of the novel fiber composites, two clone cell lines were chosen to avoid the influence of external sources and reduce the contamination potential, unlike samples from human blood peripheries. Both indirect and direct contact assays were carried out with L929 fibroblasts due to their high sensitivity[57] and model properties that can reliably determine the general biocompatibility of novel material and screen them for future *in vitro* and *in vivo* experiments[58]. The choice of Raw 264.7 macrophages to study the effect of polymer composite fibers and their extracts was due to macrophages role as the principal cells of cytokine formation, found in the pseudo-membranous tissue formed around hip implants at revision surgery[59]. A simplified drawing of macrophages main cytokine production (TNF-α) is shown in Figure 3.3 below.

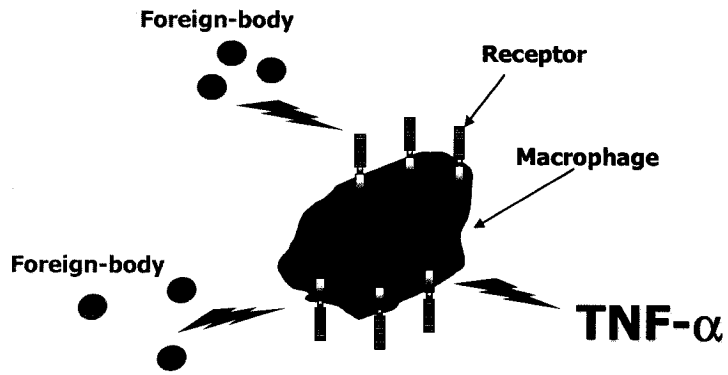

Figure 3.3 : Simplified schematic representation of macrophage Raw 264.7 cytokine production when stimulated by foreign-body

3.2.4 Culture medium

Both L929 and Raw 264.7 were grown in Dulbecco's modified Eagle's medium (DMEM; Sigma-Aldrich, Mississauga, ON, Canada), supplemented with: 3.7 g/L of sodium bicarbonate, 10% heat-inactivated (56°C for 30 min) foetal bovine serum (FBS),

100 units/ml penicillin, and 100 μg/ml streptomycin (Gibco Laboratories, Burlington, ON, Canada).

3.3 Experimental

3.3.1 Cytotoxicity – L929 fibroblasts cell culture

The cytotoxicity of the PET/HA nanocomposites charged with 0, 2, 4, 6, 8 and 10 wt% HA was evaluated either through an indirect cytotoxicity assay (extracts) or by a direct method according to AAMI 10993, Biological Evaluation of Medical Devices Series, Part 5:1999. The viability of the fibroblasts following the predetermined incubation times was determined by the Methyl tetrazolium (MTT) assay for the indirect method and by the Alamar Blue for the direct contact assay. In both cases the concentration of samples used was kept constant to 0.2 g/ml. All experiments were performed in triplicate and each measure was done three times.

3.3.2 Cytotoxicity of fiber extracts

The indirect contact method was used to measure the cytotoxicity of the possible degradation products and the effects of the HA addition into the nanocomposites chemical stability. Extracts were prepared by immersing respectively 2 g of PET0, PET2, …, PET10 fibers in 10 ml of complete DMEM medium, resulting in a fixed ratio 0.2 g/ml. In order to stimulate physiologic conditions the samples were submitted to constant agitation of 250 rpm and 37°C for 24 h. After this period, the medium was harvested and kept at –90°C until used.

In order to evaluate the cytotoxicity of the extracts, they were incubated with a confluent monolayer of the fibroblast cells (2.5×10^5 cells/ml, 200 µl/well) for 24, 48 and 72 h. Following the predetermined time period the MTT assay was performed so that the effects of the degradation particles can be evaluated on the fibroblastic cells.

3.3.3 Biocompatibility of 3D fiber scaffolds

To complement the indirect cytotoxicity contact tests with direct contact tests, the sterilized 3D fiber scaffolds were seeded with L929 fibroblast cells (1×10^4 cells/cm^2). Cells were maintained in culture for up to 14 days and at 1, 3, 7 and 14 days the cellular viability was evaluated by the Alamar Blue assay.

3.3.4 Cell morphology evaluation though FEG-SEM

Cell morphology, spreading, orientation, and growth on the 3D fiber scaffolds were evaluated using FEG-SEM on a Hitachi S-4700 apparatus (Hitachi High-Technologies Canada Rexdale, Ontario). The cells were analyzed at day 1, 7 and 14 on PET0 and PET10 fiber scaffolds in order to determine the differences induced by HA addition in the cell–substrate interactions.

3.3.5 Inflammatory mediators

The potential inflammation response of the novel nanocomposites was evaluated by quantifying TNF-α macrophages release following incubation of the macrophages with the fiber extracts as well as the 3D PET/HA fiber scaffolds. In both cases the concentration of samples used was 0.2 g/ml. Supernatants were harvested after 24, 48 and 72 h macrophages incubation with samples. The concentration of TNF-α was

measured by the enzyme-linked immunoabsorbent assay (ELISA) assay using a commercial kit as recommended by the manufacturer (Biosource, Nivelles, Belgum). This ELISA assay is mouse specific with detection limits of 5 to 1250 pg/ml. The basic principle of this method lies in the use of antibodies conjugated to an enzyme which, by reacting with its substract, forms a colorless reaction product. The color intensity is measured with the help of a spectrophotometer and is directly proportional to the quantity of the dosed substance. At the end of each cytotoxicity test, culture media were collected and stored at -80°C. The pro-inflammatory cytokine TNF-α was captured on a solid phase (matrix) with the resulting complex shown below (Figure 3.4). Subsequently, this complex was incubated with the peroxide substract and the chromogene. The resultant color changes are directly proportional to the level of TNF-α. The absorbency was read at 450 nm. The concentrations of TNF-α were established by using the standard curve generated by the ELISA assay. The minimum detectable levels were 3 pg/ml. All samples were assayed in triplicate.

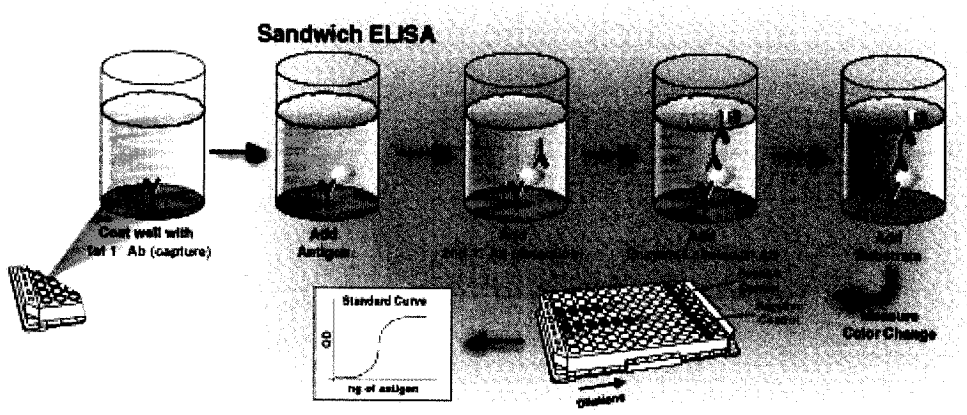

Figure 3.4: Illustration of the ELISA assay principle (Figure adapted from www.chemicon.com).

3.3.6 TNF-α stimulation by fiber extracts

In order to evaluate the potential of the fiber degradative particles to stimulate macrophages, the pro-inflammatory cytokine TNF-α was quantified following incubation of the above detailed extracts with a confluent monolayer of the macrophages (2×10^4 cells/well in 1 ml of DMEM) for 24, 48 and 72 h. Supplemented DMEM was used as a negative control while LPS was used as a positive control. Supernatants were harvested after 24, 48 and 72 h for assaying the levels of TNF-α with sandwich ELISA as recommended by the manufacturer (Biosource, Nivelles, Belgium). All samples were assayed in triplicate.

3.3.7 TNF-α stimulation by 3D fiber matrix

To test the nanocomposite 3D fiber scaffolds potential in macrophages activation, murine Raw 264.7 macrophages were seeded on PET0 and PET10 3D fiber scaffolds at a density of 2×10^5 cells/well in 1 ml of DMEM as shown in Figure 3.5.

Supplemented DMEM was used as a negative control while LPS, was used as a positive control. Supernatants were harvested for assaying the levels of TNF-α with sandwich ELISA as recommended by the manufacturer (Biosource, Nivelles, Belgium).

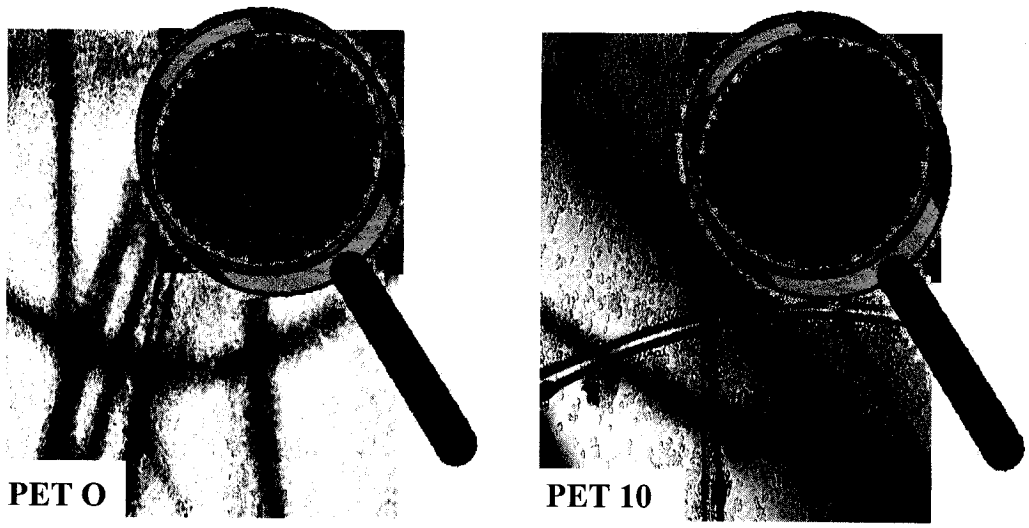

Figure 3.5 Visual representation of Macrophages Raw 264.7 co-culture with PET0 (left) and PET10 (right) fibers scaffolds. Lower Magnification used: 10X, and higher magnification: 40X.

3.4 Surface modification induced by HA and Sterilization of fibers

To verify effects of HA nanoparticle addition in the polymeric fibers on their surface chemistry, the surface chemistry of untreated PET/HA was characterized by XPS and FTIR. As one of the essential preconditions for the practical applications of the novel temperature sensitive implantable material is sterility, the effects induced by EtO and LTP sterilization technologies on the fibers chemical composition and *in vitro* cytotoxicity were compared.

3.4.1 Samples used

The samples used for the following *in vitro* studies are already described in paragraph 3.2.1. For all chemical analysis the samples used were prepared as described in paragraph 3.1.1. Prior to sterilization all samples were cleaned as described in paragraph 3.2.1.

3.4.2 Sterilization

Two widely accepted low temperature sterilization technologies were used: EtO and LTP. The choice of EtO and LTP as sterilization methods was due to their less invasive character leading to common usage to sterilize medical devices in hospitals and medical institutions. However, due to their prevailing general controversy they are also frequently studied in literature as sterilization methods.

Fibers were wrapped in plastic sterilization pouches and sterilized using one of the two different methods: a) EtO in SteriVac® at the Hearth Institute of Montreal or b) LTP in the Physics Department of University of Montreal.

3.4.3 XPS

XPS measurements were conducted on:

- Untreated composite PET fibers charged from 0% to 10% HA, in order to chemically characterize the surface modification of the fibers induced by the progressive HA addition.
- LTP and EtO treated PET fibers charged from 0% to 10% HA, in order to study chemical effects of the sterilization treatments.

The surface analysis technique that was mainly applied throughout this work was XPS. XPS is a quantitative spectroscopic technique that measures the elements within a material. The information obtained can than be used to elucidate the empirical formula, chemical state and electronic state of the elements present in the material. XPS spectra are obtained by irradiating a material with a beam of X-rays while simultaneously measuring the kinetic energy (K) and number of electrons that escape from the top 1 to 10 nm of the material being analyzed. XPS requires ultra-high vacuum (UHV). The analyses performed in this work were carried out on an ESCLAB-3 MKII spectrometer (VG Instruments) equipped with a non-monochromatised Al K_α radiation (h_v = 1486.6 eV). The chemical information contained within the first 10 nm of the fiber surface was elucidated with the use of Advantage software.

XPS tests were performed on EtO, LTP and non-treated samples in order to determine the chemical composition of the composite surfaces.

3.4.4 Sterilization effects on in vitro biocompatibility

The influences of the EtO and LTP treatments on the cytotoxicity of the composite materials were tested. The assays performed under sections 3.3.1 to 3.3.7 were reproduced with EtO and LTP-sterilized samples. The sterilization effects were evaluated in indirect contact as well as in direct contact.

3.5 Mechanical characterization of the fiber nanocomposites

The mechanical properties of the fibers were evaluated in order to estimate the effects of HA addition on the fibers mechanical properties. The fibers mechanical properties were evaluated using tensile tests. In order to calculate the stress during tensile tests, the fiber diameter was measured assuming constant circular fiber cross sections using an Optical Microscope (Leitz Wetzlar Dialux 20). Tensile tests on fibers were achieved with an Instron 5548R using a 5 N cell with small pneumatic clamps. The sample gage length was 50 mm and elongation rate was set to 120 mm/min from ASTM D3822. The load vs. elongation curves were recorded upon fiber stretching until their rupture point. From this curve, the tensile modulus and yield stress were measured. The mechanical characterization overview is presented under Appendix 1, as it was not the main interest of this work.

Chapter 4: Biocompatibility of Novel Polymer-Apatite Nanocomposite fibers

Most studies focus on novel composites entirely synthesized in research laboratories, *i.e.,* in an optimized small scale production. In reality, biomaterials used today for the fabrication of medical devices are commercially available. Novel implantable composite biomaterials thus need to be processed in production scale conditions, from commercially available biomaterials.

The focus of the first part of this work was twofold: evaluate the *in vitro* biocompatibility of the novel PET/HA composite fibers and evaluate the effects of addition of the second phase, HA, on the fibers biocompatibility and stability. The above listed parameters were evaluated trough a multi-end point approach where all tests were paralleled in indirect and direct contact by keeping the same parameters in terms of material weights tested, number of cells seeded, time points evaluated and techniques employed. More specifically the results presented in this chapter reflect the PET/HA fibers chemical stability and degradation under a physiological environment:

- by evaluating the toxic potential of the degradation products upon L929 fibroblast viability;
- by assessing the degradative particles inflammation potential on macrophages Raw 264.7.

The results presented here also reflect the PET/HA 3D fiber scaffolds and their potential to support:

- cellular proliferation, migration and spreading, in direct contact with L929 fibroblast cell line;

- acute inflammatory response, determined by the inflammatory cytokine TNF-α release from Raw 264.7 macrophages in the presence of 3D fiber scaffolds.

The results are presented in the article "Biocompatibility of Novel Polymer-Apatite Nanocomposite fibers" (Article 1), which was accepted and is now in press, for publication at the Journal of Biomedical Research, part A.

Biocompatibility of Novel Polymer-Apatite Nanocomposite fibers, Part 1

Sashka Dimitrievska[a], Alain Petit[b], Abdellah Ajji[c], Martin N. Bureau[c], L'Hocine Yahia[a]

[a] École Polytechnique de Montréal

Laboratoire d'Innovation et d'Analyse de Bioperformance-LIAB-Institut de génie biomédical-École Polytechnique de Montréal , QC H3C3A7 , Canada

[b] Division of Orthopaedic Surgery, McGill University,

Lady Davis Institute for Medical Research, SMBD - Jewish General Hospital,

3755 Chemin de la Côte Ste-Catherine, Montreal, QC H3T 1E2, Canada

[c] Industrial Materials Institute – National Research Council Canada

75 boul de Mortagne, Boucherville, QC J4B 6Y4 , Canada

4.1 ABSTRACT

Based on the bioactivity of hydroxyapatite (HA) and the excellent mechanical and biocompatible performance of polyethylene terephthalate (PET), composite micro-fibers made of nanograde HA with PET was designed and fabricated to mimic the structure of biological bone which exhibits a composite of nanograde apatite crystals and natural polymer. The PET/HA nanocomposite was molded into fibers so that the bulk structures mechanical properties can be custom tailored by changing the final 3D orientation of the fibers. This study focused on the *in vitro* biocompatibility evaluation of the PET/HA composite fibers as potential bone fixation biomaterial for total hip replacement prosthesis surfaces. The MTT assay was performed with the extracts of the composite fibers in order to evaluate the short-term effects of the degradation products. The cell morphology of L929 mouse fibroblast cell line was analyzed after direct contact with the fibers scaffolds for different time periods and the cell viability was also analyzed by the Alamar Blue assay. The release of the inflammatory cytokine, tumor necrosis factor-alpha (TNF-α) from Raw 264.7 macrophages in the presence of fibers extracts and fibers was used as a measure of the inflammatory response. The ability of the fiber matrices to support L929 attachment, spreading and growth *in vitro*, combined with the compatible degradation extracts and low inflammation potential of the fibers and extracts, suggests potential use of these fibers as load-bearing bone fixation biomaterial structures.

4.2 INTRODUCTION

The concept of bioactive particulate reinforced polymer composite as bone analogue was first introduced in the early 1980's by Bonfield *et al.*[39,60,61] with the development of hydroxyapatite (HA) reinforced high density polyethylene (HDPE) composite HAPEX™ used to produce bulk isotropic 3D products. This pioneering work inspired many other bioactive polymer/HA composites, designed in an attempt to match the properties and structure of those of bone for ultimate orthopaedic applications [62-65]. However, these particulate composites do not present mechanical properties, namely the strength and stiffness, of cortical bone, which have limited their applications as load-bearing bone substitutes. Considering the excellent mechanical properties of polyethylene terephthalate (PET)[66] as a matrix and the expected stiffening and strengthening effects of ceramic nano-fillers[67], micro-fibers of PET/HA nanocomposite is a promising biocomposite which can be molded into 3D anisotropic structures with tailored properties by controlling the micro-fiber 3D orientation. A very interesting application of these non-resorbable micro fibers is a composite coating for total hip replacement prosthesis or other load-bearing biomaterials in order to improve their osteointegration.

Due to HA similarity to the main mineral component of hard tissues, as well as its osteoconduction and bone binding properties, successful applications as bone substitutes with excellent bioactivity and biocompatibility have resulted[68]. However, in order to preserve HA attractive properties in a HA/polymer nanocomposites, new variables come into play. Namely, the physico-chemical properties of the composite;

which are highly affected by: a) the chemical interactions between HA particles and matrix and b) the structural organization of the matrix itself. At this purpose, a stress-induced process for the alignment of nanoparticles in PET polymeric suspension under a high shear rate has been used to compound the HA nanocrystals using a twin-screw (TSE) and using this PET/HA compound to produce oriented fibers from polymer/HA by melt spinning. The polymer, PET, has been successful for cardiovascular grafts since the 1950's in critical procedures where high strength and predictable long-term performance is needed[69], mainly due to its chemical structure, which promotes resistance to hydrolysis due to the hydrophobic aromatic groups and its high crystallinity[52]. Paradoxically, the same characteristics that allow PET its long history in vascular related human implantation renders it bio-inert in terms of bone related functions. It is anticipated that by loading oriented PET fibers with increasing amounts of bioactive inorganic HA particles, the nanocomposite fibers could theoretically function as bioactive material due to the known tendency of HA nanocrystals to aggregate. Our second hypothesis concerning the HA loading of the fibers is that they will be able to sustain the physiological loads required from surface bone fixation material for total hip replacement prosthesis. The PET fibers were charged with a maximum of 10 wt% HA proportion, as higher HA fills induced fiber breakage during the manufacturing process. Lastly, the process by which these fibers are apposed to the surface of the total hip prostheses and their resulting mechanical properties are under investigation and will be published elsewhere.

One of the first stage in the development of the PET/HA nanocomposite micro fibers is to evaluate their cytotoxicity. It is desirable that these nanocomposite micro fibers elicit a minimal cytotoxicity response and facilitate cell attachment for their use as a tissue engineering scaffolds. *In vitro* cytotoxicity testing provides a convenient and reliable method to assess the biological response to a biomaterial and also serves as an initial screening process for future *in vivo* studies. The initial step in an *in vitro* biocompatibility study is the evaluation of the *in vitro* cytotoxicity of a biomaterial based of the morphological examination of cell damage and growth when in direct or indirect contact with the materials. Toxicity of the proposed biomaterials involves disturbance of the cellular homeostasis leading to a multiplicity of biochemical changes. High importance is given to cell death, cell proliferation, cell morphology and cell adhesion, all being parameters directly correlated with *in vitro* toxicity [4]. Additionally, the inflammatory response is a significant element of the host response to biomaterials as it also contributes in the phenomenon of aseptic loosening of orthopaedic prosthesis and as such, is used as an assessment of biocompatibility[70]. Macrophages Raw 264.7 were cultured *in vitro* to determine the direct and indirect effect the PET/HA composites on the production and release of tumour necrosis factor (TNF-α). TNF-α was selected based on its well known control over local inflammation, cellular activation, and chemotaxis[71] as well as its established role as a potent stimulator of bone resorption via its inhibitory effect on osteoblasts[72], and its ability to activate osteoclasts[70,73]. Furthermore, the addition of HA reinforcement presents contradictory results as some authors report improved performance of HA reinforced implants[74], while others report

that ceramic coatings may produce particulate wear debris, enhanced the production of cytokines, and induce osteolysis[75,76].

In vitro experiments can be particularly beneficial for polymer/ceramic composites because they can individually test all three phases that occur in the materials life cycle during implantation, namely, unreacted macromers (if any), cross-linked network, and possible degradation products. In the present study, we evaluated the *in vitro* cytotoxicity of these three phases of the novel nanocomposites PET/HA fibers. We hypothesized that PET/HA nanocomposites with 10% HA would demonstrate acceptable biocompatibility *in vitro* and superior surface properties for cell proliferation.

4.3 MATERIALS AND METHODS

4.3.1 PET-HA nanocomposite preparation

The PET used in this study to prepare the fibers was obtained from M&G Polymers (Traytuff 8506) with an intrinsic viscosity of 0.85 (dl/g) The HA particles were obtained from Plasma Biotal (UK, Captal 30). A master batch of PET and HA containing 38 wt% HA was compounded in the form of pellets using a twin screw extruder at 280°C. Scanning electron microscopy (SEM) indicated a good dispersion of HA in the PET matrix.[67] The master batch was then diluted by dry blending prior to feeding in a fiber spinning line to prepare PET fibers with 0, 2, 4, 6, 8 and 10 wt% HA, designated in Table 1. The fiber spinning line consisted in a single screw extruder equipped with a 15 cm linear die with 150 holes of 380 microns each. The fibers were

drawn from the die using a roller positioned at about 2 m from the die exit. The extrusion temperature was 285°C. The final diameter of the fibers was in the range of 25 to 80 microns. X-ray diffraction analysis of the fibers revealed that the PET was essentially amorphous[67]. Optical micrographs observations of the PET0 and PET10 nanocomposite fibers are shown in Figure 4.1.

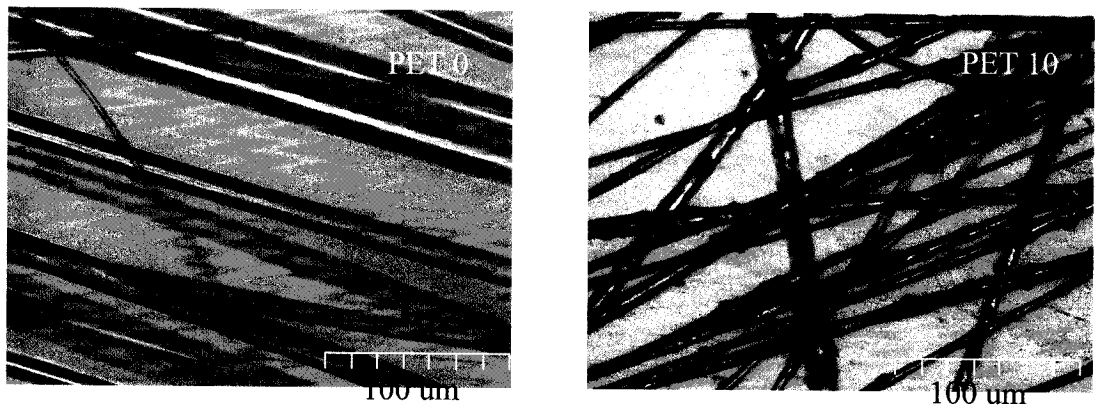

Figure 4.1 : Optical microscope images of PET0 and PET10 fibers

Table 4.1 : Morphological features of fiber nanocomposites

Name	HA Fraction (%)	Fiber Density (g/cm^3)	Fiber Diameter (μm)	Porosity (%)
PET0	0	1.30	52	88.7
PET2	2	1.34	58	89.0
PET4	4	1.37	54	89.3
PET6	6	1.41	53	89.5
PET8	8	1.44	64	89.8
PET10	10	1.48	57	90.0

4.3.2 Ultrasonic cleaning and sterilization of nanocomposite fibers

Equal amount of samples (2 g) of each fiber batches were cleaned by a 2-step ultrasonification procedure involving 99.9% ethanol and 98.9% acetone for 10 min cycles. The samples were then wrapped in plastic sterilization pouches and sterilized using pure ethylene oxide (EtO). EtO sterilization was carried out in SteriVac® (3M), with a 4-h cycle followed by 24 h aeration to remove residual EtO.

4.4 Biocompatibility – Effect of material extracts

4.4.1 Cell culture

Murine L929 fibroblast and Raw 264.7 macrophage cell lines (ATCC, Rockville, MD, USA) were used in this study. Cells were grown at 37°C in a 5% CO_2 humidified atmosphere in Dulbecco's modified Eagle's medium (DMEM; Sigma-Aldrich, Mississauga, ON, Canada), supplemented with 3.7 g/L of sodium bicarbonate, 10% heat-inactivated (56°C for 30 min) fetal bovine serum (FBS), 100 units/ml penicillin, and 100 µg/ml streptomycin (Gibco Laboratories, Burlington, ON, Canada).

4.4.2 Preparation of the extracts

Extracts were prepared from the material samples in agreement with the ISO specification (10993-5) governing *in vitro* tests [77]. Each polymer nanocomposite was immersed in serum free DMEM at a ratio of 0.2 g/ml and incubated for 24 h at 37°C under constant agitation (250 rpm). After this period, the medium was harvested and

kept at –90°C until used. The extracts were used undiluted and supplemented with 10% FBS.

4.4.3 Cytotoxicity of fiber extracts

The cytotoxicity of fiber extracts was evaluated against L929 fibroblasts using the methyl tetrazolium (MTT) assay in 96-well plates as described by the manufacturer (Sigma-Aldrich). The MTT assay is based on the ability of living cells to convert a water-soluble yellow dye, 3-(4,5-dimethylthiazole-2-yl)-2,5-diphenyl tetrazolium bromide (MTT) into purple formazan crystals. Briefly, L929 cultured cells were seeded in 96-well plate (2.5×10^5 cells/ml, 200 µl/well) and allowed to adhere for 24 h at 37°C in a 5% CO_2 humidified atmosphere. The culture medium was replaced by the previously prepared extracts, and the plates were further incubated for 24, 48 and 72 h. Control samples consisted of L929 cells grown on tissue culture plastic supplemented with complete DMEM, but not in contact with fiber extracts, as previously described for the study of glass-ceramics[22] and nano-sized HA[24]. After the incubation periods, the extracts were removed and each well was treated with the MTT solution for 4 h at 37°C. Liquid was then removed, solubilisation solution added, and microplate was shaken for 15 min before reading at 550 nm on a microplate reader. Cytotoxicity was calculated as the percentage of negative control cell viability. Results are the mean ± standard deviation of three (3) experiments performed in triplicate.

4.4.4 TNF-α release

Murine Raw 264.7 macrophages were seeded in 24-well culture plates at a density of 2 x 10^4 cells/well in 1 ml of DMEM supplemented with 10% heat-inactivated FBS, 100 units/ml penicillin, and 100 µg/ml streptomycin. After overnight equilibration, the medium was replaced by the polymer nanocomposite fiber extracts. Supplemented DMEM was used as a negative control while 10µg/ml of lipopolysaccharide (LPS, *E. coli*; Sigma-Aldrich) was used as a positive control. Supernatants were harvested for assaying the levels of TNF-α with sandwich ELISA as prescribed by the manufacturer (Biosource, Nivelles, Belgium). The optical density was then determined using a microplate reader set to 450 nm and corrected at 570 nm. The minimum detectable levels were 3 pg/ml. Results are the mean ± standard deviation of three (3) experiments performed in triplicate. Numerical data were analyzed statistically using Student t tests. Statistical significance was considered at $p < 0.05$.

4.5 Biocompatibility – Direct contact assay

4.5.1 Fiber scaffold preparation

Specimen of non-woven fiber scaffolds for direct contact assay tests were prepared by compression molding using a laboratory Carver press. The scaffolds were heated between the press platens at a temperature of 85°C under a pressure of 1 metric ton applied for 1 min and then under 2 metric tons for 2 min. Heating was then stopped to allow specimens to cool down until room temperature is reached. The fiber scaffolds

had a high porosity of approximately 90% to mimic the porosity of spongy (trabecular) bone. Details of the scaffolds morphology are given in Table 1.

4.5.2 Cells and matrix seeding

To test the long-term biocompatibility of the polymer nanocomposite fibers, the fibers were placed in 24-well plates and sterilized by EtO. After the five days aeration time, the fiber scaffolds were promptly soaked in phosphate buffered saline (PBS) and then soaked overnight in DMEM supplemented with 10% heat-inactivated fetal bovine serum (FBS), 100 units/ml penicillin, and 100 μg/ml streptomycin prior to L929 fibroblast seeding (1×10^4 cells/cm^2). This procedure facilitates protein absorption and cell attachment onto the fibers. L929 fibroblasts cultured on the regular polystyrene surface (TCP, tissue culture plate) were used as control. Cells were maintained in culture for up to 14 days. Medium was changed every 3 days.

4.5.3 Cell morphology

Cell morphology, spreading, orientation, and growth on the surfaces of the fiber scaffolds were evaluated using the common qualitative technique, Field Emission Gun Scanning Electron Microscope (FEG-SEM) on a Hitachi S-4700 apparatus (Hitachi High-Technologies Canada, Rexdale, Ontario). Harvested L929 fibroblasts were washed twice with PBS and fixed with 1% glutaraldehyde, first for 1 h at room temperature, then overnight at 4°C. The samples were rinsed with PBS for 30 min and then dehydrated through a series of graded alcohol solutions. The specimens were air-dried overnight and

the dry cellular constructs were finally sputter-coated with palladium and observed under the FEG-SEM at an accelerating voltage of 2.0 kV.

4.5.4 Cell proliferation

Cell proliferation was monitored using the Alamar Blue™ assay as specified by the manufacturer (Biosource, Nivelles, Belgium). The assay is based on a fluorometric/colorometric growth indicator that detects metabolic activity. Specifically, the system incorporates an oxidation-reduction (REDOX) indicator that both fluoresces and changes color in response to chemical reduction of growth medium resulting from cell growth[78]. The directly plated fibroblasts were incubated at 37°C in a humidified atmosphere of 5% CO_2 and 95% air. At selected time points of 1, 3, 7 and 14 days, medium was removed and 1 ml aliquots of Alamar Blue (diluted 1:10 in phenol red-free medium) were added to each well and incubated for a further 4 hr at 37°C, 5% CO_2. Wells without cells were used as the blank control and L929 cells grown on tissue culture plastic (TCP) supplemented with complete DMEM were used as a negative control as reported elsewhere [79]. Following the incubation 3 x 100 aliquots from each well were taken and transferred to a 96-well plate for reading. Absorbance was measured on an ELISA microplate reader at 570 nm and 600 nm. The intensity of red color (570 nm) is proportional to the percent reduced of Alamar Blue that can than be related to the metabolic activity of the cell population through the following:

$$\%\ \text{metabolic activity} = \frac{\varepsilon_{ox}(\lambda_2)\cdot A(\lambda_1) - \varepsilon_{ox}(\lambda_1)\cdot A(\lambda_2)}{\varepsilon_{red}(\lambda_1)\cdot A'(\lambda_2) - \varepsilon_{red}(\lambda_2)\cdot A'(\lambda_1)}\cdot 100 \qquad (1)$$

where ε_{ox} is the molar extinction coefficient of Alamar Blue oxidized form (BLUE), ε_{red} is the molar extinction coefficient of Alamar Blue reduced form (RED), A is the absorbance of test wells, A' is the absorbance of negative control well, λ_1 is given by 570 nm and λ_2 by 600 nm. Results are the mean ± standard deviation of three (3) experiments performed in triplicate. Numerical data were analyzed statistically using Student t tests. Statistical significance was considered at $p < 0.05$.

4.5.5 TNF-α release

To test the polymer nanocomposite fibers potential in macrophages activation, murine RAW 264.7 macrophages were seeded on PET0 and PET10 fiber scaffolds at a density of 2×10^5 cells/well in 1 ml of DMEM supplemented with 10% heat-inactivated fetal bovine serum (FBS), 100 units/ml penicillin, and 100 μg/ml streptomycin. Supplemented DMEM was used as a negative control while 10 μg/ml of lipopolysaccharide (LPS, *E. coli*; Sigma-Aldrich) was used as a positive control. Supernatants were harvested for assaying the levels of TNF-α with sandwich ELISA as prescribed by the manufacturer (Biosource, Nivelles, Belgium). The optical density was then determined using a microplate reader set to 450 nm and corrected at 570 nm. The minimum detectable levels were 3 pg/ml. Results are the mean ± standard deviation of three (3) experiments performed in triplicate. Numerical data were analyzed statistically using Student t tests. Statistical significance was considered at $p < 0.05$.

4.6 RESULTS

4.6.1 Biocompatibility – Effect of material extracts

4.6.1.1 Cytotoxicity

Figure 4.2 shows the short-term effects of the extractable products on L929 fibroblasts. Cytotoxicity was calculated as the percentage of cell viability over control values. Results clearly show that, at 24 h, the extracts have no significant effect on the cell viability, as it remains roughly constant around 100% for all nanocomposite fibers. At 48 and 72 h, the cellular viability also remains around 100% for all fiber composition. No statistical differences can be observed with respect to incubation time.

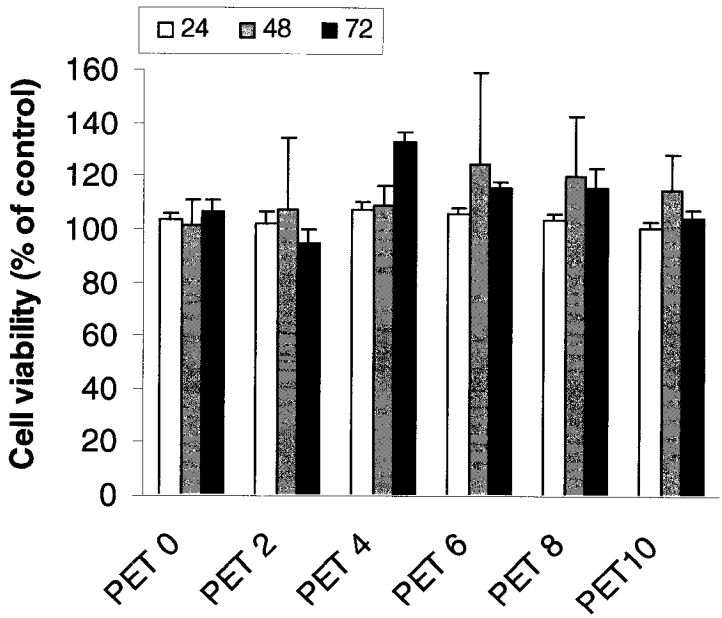

Figure 4.2: Effect of PET/HA fiber extracts on the viability of L929 fibroblast cells as determined by the MTT assay. L929 cells were incubated in the presence of undiluted fiber extracts (0.2 g/ml) and the fibroblast viability was determined by the MTT assay at 24, 48 and 72 h. L929 cells grown on tissue culture plastic (TCP) supplemented with complete DMEM was used as the negative control. Results are expressed as % of negative control and are the mean ± standard deviation of 3 different experiments.

4.6.1.2 TNF-α release from extracts

The effects of the material extracts on TNF-α release by Raw 264.7 macrophages are shown in Figure 4.3. Significant variations according to the percentage of HA and the time of culture were seen. However, an unequivocal dose-response as a function of HA in the materials could not be established. All nanocomposite fibers had no effect on TNF-α release (compared to control) after 1 h in presence of materials extracts. However, the extract from the polymer without HA (PET0) significantly stimulated 10 and 2 times (compared to negative control) respectively the release of TNF-α after 24 h (279 pg/ml vs. 27 pg/ml) and 48 h (270 pg/ml vs. 107 pg/ml). The presence of HA in the polymer (PET2 to PET10) had few additional effect on TNF-α release after 24 h. At 48 h, the release of TNF-α (compared to negative control) was significantly increased in presence of 8% HA (642 pg/ml) and decreased with 4% HA (221 pg/ml) and 6% HA (149 pg/ml). PET10, the fibers with the highest amount of HA, stimulated 12 and 2 times (with respect to negative control) the release of TNF-α after 24 h (326 pg/ml) and 48 h (288 pg/ml), representing 25% of the positive control LPS at both 24 and 48 h. As a control, LPS stimulated TNF-α release (with respect to control) by 23 times (160 pg/ml), 55 times (1450 ml), and 13 times (1380 ml) after 1 h, 24 h and 48 h respectively.

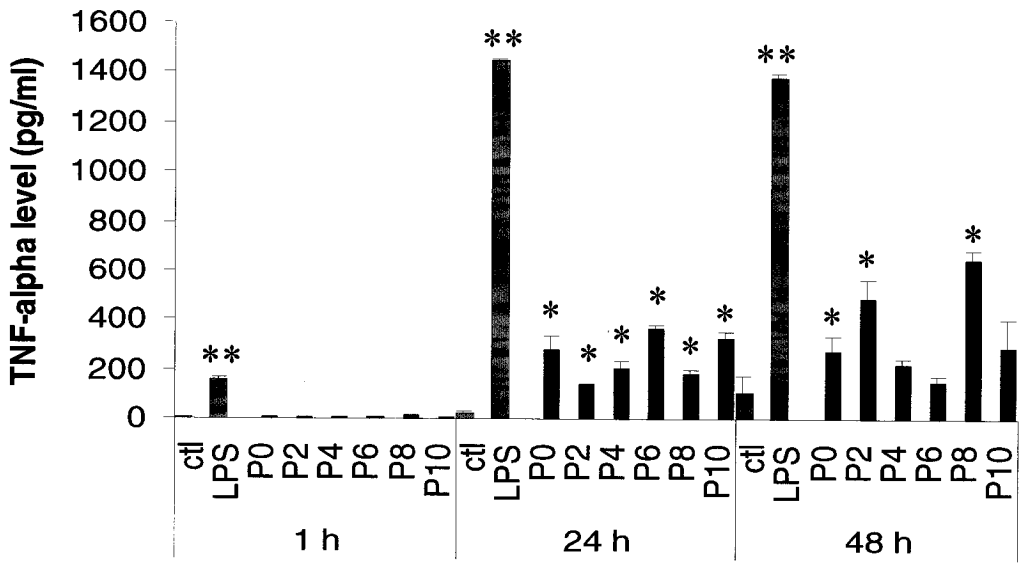

Figure 4.3 : Effect of fiber extracts on TNF-α release Raw 264.7 macrophages were incubated for 1 to 48 h with undiluted extracts (0.2 g/ml) of PET0 to PET10 fibers. Supplemented DMEM was used as a negative control while 10 µg/ml of lipopolysaccharide (LPS) was used as a positive control. Results are the mean ± standard deviation of 3 experiments.

4.7 Biocompatibility – Direct contact assay

4.7.1 Cell proliferation

Figure 4.4a) shows the proliferation of L929 fibroblasts on PET0 to PET10 fiber scaffolds after 3 days in culture, as determined by Alamar Blue. The pure polymer fiber (PET0) reduced the metabolic activity of L929 fibroblasts by 35%. The presence of HA increased this metabolic activity in a dose-dependant manner with maximal level reached with 10% HA (91% of control). Proliferation of L929 fibroblasts was then assayed for 1 day up to 14 days on all composite fibers, but only PET0 and PET10 are shown in Figure 4.4b. Significant differences were observed between PET0 and PET10

after 1 and 3 days in culture. This difference disappeared after 7 days with metabolic activities reaching 93% and 99% of control for PET0 and PET10, respectively.

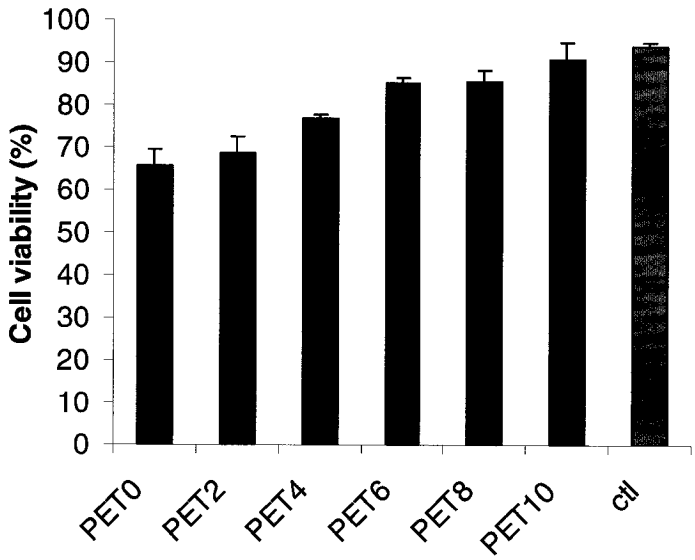

Figure 4a

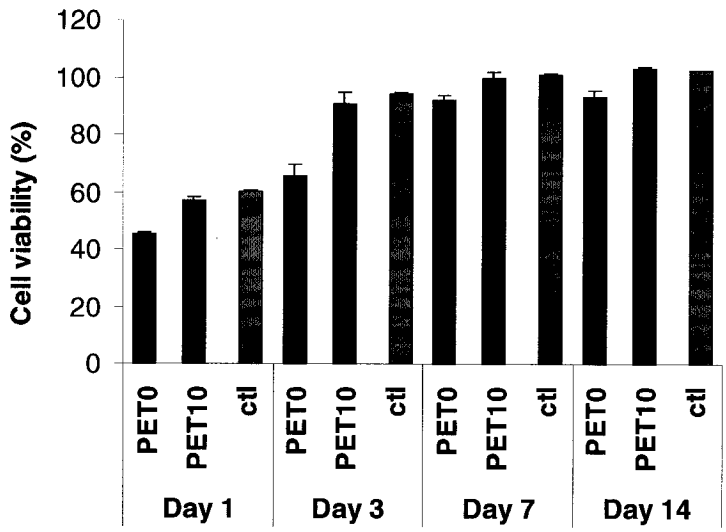

Figure 4b

Figure 4.4 : Effect of HA nanoparticle dosage in the PET fibers on the proliferation of L929 fibroblast cells. (a) L929 fibroblasts were seeded on PET0 to PET10 fiber scaffolds and their viability was assessed after 3 days by the Alamar Blue assay. Negative control samples consisted of L929 cells grown on tissue culture plastic (TCP) supplemented with complete DMEM. Results are expressed as % reduced of Alamar Blue and are the mean ± standard deviation of 3 different experiments. (b) L929 fibroblasts were seeded on PET0 and PET10 fiber scaffolds and their viability was assessed after 1, 3, 7 and 14 days by the Alamar Blue assay. Negative control samples consisted of L929 cells grown on tissue culture plastic (TCP) supplemented with complete DMEM. Results are expressed as % reduced of Alamar Blue and are the mean ± standard deviation of 3 different experiments.

4.7.2 Cell adhesion

The interactions between L929 fibroblasts and nanocomposite fibers were studied *in vitro* by FEG-SEM up to 14 days in culture (Figure 4.5). Although all fibers supported healthy attachment and spreading of L929 fibroblasts, the cell-fiber scaffold interactions varied for different fiber composition. At day 14, PET10 demonstrated a denser and greater cell sheet after 14days than the PET0 fibers indicating the differences in cell proliferation.

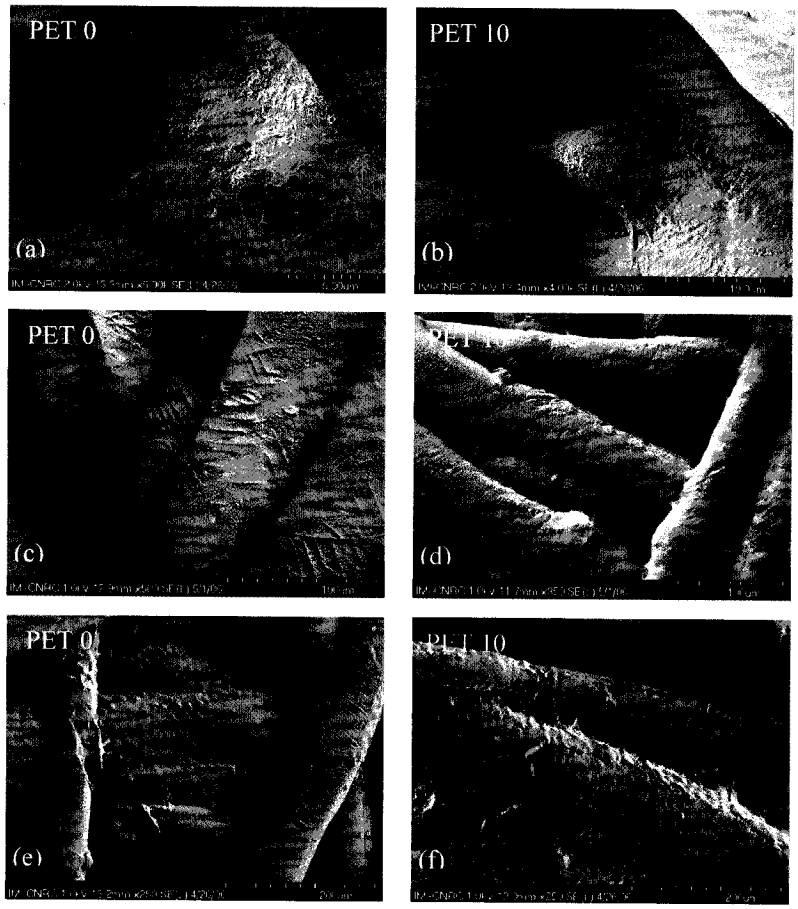

Figure 4.5: FEG-SEM images of L929 fibroblasts cells seeded on fiber scaffolds. L929 fibroblasts were cultured for 1 day on (a) PET0 and (b) PET10, for 7 days on (c) PET0 and (d) PET10, and for 14 days on (e) PET0 and (f) PET10.

4.7.3 TNF-α release after direct contact with fiber scaffolds

The effects of the nanocomposite fibers on TNF-α release by Raw 264.7 macrophages are shown in Figure 4.6. The trends are comparable to the previously discussed for the stimulation of TNF-α by the fiber extract. Indeed, macrophages plated on fiber scaffolds had no effect on TNF-α release after 1 h. However, PET0 stimulated 9times the release of TNF-α after 24 h (296 pg/ml) and 48 h (226 pg/ml), respectively.

As opposed to PET0, PET10, the main focus of this study, significantly decreased the TNF-α release down to 0.8 and 1.5 times after 24 h (25 pg/ml) and 48 h (41 pg/ml), representing a fraction of the positive control LPS. As a control, LPS stimulated TNF-α release by 3 times (26 pg/ml), 18 times (566 pg/ml), and 23 times (588 pg/ml) after 1 h, 24 h, and 48 h respectively.

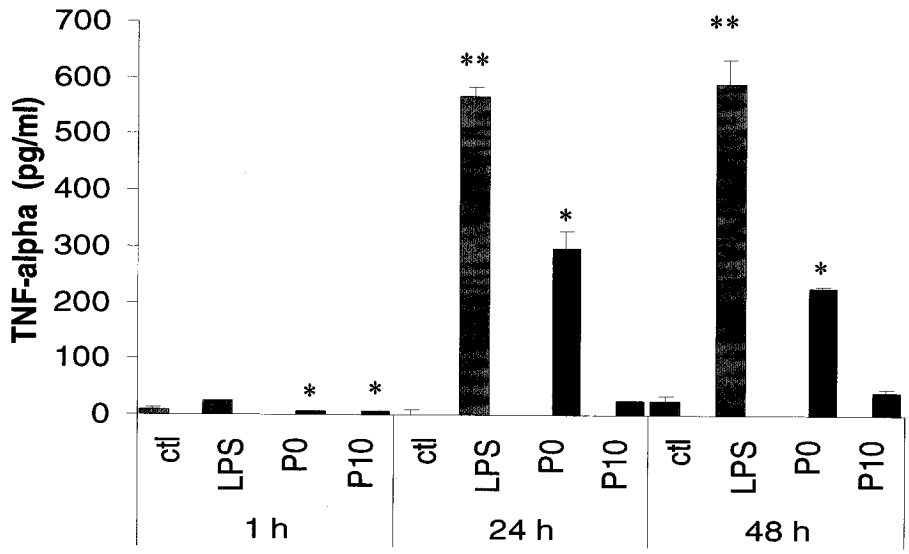

Figure 4.6: Effect of fiber scaffolds on TNF-α release Raw 264.7 macrophages were seeded on PET0 and PET10 fiber scaffolds for 1 to 48 h. Supplemented DMEM was used as a negative control while 10μg/ml of lipopolysaccharide (LPS) was used as a positive control. Results are the mean ± standard deviation of 3 experiments.

4.8 DISCUSSION

Polymer composites are increasingly evaluated for biomedical applications in hopes to marry the positive effects of the materials and overcome their independent shortcomings. In the present study, the effect of HA reinforcement on the PET micro

fibers was investigated on L929 fibroblasts viability and proliferation, as well as RAW 264.7 macrophages activation were investigated. Although PET/HA micro fibers are being developed for orthopaedic applications, both the indirect and direct contact assays were carried out with L929 fibroblasts due to their high sensitivity [57]. Also the choice of L929 fibroblasts was due to their model properties that can reliably determine the general biocompatibility of novel material and screen them for future *in vitro* and *in vivo* experiments[58]. The effect of polymer composite fibers and their extracts on Raw 264.7 macrophages were also studied because macrophages are the principal cells found in the pseudo-membranous tissue formed around hip implants at revision surgery[59]. This study is the first one looking at the biocompatibility of the novel fiber composites.

The effect of extractable products of polymers on their biological environment is important in determining the biocompatibility of promising biomaterials. In this work, the well-known MTT assay was used to quantify the short-term effects of the extractable products on the viability of L929 fibroblasts. Results showed that the extracts from the polymer fibers without HA and the polymer fibers reinforced with HA had no effect on the cell viability, which suggests the biocompatibility of the extracts. However, it is not impossible that the conditions of the present study (250 rpm agitation for 24 h at 37°C) may be insufficient to generate the same levels of extractables or leachables products than in an *in vivo* environment with mechanical constraint. For example, as a potential composite coating material for total hip replacement prosthesis, the effect of wear debris on cell viability and activity should be determined in the future. The size, shape and exact composition of these putative particles are not yet known. It should not be

forgotten that the polymer fibers reinforced with 10% HA, the main focus of this study as they will potentially have the highest bioactivity, presented a minimal cellular viability of 105% at the three different time points (24, 48 and 72 h), which amply demonstrates an acceptable biocompatibility of the extracts under the conditions used in the present study.

As the ultimate application of the fibers used in the present study would be a bone fixation material for total hip replacement prosthesis surfaces, the inflammatory responses due to extractable products was also quantified by looking at the release of TNF-α by Raw 264.7 macrophages. The present experiments demonstrated that macrophages cultured with PET/HA composite fibers extracts released more TNF-α than control cells. The variations in TNF-α release following incubation with the material extracts cannot be qualified as a dose-response to the initial percentage of HA present in the materials. This could be due to the fiber composite nature (polymeric/ceramic) that may release degradation products such as undesired additives (processing aids) or impurities or/and the surface exposed HA. The extracts chemical nature is under further chemical characterization and will be published elsewhere. Furthermore, to the authors' knowledge, no studies examining the TNF-α levels released following *in vitro* incubation of cells and HA composites materials extracts have been reported. However, the stimulation of TNF-α is comparable to other materials of orthopaedic interest, such as ceramic particles [80] and with metal ions [81]. Additionally, the stimulation is less important than observed with ultra-high-molecular-weight polyethylene particles[81], also of orthopaedic interest. The effect of PET/HA fiber

leachables on TNF-α release is also very low compared to positive LPS control cultured macrophages. Taken together, these results suggest that extracts from PET/HA fibers had comparable inflammatory responses to different materials of orthopedic interest. This is supported by optical microscopic analyses of Raw 264.7 macrophages in contact with PET fiber extracts that remained round without the formation of foreign body giant cell (results not shown).

The inflammatory responses due to the initial interactions between PET0 and PET10 scaffolds and Raw 264.7 macrophages were also quantified by looking at the release of TNF-α. The interaction between macrophages and HA charged orthopedic implants is an important parameter since macrophages can produce a variety of inflammatory factors, such as cytokines and prostaglandins, that are known to stimulate inflammation and osteoclastic bone resorption.[82] Several factors modulate the activation of macrophages and mediate the production of cytokines. Among these factors, surface physical and chemical properties and adhesion specific signals are believed to have important roles.[76] Concerning HA reinforced composites, contradictory results in terms of cytokines production are presented in literature. Ninomiya *et al.*[83] reported that HA enhanced the production of TNF-α by human fibroblasts *in vitro*. Marques *et al.*[76] on the other hand found that the addition of HA resulted in a significant reduction of those inflammatory cytokines, by monocytes and lymphocytes *in vitro*. Furthermore, Huang *et al.*[84] found no correlation between the TNF-α release and the concentration of HA added to *in vitro* macrophage culture. In the present study, the presence of HA in the fiber scaffolds significantly decreased the TNF-α release as compared to the pure PET fibers

scaffolds. Finally, the release of TNF-α in PET10 fibers and macrophages co-culture was not significantly greater than the negative control, indicating that PET10 fibers may not trigger a severe inflammatory response.

The indirect cytotoxicity contact tests were complemented with direct contact tests. This allows evaluating the cell-material contact arrangements dictated by material surface features and properties, which may lead to differences in cytotoxicity. The direct contact proliferation assay showed that L929 fibroblasts remained viable for at least 14days on PET/HA fibers. It also showed that the metabolic activity, associated with cell number, increased proportionally with the amount of HA in the composite fibers, up to 7days. This trend in the increased cell viability relatively to the HA amount may be explained by the followings: a) the increased surface roughness of the composite fibers with higher HA concentrations, as the HA nanocrystals tend to aggregate on the surface of the fibers (Figure 4.1), b) the chemical exposure of the HA nanocrystals aggregates, or 3) both possibilities. Although a conclusive mechanism of cell adhesion is not yet established, the shape and surface texture of an implant are important factors determining the cell-material contact and influencing cell proliferation[4]. Other studies have also reported that cell adhesion and proliferation of different types of cells onto various surfaces depend on the material surface characteristics like surface charge, wettability and most importantly topography. More specifically, it has been reported that there is a favoured cell attachment on roughened surfaces[4].

However, increased fibroblast proliferation proportional to the HA dosage was not observed after 7 days in culture, as at day 7 cellular viability on PET0 and PET10

fibers approximately level off, suggesting that the number of fibroblasts is similar on both scaffolds. However, the direct contact Alamar Blue results beyond day 7 cannot be extrapolated to *in vivo* conditions; they for example contradict the SEM analysis, which demonstrates a more important proliferation of L929 fibroblasts on PET10 than on PET0 fibers, especially beyond day 7. These contradicting results can be explained by the fact that as cells grow in culture, their metabolic activity maintains a reductive environment in the surrounding culture medium, while growth inhibition produces an oxidative environment[85]. In this test, metabolic activity (reduction) causes color change of the Alamar Blue indicator from nonfluoresent (blue) to fluorescent (red). As cell growth is inhibited by the physical constraints of the tissue culture well beyond day 7 on the PET10 fibers, the surrounding culture medium starts being oxidized as well as reduced leading to an underestimation of the cell metabolic activity and the cell number by the Alamar Blue assay. It should not be forgotten that the direct contact assay performed in this work demonstrated that the three-dimensional form of the PET10 composite fibers did not present any toxicity, reduced cell adhesion, or delayed proliferation rate and therefore can be considered as a potential biomaterial.

It is well known that the initial interaction between biomaterials and cells is mediated by a previously absorbed layer of proteins resulting from cell culture medium *in vitro*[86]. In the present study, a new variable factor is introduced in the outer layer of the PET composite fibers formed of HA nano- and micro-crystals (aggregated nanocrystals). In this context, based on the surface modifications induced by the addition of the HA nanocrystals, it seems that proteins are differently absorbed on the composites

and consequently the cells interactions with the different composites modified. This fact may not only affect the pattern of adhesion of fibroblasts cells to the material, but also the reorganization in their cytoskeleton[87]. In this regard, the hypothesis of the present *in vitro* study was that the novel composites fibers, PET10, would be highly biocompatible in that it will be a suitable substrate for adhesion and cell–matrix interactions to support cell growth and differentiation, and organization of cells to form a specific tissue [88]. This hypothesis is further supported by the SEM results, which revealed that at day 1 the fibroblasts seeded on PET10 fibers have a more spread and flattened morphology than those seeded on PET0 fibers, indicating a stronger cellular adhesion. By the end of the second week, the degree of colonization of the PET10 fibers appeared higher and denser as compared to PET0. This is coherent with studies demonstrating that small modifications in the composition and texture of the surfaces of materials can have an impact on the subsequent host-implant interactions. Although more conclusive studies are needed to characterize the extracellular-like matrix formed, the results suggest that the novel composites fibers would be able to support three-dimensional proliferation as they sustain adhesion, growth, healthy cell morphology, and migration upon fibroblast culturing. However, further studies with cell lines that have the potential to differentiate into the osteoblast phenotype are necessary in order to evaluate PET10 composite fibers potential as bioactive scaffolds.

4.9 CONCLUSION

The effects of HA nanocrystals dosage in PET polymer based fibers were investigated on L929 fibroblasts and RAW 264.7 macrophages. The results of cell behavior on the nanocomposite fibers showed that throughout the time points, L929 fibroblasts proliferated well as monolayer cultures, which is expected to have a final outcome on the support of new tissue formation at the interface. It was also possible to demonstrate that the 3D structures with high HA content PET fibers have low inflammation effect on Raw 264.7 macrophages. Overall, these results strongly support the biocompatibility of the PET10 nanocomposite fibers.

4.10 ACKNOWLEDGMENTS

The authors gratefully acknowledge Natural Sciences and Engineering Research Council of Canada (NSERC) for their financial support and Dr. Yahye Merhi of the Montreal Heart Institute and Laura Epure of École Polytechnique of Montréal for their time and help.

4.11 REFERENCES

See general references in the Bibliography section.

Chapter 5: Surface chemical characterization of novel nanocomposite fibers and Sterilization effect on *in vitro* biocompatibility

The studies fulfilled in this Chapter were conducted in order to better understand the previously seen cellular variations with respect to HA present in the PET/HA fibers (Chapter 4). In addition, since the development of new biomedical devices should include from the outset a concept for sterilization the two most commonly used low temperature sterilization techniques (EtO and LTP) were evaluated taking into consideration the functional aspects of the novel composites.

In order to evaluate the above described parameters the following studies were undertaken:

- Untreated fibers with HA additions from 0 to 10 percent were chemically analyzed in order to elucidate the chemical modifications induced by the HA additions. The well know XPS technique was employed as it is surface sensitive and allows a detailed qualification and quantification of the surface chemistry of a biomaterial. This parameter was central as the fibers surface chemistry (in the nanometer range) describes the fibers-*in vitro* environment interface, and consequently the *in vitro* variations seen in Chapter 4.

After elucidating the surface modifications induced on the PET/HA fibers by the progressive HA addition, the fiber scaffolds were sterilized by the two most commonly used low temperature sterilization techniques: LTP and EtO.

- For the practical applications of the PET/HA fibers as novel implantable material, the sterilization induced modifications were evaluated by XPS in the same fashion as the untreated PET/HA fibers surface chemistry. Hence the previously chemically characterized untreated fibers were used as negative controls.
- The *in vitro* biocompatibility of the fibers and fibers scaffolds following the LTP and EtO treatments was evaluated in order to determine sterilization method effect of on the PET/HA fibers established biocompatibility as it remains an important aspect for novel implantable materials.

The results are presented in the article "Sterilization Effects on Bioactive Polymer-Apatite Nanocomposite Fibers" which was submitted at Biomaterials.

Sterilization Effects on Bioactive Polymer-Apatite Nanocomposite Fibers

S. Dimitrievska[a], M. N. Bureau[b,*], A. Ajji[b], A. Petit[c],

L. Epure[a], D.Q. Yang[a], L'H. Yahia[a]

[a] Laboratoire d'Innovation et d'Analyse de Bioperformance (LIAB)

Institut de génie biomédical, École Polytechnique de Montréal

Montreal, QC H3C3A7, Canada

[b] Industrial Materials Institute – National Research Council Canada

75, de Mortagne, Boucherville, QC J4B 6Y4, Canada

[c] Division of Orthopaedic Surgery, McGill University,

Lady Davis Institute for Medical Research, SMBD - Jewish General Hospital,

3755 Chemin de la Côte Ste-Catherine, Montreal, QC H3T 1E2, Canada

---

* To whom correspondence should be addressed; martin.bureau@cnrc-nrc.gc.ca, 450-641-5105

5.1 ABSTRACT

Nanocomposite in the form of fibers, compounded from synthetic hydroxyapatite (HA) nanoparticles and polyethylene terephthalate (PET) is a new biomaterial made to simulate bone for ultimate applications in load bearing bone replacements. The sterilization of those materials with the use of accepted protocols and minimal effects on their established biocompatibility is a crucial requirement for their biomedical application. This work compares the effects induced by ethylene oxide (EtO) and low temperature plasma (LTP) sterilization technologies on the composite surface chemistry and *in vitro* cytotoxicity. The chemical composition of the PET/HA fiber surface was carried out by X-ray photoelectron spectroscopy (XPS) analysis before and after LTP and EtO sterilization. The addition of the second phase, HA, in PET significantly oxidized the fiber surface, leading to an improved biological response at higher HA additions. LTP sterilization led to a modified C-O/C=O ratio, thus to a better biologic response, while EtO sterilization induced slight alkylation of PET. The *in vitro* cytotoxicity to L929 fibroblasts was evaluated after the LTP and EtO treatments. It was seen that, despite the surface modifications produced, the cell viability remained similar on both LTP- and EtO-treated fibers scaffolds. Following macrophage incubation with the nanocomposite scaffolds, a trend of higher TNF-α release by the EtO-treated scaffolds, as compared to the LTP-sterilized ones, was observed, indicating a higher inflammatory potential present by the EtO-sterilized fibers. The influences of the different sterilization techniques on the cytotoxicity of the composite materials, as well as the clinical relevance of the described differences are discussed.

5.2 INTRODUCTION

The substantial recent advancements in orthopedic surgery are partially attributed to the continuous innovation of novel implantable bioactive materials. In our last study, we introduced a nanocomposite in the form of fibers compounded from synthetic hydroxyapatite (HA) nanoparticles and polyethylene terephthalate (PET) polymer, fabricated to mimic the structure of biological bone[89]. Our laboratory has been investigating the biocompatibility of the novel PET/HA nanocomposite fibers, as potential orthopedic/dental biomaterials. As one of the essential preconditions for the practical applications of the novel implantable material is sterility, its development should include from the outset a concept for sterilization taking into consideration both microbiological and functional aspects[90]. Yet, many studies pioneering in biocompatibility evaluation of novel implantable materials do not specify the sterilization method used if any[87,91,92]. Others use the immersion in aqueous alcohol solutions[93,94] in spite of the fact that ethanol is not a sterilizing agent but a good disinfectant[95]. This general trend of excluding the sterilization in the development of novel implantable composite materials may be due to the physico-chemical properties of polymeric materials sensitive to sterilization methods[96]. In this study, we focused on the current widely accepted low temperature sterilization technologies: ethylene oxide (EtO) and low temperature plasma (LTP), due their less invasive character and prevailing general controversy.

EtO is the most commonly used among low temperature sterilization techniques due to its valuable advantages, such as adequate effectiveness at low temperature, high

penetration, and compatibility with a wide range of materials[95]. Nonetheless, it is flammable and explosive, produces toxic residues and can react with polymeric functional groups[95], increasing the risk of material toxicity, not to mention health hazards they poses. These residual EtO toxic effects on humans have been extensively documented allowing the American National Standard ANSI/AAMI ST27-1998[97] to establish strict regulations concerning EtO sterilization (*e.g.*, < 25 ppm for implantable devices). Despite this precaution, levels of EtO residues above the FDA/AAMI standards have been detected in materials sterilized by EtO[98].

To compensate for EtO shortcomings, the gas plasma sterilization technology was introduced in 1992 as a low-temperature sterilization alternative that poses fewer health and environmental risks with faster turnaround times[99]. However, relatively little is known about the influence of plasma-based sterilization on the physico-chemical and mechanical properties of polymeric biomaterials and whether this affects the biocompatibility of polymeric devices[100]. The handful of scientists that have examined LTP effects on polymeric materials can be quickly summarized: following LTP sterilization, Tabrizan *et al.* have shown surface oxidation in different types of polymers tested[101]; Bathina *et al.* have discovered mechanical damage at an insulation-electrode interface tested [102], and Lerouge *et al.* detected oxidation at the near surface layer of polyurethane as well as oligomer alteration[98]. Additionally when the latter study compared plasma-sterilized, EtO-sterilized and non-sterilized samples, they discovered an increase of released oligomers following LTP sterilization when polyurethane was incubated in physiological serum.

As PET/HA nanocomposite fibers will ultimately represent an interface to surrounding tissues, the influence of the sterilization technique on their *in vivo* performance becomes a very important parameter. Since it is difficult to examine the *in vivo* reactions of a specific cell type to the implant, because of the variety of cell populations and biofactors present at the implantation site, *in vitro* models are used[103]. *In vitro* cytotoxicity testing provides a convenient and reliable method to assess the biological response to a biomaterial and also serves as an initial screening process for future *in vivo* studies. Although the materials are being developed for orthopedic applications, both indirect and direct contact assays were carried out with L929 fibroblasts due to their high sensitivity[57]. Also the choice of L929 fibroblasts was due to their model properties that can reliably determine the general biocompatibility of novel material and screen them for future *in vitro* and *in vivo* experiments[58]. The effect of polymer nanocomposite fibers and their extracts on RAW 264.7 macrophages were also studied because macrophages are the principal cells found in the pseudo-membranous tissue formed around hip implants at revision surgery[59]. As the influence of the appropriate sterilization method has been stated to be of primary importance in the development of the novel biomaterials[90], we undertook this study to evaluate the effects on the cytocompatibility of PET/HA fibers following LTP and EtO sterilization treatments.

5.3 MATERIALS AND METHODS

5.3.1 Materials

The masterbatch of PET and HA containing 38 wt% HA was compounded in the form of pellets using a twin screw extruder at 280°C. The masterbatch was then diluted in a fiber spinning line to prepare PET fibers with 2, 4, 6, 8 and 10 wt% HA (respectfully designated as PET0, PET2, PET4, PET6, PET8 and PET10) The fiber spinning line consisted in a single screw extruder equipped with a 15 cm linear die with 150 holes of 380 microns each. The fibers were drawn from the die using a roller positioned at about 2 m from the die exit. The extrusion temperature was 285°C and the fibers final diameter was in the range of 25 to 80 microns. X-ray diffraction analysis revealed that the PET in the fibers was essentially amorphous.

5.3.2 Fiber matrix preparation

Specimen of non-woven fiber scaffolds for direct contact assay tests were prepared by compression molding using a Carver laboratory press. The scaffolds were heated between the press platens under a pressure of 1 metric ton applied for 1 min and then under 2 metric tons for 2 min. Heating was then stopped to allow specimens to cool down until room temperature was reached. The fiber scaffolds had a high porosity of approximately 90% to mimic the porosity of spongy (trabecular) bone. Details of the scaffolds morphology are given in previous publication[89].

5.3.3 EtO and LTP sterilization of composite fibers

Equal amount of samples (2 g) of each fiber batches were cleaned by a 2-step ultrasonication procedure involving 99.9% ethanol and 98.9% acetone for 10 min cycles. The samples were then wrapped in plastic sterilization pouches and sterilized using one of the two different methods: (a) EtO or (b) LTP. EtO sterilization was carried out in SteriVac® (3M), with a 4-h cycle followed by 24 h aeration to remove residual EtO. LTP sterilization was performed using a 20l volume and a 2.45-GHz surface-wave discharge operated at the 100-W power level. The gas flow rate (one standard l/min of N plus % of added χ O2) has been extensively explained by Philip *et al.*[104]

5.3.4 XPS analysis

X-ray photoelectron spectroscopy (XPS) tests were performed on EtO, LTP and non-treated samples in order to determine the chemical composition of the composites surface. XPS measurements were acquired on an ESCALAB MKII spectrometer (VG Instruments) using non-monochromatised Al Kα radiation (h_v = 1486.6 eV) from a twin Mg/Al anode operating at 15 kV and 300 W. The operating system pressure during the scans was ~8×10^{-9} Torr over a sample area of 3 x 2 mm^2. For each sample, the survey spectra (0–1200 eV) were recorded at pass energy of 50 eV and for the high-resolution scans for the elements of interest O 1s, C 1s and Ca 2p, at 20 eV. The resolution of the spectrometer was 1 eV for survey scans and 0.7 eV for high-resolution scans. All spectra have been corrected for sample charging, with the adventitious C 1s peak (284.7 eV) used as an internal reference.

5.3.5 Scanning electron microscopy in combination with energy dispersive X-ray analysis (SEM-EDX)

The PET/HA nanocomposite fiber morphology was examined by Field Emission Gun Scanning Electron Microscope (SEM) on a Hitachi S-4700 apparatus (Hitachi High-Technologies Canada Rexdale, Ontario) equipped with a Link AN10/55 S (Link Analytical, England) energy dispersive spectrometer unit. The EDX spectra were observed with Kontron Electronic GmbH (KS 3000) program. The specimens were mounted on conducting carbon tape and sputter coated with palladium and observed under the FEG-SEM at an accelerating voltage of 2.0 kV.

The SEM samples were examined at magnifications between 200x and 13000x using an accelerating voltage of 15 kV. EDX was used to determine their chemical surface composition with approximate 1μm^2 resolution and source energy of 10 keV. Three runs on different spots on each specimen were made. Samples photographs were chosen to demonstrate differences in particles morphology.

5.3.6 In vitro biocompatibility – Effect of sterilization on cellular behavior indirect and direct contact

5.3.6.1 Cell culture

Murine L929 fibroblast and RAW 264.7 macrophage cell lines (ATCC, Rockville, MD, USA) were used in this study. Cells were grown at 37°C in a 5% CO_2 humidified atmosphere in Dulbecco's modified Eagle's medium (DMEM; Sigma-Aldrich, Mississauga, ON, Canada), supplemented with 3.7 g/L of sodium bicarbonate, 10% heat-inactivated (56°C for 30 min) fetal bovine serum (FBS), 100 units/ml penicillin, and 100 µg/ml streptomycin (Gibco Laboratories, Burlington, ON, Canada).

5.3.6.2 Cytotoxcity of EtO- and LTP-sterilized PET/HA extracts

Extracts were prepared from the material samples in agreement with the ISO specification (10993-5) governing *in vitro* tests[77]. EtO- and LTP-sterilized polymer nanocomposite were independently immersed in complete DMEM at a ratio of 0.2 g/ml and incubated for 24 h at 37°C under constant agitation (250 rpm). After this period, the medium was harvested and kept at -90°C until used. The extracts were used undiluted.

The cytotoxicity of composite extracts was evaluated against L929 fibroblasts using the methyl tetrazolium (MTT) assay in 96-well plates as described by the manufacturer (Sigma-Aldrich). Briefly, L929 cultured cells were seeded in 96-well plate (2.5×105 cells/ml, 200 µl/well) and allowed to adhere for 24 h at 37oC in a 5% CO_2 humidified atmosphere. The culture medium was replaced by the EtO- and LTP-sterilized nanocomposite extracts, using culture medium itself as control, and further incubated for 24, 48 and 72 h. After the incubation periods, the extracts were removed and each well was treated with the MTT solution for 4 h at 37°C. Liquid was then removed, solubilization solution added, and microplate was shaken for 15 min before reading at 550 nm on an ELISA microplate reader. Control samples consisted of L929 cells grown on tissue culture plastic supplemented with complete DMEM not in contact with fiber extracts. Cytotoxicity was calculated as the percentage of control cell viability. Results are the mean ± standard deviation of three (3) experiments performed in triplicate.

5.3.6.3 Cytotoxcity of EtO- and LTP- sterilized 3D PET/HA matrix in direct contact

To test the long-term effects of the sterilization method on the nanocomposite biocompatibility, the fiber matrix were deposited in 24-well plates and sterilized by EtO or LTP. After five (5) days aeration time, the scaffolds were soaked in phosphate buffered saline (PBS) and then overnight in DMEM supplemented with 10% FBS, 100 units/ml penicillin, and 100 μg/ml streptomycin prior to L929 fibroblast seeding (1×10^4 cells/cm^2). L929 fibroblasts cultured on the regular polystyrene surface were used as control. Cells were maintained in culture for up to 14 days. Medium was changed every 3 days.

Cell proliferation on the EtO- and LTP-sterilized scaffolds was monitored using the Alamar BlueTM assay as specified by the manufacturer (Biosource, Camarillo, CA). The directly plated fibroblasts were incubated at 37°C in a humidified atmosphere of 5% CO2 and 95% air. At selected time points 1, 3, 7 and 14 days medium was removed from the wells containing the test scaffolds. An aliquot of 1 ml Alamar Blue diluted 1:10 in phenol red-free medium was added to each well and incubated for a further 4 hr at 37°C, 5% CO2. Wells without cells were used as the blank control and L929 cells grown on tissue culture plate (TCP) supplemented with complete DMEM were used as a negative control. Following the incubation 3 x 100 aliquots from each well were taken and transferred to a 96-well plate for reading. Absorbance was measured on an ELISA microplate reader at 570 nm and 600 nm. The intensity of red color (570 nm) is proportional to the percent reduced of Alamar Blue that can than be related to the metabolic activity of the cell population through the following:

$$\%\ \text{metabolic activity} = \frac{\varepsilon_{ox}(\lambda_2)\cdot A(\lambda_1) - \varepsilon_{ox}(\lambda_1)\cdot A(\lambda_2)}{\varepsilon_{red}(\lambda_1)\cdot A'(\lambda_2) - \varepsilon_{red}(\lambda_2)\cdot A'(\lambda_1)}\cdot 100 \quad (1)$$

where ε_{ox} is the molar extinction coefficient of Alamar Blue oxidized form (BLUE), ε_{red} is the molar extinction coefficient of Alamar Blue reduced form (RED), A is the absorbance of test wells, A' is the absorbance of negative control well, λ_1 is given by 570 nm and λ_2 by 600 nm. Results are the mean ± standard deviation of three (3) experiments performed in triplicate. Numerical data were analyzed statistically using Student's t tests. Statistical significance was considered at $p < 0.05$.

5.3.7 Effect of sterilization on macrophages activation

Murine RAW 264.7 macrophages were seeded in 24-well culture plates at a density of 2 x 104 cells/well in 1 ml of DMEM supplemented with 10% FBS, 100 units/ml penicillin, and 100 µg/ml streptomycin. After overnight equilibration, the EtO- and LTP-sterilized nanocomposite extracts replaced the medium. Supplemented DMEM was used as a negative control while or 10 µg/ml of lipopolysaccharide (LPS, *E. coli*; Sigma-Aldrich) was used as a positive control. Supernatants were harvested for assaying the levels of TNF-α with sandwich enzyme linked immunosorbent assays (ELISAs) as prescribed by the manufacturer (Biosource, Nivelles, Belgium). The optical density was then determined using a microplate reader set to 450 nm and corrected at 570 nm. The minimum detectable levels were 3 pg/ml. Results are the mean ± standard deviation of three (3) experiments performed in triplicate. Numerical data were analyzed statistically using Student's t tests. Statistical significance was considered at $p < 0.05$.

To test the long-term effects of the sterilization method on the nanocomposite potential in macrophages activation, the PET0 and PET10 fiber matrix were deposited in 24-well plates and sterilized by EtO or LTP. After five days aeration time, the scaffolds were soaked in phosphate buffered saline (PBS) and then overnight in DMEM supplemented with 10% FBS, 100 units/ml penicillin, and 100 µg/ml streptomycin prior RAW 264.7 macrophages seeding (2 x 105 cells/cm^2). Supplemented DMEM was used as a negative control while 10 µg/ml of LPS was used as a positive control. Supernatants were harvested for assaying the levels of TNF-α with ELISA as prescribed by the manufacturer (Biosource, Nivelles, Belgium). The optical density was then determined using a microplate reader set to 450 nm and corrected at 570 nm. The minimum detectable levels were 3 pg/ml. Results are the mean ± standard deviation of three (3) experiments performed in triplicate. Numerical data were analyzed statistically using Student's t tests. Statistical significance was considered at $p < 0.05$.

5.4 RESULTS

5.4.1 XPS characterization of surface modifications induced by HA addition in the PET fibers

In order to chemically characterize the surface modification of the fibers induced by the progressive HA addition, XPS measurements were conducted on untreated nanocomposite PET fibers charged from 0% to 10% HA. The main interest was the effect of the HA nanoparticle addition on the surface chemistry of the resulting nanocomposite fibers. For simplicity purposes, only the 0% HA (PET0), 4% HA (PET4)

and 10% HA (PET10) nanocomposite fibers are presented. In Figure 5.1, the C 1s and O 1s core level graphs are shown superimposed for a graphic representation. In Table 5.1, the estimation of carbon and oxygen species relative concentration is shown for a numerical representation.

The main observations due to the progressive addition of HA nanoparticles into the PET fibers were:

(1) Regardless of the HA content in the PET/HA fibers, HA is not exposed to the fibers surface as the XPS survey detected carbon and oxygen atoms only. The typically detected atoms signaling HA presence, Ca and/or P, are not present in the XPS survey spectrums. However HA addition greatly modified the surface of the PET/HA nanocomposite fibers as new C 1s and O 1s line-shape peaks were found in fibers containing HA nanoparticles. Moreover the changes in the C 1s and O 1s peaks became more pronounced as the HA nanoparticles content added to the fibers increased.

(2) C_{1S} spectra showed that HA addition resulted in a new compound formation as the typical PET spectrum (PET0) is modified with the new line-shape peak growth at 286.5 eV proportional with the addition of HA. The emergence of a peak growth at ~286.5 eV clearly indicates –C-OH hydroxyl group addition to the surface as shown in the deconvolved C 1s XPS spectrum in Figure 5.2. The appearance of such a component has been shown favorable for cell attachments[105], as we showed by previous *in vitro* cell studies[89].

(3) Furthermore, with the addition of 10% HA to PET, the C_{1S} spectra also showed a 84% increase in the –C-O groups and a 165% increase in the –O-C=O groups,

as seen in Table 5.1. This additional surface oxidation seen in the C_{1S} spectra is important for the resulting surface exposed to the *in vitro* environment.

(4) The O_{1S} deconvolution spectra (not shown) indicated the components of –C-OH at 533.5 eV and –C-O-OH at 532.0 eV. The superposition of the variously charged PET fibers O_{1S} spectra (Figure 5.1b) showed an increase of the carbonyl peak (C=O) respective to the ether peak (C-O-C), as a consequence of the HA nanocrystals addition. The ether peak decrease suggests it is the preferential location for the newly formed PET-HA bonds. The increase of the carbonyl confirms the newly formed hydroxyl peak found in the C_{1S} spectra.

(5) Table 5.1 lists the estimation of carbon and oxygen species, indicating that the total oxygen concentration doubles from 17% to 30% upon 10% HA addition into the PET fibers. The same trend is seen with the pure carbon content (C-C/C-H bonds) as the concentration decreases from 75% to 52% with the addition of 10% HA.

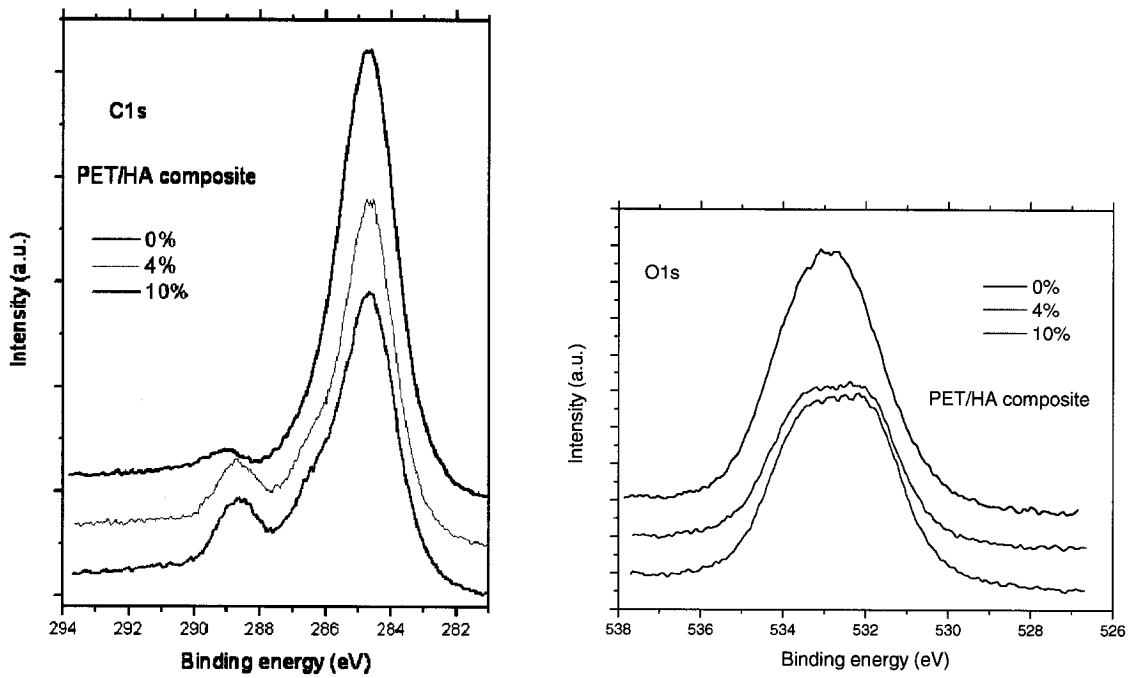

a) b)

Figure 5.1: Effect of HA nanoparticle dosage in the PET fibers on the a) XPS carbon signal spectra and b) XPS oxygen signal spectra of non-sterilized PET nanocomposite fibers charged with 0% HA (PET0), 4% HA (PET4) and 10% HA (PET10).

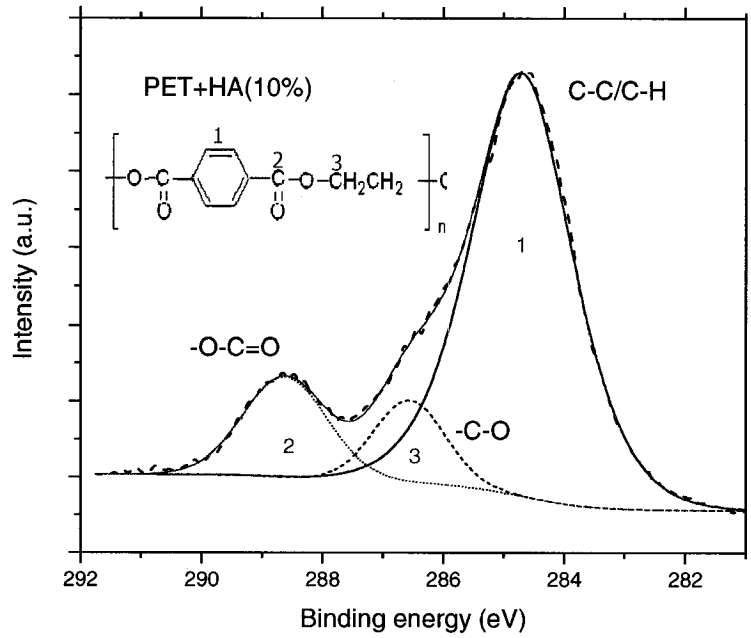

Figure 5.2: XPS analysis of PET10 carbon signal spectra.

Table 5.1: XPS estimation of carbon and oxygen species relative concentration of non-sterilized PET nanocomposite fibers charged with 0% HA (PET0), 4% HA (PET4) and 10% HA (PET10) untreated [a] from C 1s deconvolution, [b] from O 1s and C 1s peak area estimation

HA %	Carbon[a]			Oxygen[b]
	C-C/C-H	-C-O	-O-C=O	
0	74.9	3.7	3.7	17.6
4	57.5	5.8	10.8	25.7
10	52.6	6.8	9.8	30.7

5.4.2 Morphologic evaluation of untreated fibers

The influence of the progressive HA addition, on the PET/HA nanocomposites fibers microstructure was studied by SEM. EDX coupled with SEM was applied to associate the elemental composition with the morphological features of an area. The SEM micrographs of the PET0 (pure PET) and PET10 fibers are shown in Figures 3 and 4 respectively. The high magnification images (1 mm) present general features of each sample. In each figure, two areas of interest are magnified further; these are referred to as Areas 1 and 2. Note that these areas were selected because their morphologies are obviously different. The elemental compositions of spots within the areas were analyzed by EDX and the analyses are included next to the image they represent.

Although the SEM and the EDX tests were performed for all PET/HA nanocomposite fibers (PET0, PET2, ..., PET10) samples, only the results for PET0 (Figure 3) and PET10 (Figure 4) fibers are presented. The reason was twofold: a) the samples with in between amounts of HA exhibited similar morphology to the closest end spectrum sample, rendering the entire samples overview redundant; and b) PET10 is the main candidate for orthopedic surgery and the main interest of the study. Comparing PET10 to pure PET fibers exhibits the changes induced by the HA addition more clearly.

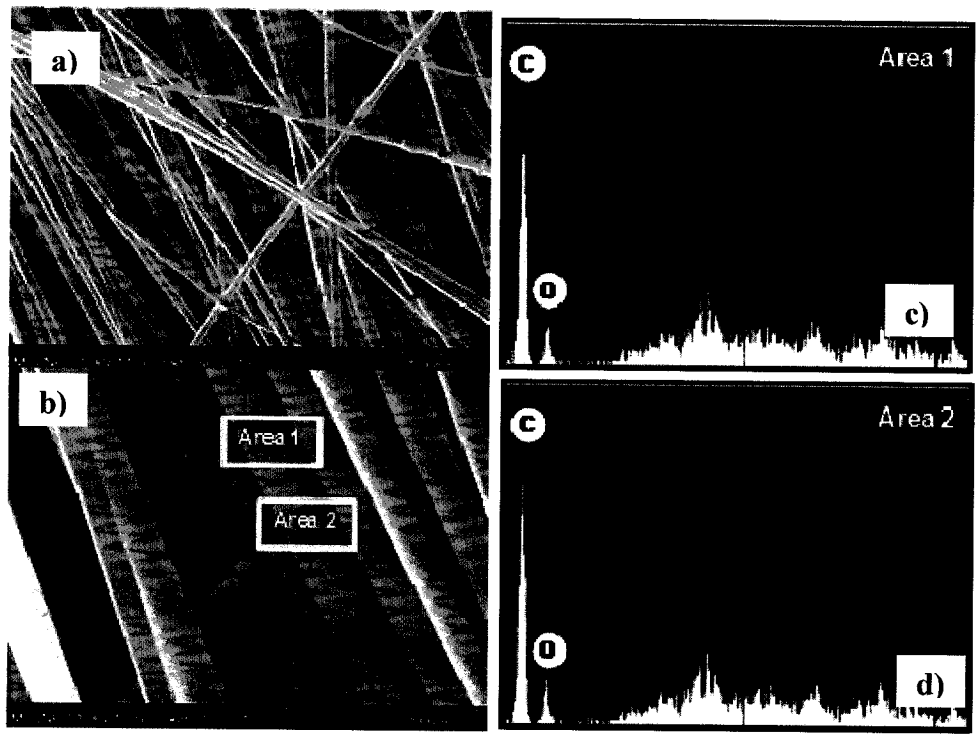

Figure 5.3 SEM micrograph of PET0, a) general view (original magnification x1000); (b) SEM micrograph of PET0 fiber, selected Area 1 and 2; (c) EDX analysis of the irregular part of the fiber; (d) EDX analysis of the smooth and more predominant morphology of the fiber.

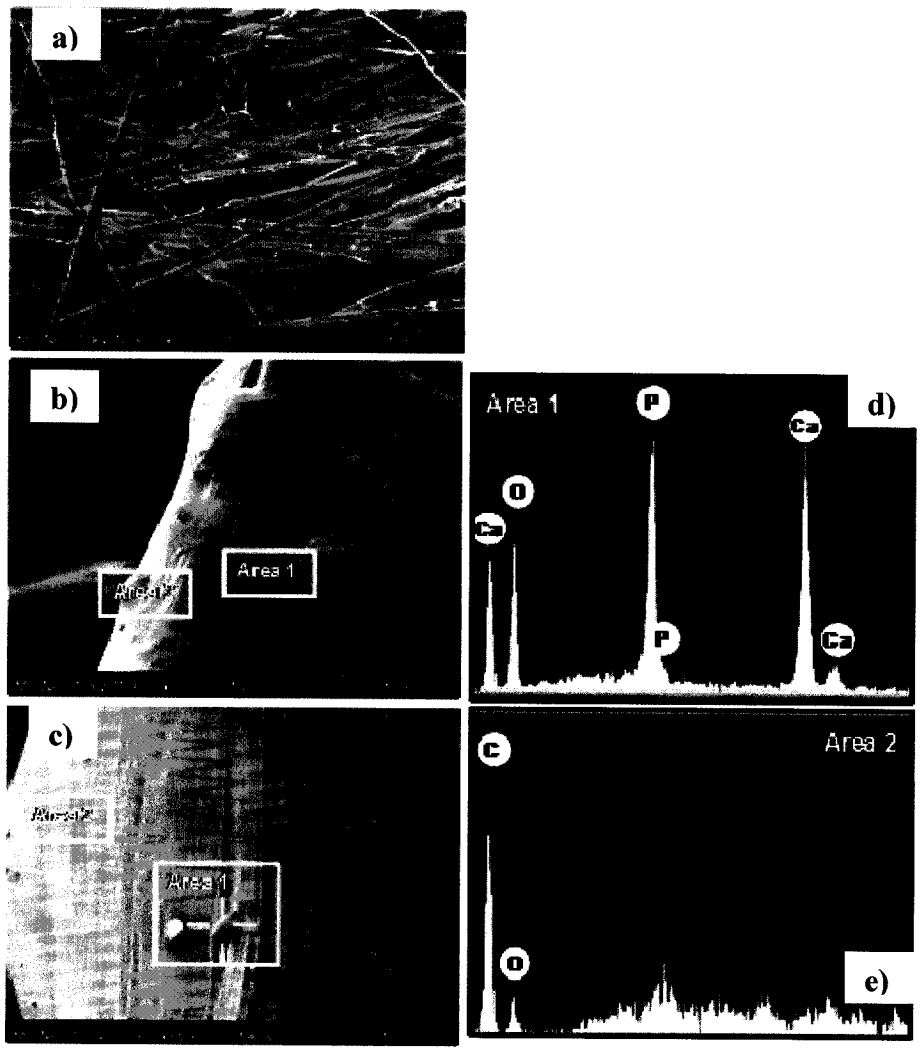

Figure 5.4 SEM micrograph of PET10, a) general view (original magnification x1000); (b) SEM micrograph fiber, selected Area 1 and 2; (c) same area as in b but shown in higher magnification (d) EDX analysis of the irregular part of the fiber, the particle like; (e) EDX analysis of the smooth morphology of the fiber.

The PET0 fibers clearly had a smooth unmodified morphology as the only chemical component of the fibers was the PET polymer. The EDX chemical analysis associated with the small irregularities as well as the smooth parts of the fibers clearly demonstrate that the fibers are composed of carbon and oxygen only, constituting elements of PET.

PET10 fibers on the other hand exhibited two distinct morphologies in their structure. The first morphological feature was a granular aggregation corresponding to the HA particles (Area 2 of Figure 5.4c). The large HA aggregates however are covered by a layer of PET, as the corresponding EDX (Figure 5.4e) graph only detects PET elemental composition of carbon and oxygen atoms only. This observation is coherent with the previously presented XPS results that did not reveal HA presence. The second morphology seen on PET10 fibers was a mixture of nano- and micron-sized HA particles partially embedded in the fibers. One of those micron sized particles is clearly shown in higher magnification Figure 5.4c area 1. The EDX spectra of the nano and micron sized HA particle (Figure 5.4d) showed characteristic peaks of oxygen, phosphorous, and calcium, respectively at 1.5, 1.8, and 3.75 keV, corresponding to elements oxygen, phosphorous, and calcium, which describe the characteristic constituents of HA.

5.4.3 XPS characterization of surface modifications induced by EtO and LTP treatments

Following the surface characterization, the PET/HA nanocomposite fibers were treated by LTP and EtO. The EtO and LTP effects on the nanocomposite surface were characterized by XPS and compared with the previously characterized untreated fibers. For simplicity purposes, only the C_{1S} spectra of PET0 and PET10 are shown before and after EtO or LTP treatment as obtained by XPS analysis in Figure 5.5. For a better comprehension, the results following EtO and LTP treatments are presented

quantitatively in Table 5.2. The observations for PET10, the main candidates for orthopedic applications were that: following EtO treatment, the C1s peak width increases. As listed in Table 5.2, quantitative analysis attributes the peak widening to a 14% increase of C-O/C-OH bonds and 30% decrease of the benzene ring (C-C/C-H) bonds. Although numerically EtO appears to be oxidating the fiber surface, the shape of the C 1s peak indicates that the additional C-O/C-OH is resident EtO rather than reacted C-O.

Following LTP treatment, the C1s peak widens significantly and changes in appearance. As listed in Table 5.2, quantitative analysis reveals a 62% content decrease in benzene ring and a 420% C-O/C-OH increase. Although the trend is similar as in the EtO treatment, the overall C 1s peak shape indicates a formation of C-O bonds, and defects creation probably due to the C-C bonds breakage under the plasma bombardment[106]. Furthermore the bond breaking sites (free radicals) are then free to react with the air oxygen and water in order to form C-OH groups, increasing the overall oxygen content in the fibers surface.

Both LTP and EtO treatments include slight carboxyl increase as shown in Table 5.2 and Figure 5.5 However the limitations of our XPS energy resolution do not allow a separation of the –C-O and –C-OH groups.

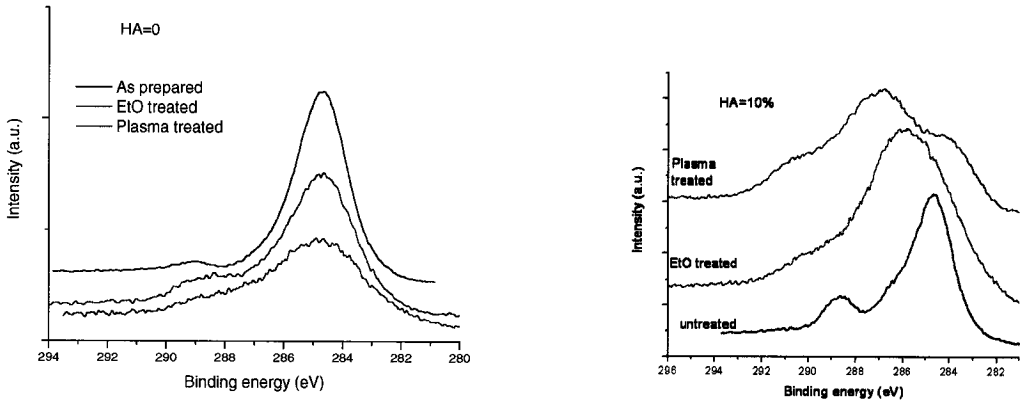

a) b)

Figure 5.5: XPS carbon signal spectra of a) PET0 and b) PET10 before sterilization, after EtO and LTP sterilization.

Table 5.2: XPS estimated relative concentration on the surface modifications on 10% HA (PET10) nanocomposites before treatment and following EtO and LTP sterilizations

Samples treatments	Carbon		
	C-C/C-H	-C-O and -C-OH	-O-C=O
untreated	52.6	6.85	8.83
ETO	36.9	27.7	11.5
LTP	20.1	35.7	13

5.4.4 Effect of sterilization method on in vitro viability

Figure 5.6 shows a comparison of EtO- and LTP-sterilized materials extracts, quantified by the MTT assay in order to measure the short-term effects of the degradation products on L929 fibroblasts. Cytotoxicity was calculated as the percentage

of cell viability over control values. Results clearly show that the extracts from both EtO- and LTP-sterilized materials have no significant effect on the fibroblasts viability, as it remains constant around 105% for all nanocomposite fibers with no statistical differences with respect to the sterilization method. The extracts were clear and no pH changes were noted.

The effects of EtO and LTP sterilization treatments were then evaluated in direct contact by incubating L929 fibroblasts on EtO- and LTP-sterilized fiber scaffolds (PET0 to PET10) for 1 to 14 days. Figure 5.7 shows the proliferation of the fibroblasts in culture as determined by Alamar Blue assay. As no significant statistical differences are demonstrated between EtO- and LTP-sterilized scaffolds, it can be stated that the fibroblastic viability is independent of the sterilization mode used. More importantly as the metabolic activities reach 100% after 7 days in culture and remain above 100% until 14 days, it can be said that both EtO and LTP sterilization methods did not present any toxicity towards fibroblastic cells.

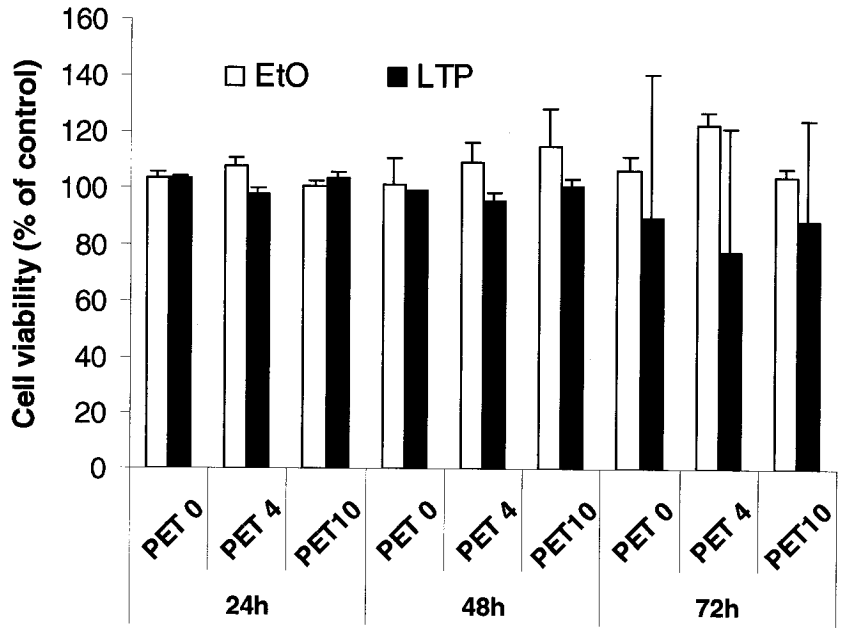

Figure 5.6: Effect of 0% HA (PET0), 4% HA (PET4) and 10% HA (PET10) extracts following EtO and LTP sterilization on the viability of L929 fibroblast cells; as determined by the MTT assay. L929 cells were incubated in the presence of undiluted fiber extracts (0.2 g/ml) and the fibroblast viability was determined by the MTT assay at 24, 48 and 72 h. L929 cells grown on tissue culture plastic (TCP) supplemented with complete DMEM was used as the negative control. Results are expressed as % of negative control and are the mean ± standard deviation of three (3) different experiments

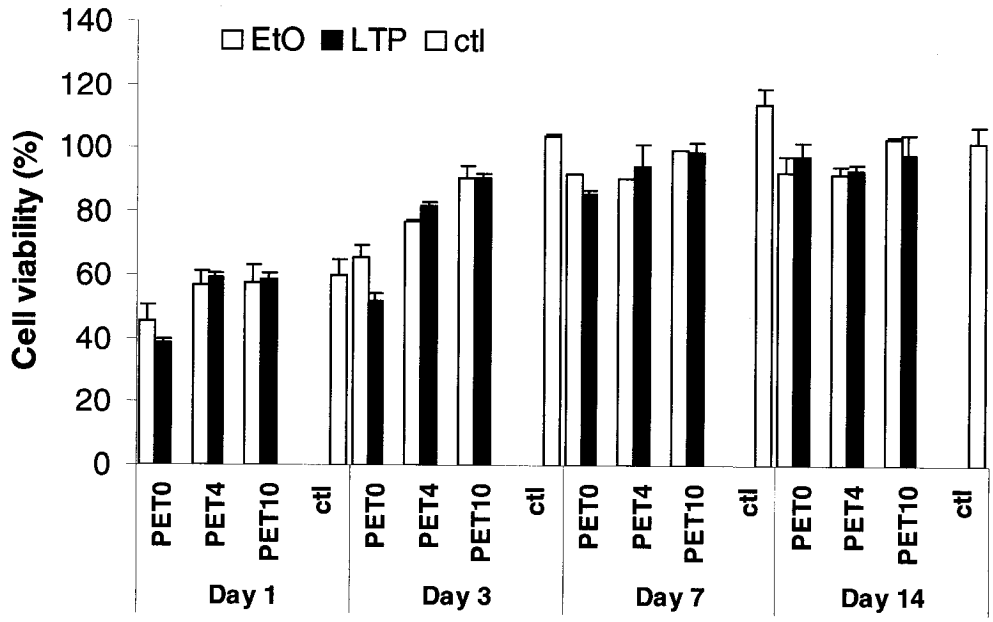

Figure 5.7: Effect of 0% HA (PET0), 4% HA (PET4) and 10% HA (PET10) fiber scaffolds following EtO and LTP sterilization on the proliferation of L929 fibroblast cells. L929 fibroblasts were seeded on PET0, PET4 and PET10 fiber scaffolds and their viability was assessed after 1, 3, 7 and 14 days by the Alamar Blue assay. Negative control samples consisted of L929 cells grown on tissue culture plastic (TCP) supplemented with complete DMEM. Results are expressed as % reduced of Alamar Blue and are the mean ± standard deviation of three (3) different experiments

5.4.5 Effect of sterilization method on in vitro macrophage activation

The effects of the material extracts following the two different sterilization treatments on TNF-α release by Raw 264.7 macrophages are shown in Figure 5.8. After 1 h in presence of materials extracts, both EtO- and LTP-sterilized nanocomposite fibers extracts had no effect on TNF-α release (with respect to control). However, a trend of higher TNF-α release following longer incubation time with EtO-treated fibers extracts is observed. For instance after 24 h, EtO-sterilized PET0 extracts stimulated 10 times the release of TNF-α (279 pg/ml) versus 2 times (62 pg/ml) LTP-sterilized PET0 extracts

(with respect to negative control). Similarly, at the other end of the spectrum, EtO-sterilized PET10 (the highest HA-loaded polymer) extracts stimulated 13 times the release of TNF-α (326 pg/ml) as compared to 8 times (220 pg/ml) for LTP-treated PET10 (with respect to negative control). At 24 h, all other nanocomposite fibers (PET2, PET4, PET6 and PET8) follow the same trend, with EtO-sterilized extracts maintaining one to three times higher TNF-α release than LTP-sterilized extracts. At 48 h, the same trend of slightly higher TNF-α release following EtO sterilization is generally preserved. As a control, LPS stimulated TNF-α release (with respect to negative control) 23 times (160 pg/ml), 55 times (1450 ml), and 13 times (1380 ml) after 1 h, 24 h and 48 h respectively.

The effects of the different sterilization methods on TNF-α release in direct contact with PET0 and PET10 scaffolds-Raw 264.7 macrophages are shown in Figure 5.9. The trends of direct contact stimulation are comparable to the previously discussed stimulation of TNF-α by the fibers extract. As in presence of the extracts, macrophages plated on EtO- and LTP-sterilized fiber scaffolds had no effect on TNF-α release after 1 h (with respect to control). However, after 24 h EtO-sterilized PET0 stimulated 9 times the release of TNF-α (296 pg/ml) as compared to only 3 times for the LTP-sterilized PET0 (88 pg/ml).

The main focus of this study, PET10, stimulated low levels of TNF-α release following both EtO and LTP sterilizations. After 24 h EtO- and LTP-sterilized PET10 scaffolds represented 0.8 times TNF-α stimulation of the negative control (25 pg/ml and

27 pg/ml respectively) and a fraction of the positive control. The same trend reoccurs after 48 hrs, with EtO-sterilized PET0 stimulating 9 times the release of TNF-α (226 pg/ml) as compared to only 2 times for the LTP-sterilized PET0 (60 pg/ml) of the negative control; and PET10 remained again at low levels of TNF-α release following both EtO and LTP sterilizations, down to 1 time (41 pg/ml and 30 pg/ml respectively). As a control, LPS stimulated TNF-α release by 3 times (26 pg/ml), 18 times (566 pg/ml), and 23 times (588 pg/ml) after 1, 24, and 48 h respectively.

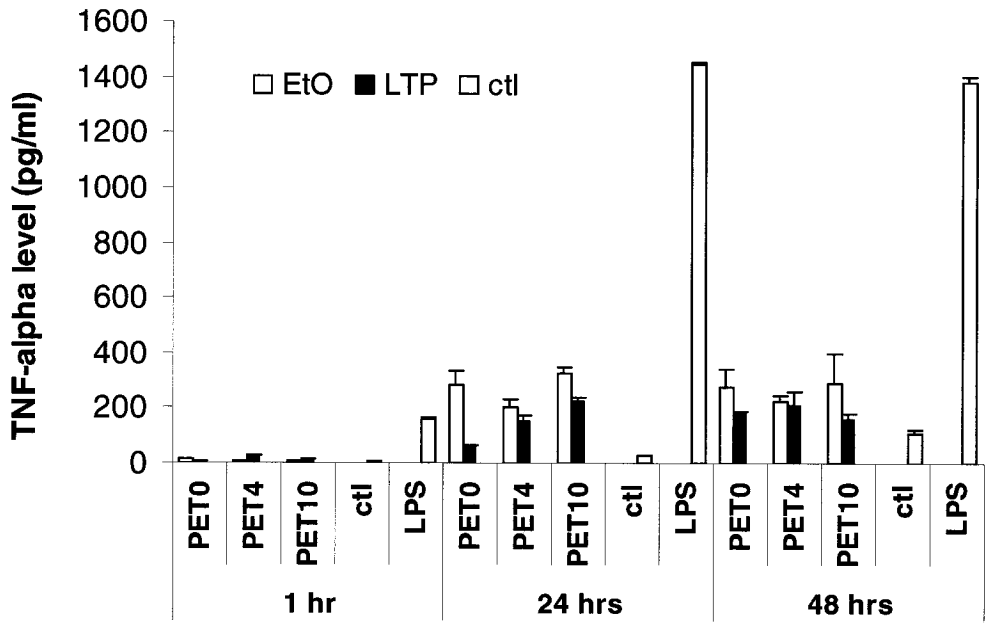

Figure 5.8: Effect of 0% HA (PET0), 4% HA (PET4) and 10% HA (PET10) extracts following EtO and LTP sterilization on TNF-α release. Raw 264.7 macrophages were seeded on PET0, PET4 and PET10 fiber scaffolds for 1 to 48 h. Supplemented DMEM was used as a negative control while 10μg/ml of lipopolysaccharide (LPS) was used as a positive control. Results are the mean ± standard deviation of three (3) experiments.

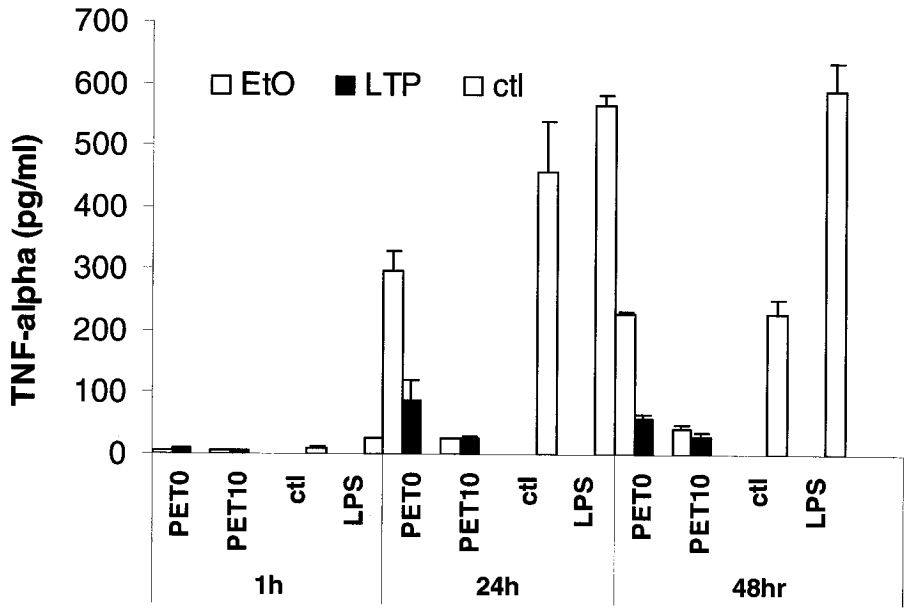

Figure 5.9: Effect of 0% HA (PET0) and 10% HA (PET10) fiber scaffolds following EtO and LTP sterilization on TNF-α release. Raw 264.7 macrophages were seeded on PET0, PET4 and PET10 fiber scaffolds for 1 to 48 h. Supplemented DMEM was used as a negative control while 10μg/ml of lipopolysaccharide (LPS) was used as a positive control. Results are the mean ± standard deviation of three (3) experiments.

5.5 DISCUSSION

As all novel biomaterials, the previously introduced PET/HA nanocomposite fibers have to be efficiently sterilized before use as biomaterials. Since it is well accepted that all sterilization processes commonly used can modify the physical and chemical characteristics of polymeric materials[100], the sterilization method has to be carefully selected. However, literature seems to present contradictory results about the effects of the sterilization procedure on the biological response, as several studies have shown that sterilization can alter biological response while other investigators have found that different sterilization protocols do not have a significant effect on the

biological response to the specific polymers[107]. Thus the continuing need to examine the effects of the sterilization protocols on novel implant materials. As PET/HA nanocomposite fibers are novel materials that have not been previously chemically characterized, their surface chemistry was elucidated in terms of HA percentage added to the PET fibers. The reason for this surface characterization was double-fronted. First, it would allow an accurate analysis of the modifications induced through sterilization by comparing the equivalent untreated fiber surface chemistry. Secondly, it would allow a potential explanation of the increased bioactivity previously reported on the nanocomposite fibers with higher HA percentages. Following the chemical surface characterization of the PET/HA fibers, the effects of LTP and EtO sterilizations on PET0 and PET10 nanocomposite fibers, specifically their surface chemistry and *in vitro* biocompatibility, were evaluated.

In terms of surface modifications induced on the PET/HA nanocomposite fibers by the increased HA addition, the reduced overall carbon surface content in favor of increased oxygen content via the formation of new hydroxyl groups is the most important one. The hydroxyl group formation is plausibly caused during fiber processing via the reaction of free hydroxyapatite -OH groups with the PET polymer; *e.g.,* the PET matrix reacted with the added HA nanoparticles through weak hydrogen bonds, encapsulating HA nanoparticles and exposing –CH/COH/-COOH groups within a 10 nm thick layer. This encapsulation under higher temperatures, such as the 280°C used in fiber processing, reinforces the weak bonds leaving the newly formed hydroxyl groups exposed to the surface. The hydrated layer encapsulating the nanoparticles is what

finally prevents the detection of HA main elements: P and Ca by XPS survey scans. However, detailed description of the PET/HA reaction goes beyond the scope and interest of this paper as XPS measurements were used to analyze the elemental composition of the outermost atom layer. In the context of this research, XPS measurements were conducted to evaluate HA nanoparticle effects on fiber surface. As explained elsewhere, in order to preserve HA attractive properties in HA/polymer nanocomposite fibers, new variables, such as their physico-chemical properties, which are affected by the chemical interactions between the HA particles and matrix, come into play. Furthermore, the chemical composition of a surface has an impact on the biological response by influencing the protein absorption on a material, and subsequently the cell behavior[105]. The initial cellular interaction and adhesion is facilitated on an oxygenated surface rendering the surface bioactive. The reason for the acquired bioactivity through a rather simple surface modification is that a biocompatible oxygenated surface will supply cells with substrates suitable for adhesion and cell–matrix interactions to promote cell growth and differentiation[108]. As previously shown by our group, PET10 fiber scaffolds presented increased growth kinetics when compared to other 3D PET/HA fiber scaffolds, including PET which is the gold standard. The *in vitro* cellular variations are expected to have a final outcome on the stimulation of new tissue formation at the interface[89]. As now explained by XPS analysis, the improved cellular response on PET10 is due to the high increase in hydroxyl groups (and oxygen content overall), known favorable for cell attachment and growth. Additionally, the SEM-EDX characterization detected some nano- and micron-sized HA particles exposed to the

surface. As HA is undetected by XPS the total surface concentration of the particles must be below 3%, the detection limit of XPS. Additionally as seen by SEM the rougher morphology at higher HA percentages induced by large HA aggregates influences the cellular response. It thus appears that the previously characterized[89] improved biological responses at higher HA percentages was probably due to the rougher surface topography of the fibers combined with the oxidized surface chemistry, and not surface exposed HA as initially anticipated.

Following the surface characterization of the novel fibers, XPS measurements were conducted on EtO- and LTP-treated novel PET/HA nanocomposite fibers to determine the more appropriate sterilization technique. The previously obtained XPS data were used as reference to determine the modifications induced by EtO and LTP treatments. In terms of quantitative chemical analysis both EtO and LTP presented similar alterations such as the significant decrease of benzene (C-C) groups in favor of advantageous C-OH and –COOH functional groups. Qualitatively speaking, both treatments seem beneficial in terms of biological responses due to the hydroxyl content increase. The results also have to be interpreted quantitatively for a complete understanding. Despite the similar quantitative analysis for both EtO and LTP treatments, oxygenated functional groups are only present following the LTP treatment. The overall C 1s peak shape following LTP treatment indicates a formation of C-O bonds in favor of C-C bonds breakage, which is not the case following the EtO treatment.

Observed alterations can be explained by the nature of the sterilizing agent as plasma modifications occurs in a mechanism particular for each gas used[109]. The LTP set-up used combined the use of strongly oxidative chemical agent, oxygen (O_2) and inert nitrogen (N_2), which are vaporized and left to diffuse into the chamber, alternately with the plasma. Although the chemical phase is used for its bactericide efficacy[98] in this particular case, it has shown beneficial side effects as it is responsible for the –COOH functional groups addition. Specifically, the surface oxidation occurred due to the oxygen containing reactive species that react with the exposed nanocomposite fiber surface during the plasma phase. Deconvolution of the C1s region indicated the formation of highly oxygenated carbon, supporting the idea that bond breaking sites have at least partially reacted with the air oxygen and water in order to form the C-OH groups, further increasing the overall oxygen content in the fiber surface. The oxygenation of the fiber surface probably induced a change in the interfacial properties of the fibers[109] but more conclusive wettability tests are needed to conclude on this aspect.

On the other hand, although the qualitative EtO results suggest an increase in oxygenated functional groups, the overall C 1s peak shape suggests simple surface alkylation artifact. The indicated alkylation was expected as alkylation is the known EtO mechanism of action on microbe sterilization. The phenomenon of alkylation by EtO gas is related to the residue of EtO molecules in the macromolecular network as well as the bounding of EtO molecules with specific chemical groups[98]. However, EtO as a reactive alkylating agent adds alkyl groups to DNA, RNA and proteins, rendering it toxic to

living organisms and cells. Despite the alkylation detected by XPS, the EtO-treated nanocomposite fibers do not present any toxicity in direct and non-direct contact with fibroblasts, indicating that most of the EtO had probably reacted with the components in the biological media. This was expected as previous works have shown that the bioavailability of EtO in culture medium with FBS is significantly reduced as EtO reacts with proteins in the solution[110]. Therefore based on XPS analysis alone, the clear advantage of the LTP treatment was the favorable surface modifications on the nanocomposite fibers resulting in a more hydrophilic surface, due to the hydroxyl end groups, in addition to a sterilized surface.

In order to evaluate the effects of the sterilization method on the PET/HA nanocomposite fibers *in vitro* biocompatibility, four methods were used: (1) evaluation of L929 fibroblast viability using extract media obtained from the differently sterilized nanocomposite fibers, (2) evaluation of L929 fibroblast viability following direct-contact incubation with the differently sterilized fiber scaffolds, (3) evaluation of the TNF-α release by Raw 264.7 macrophages following incubation with extract media obtained from the differently sterilized nanocomposite fibers, and (4) direct-contact Raw 264.7 macrophages incubation with the differently sterilized fiber scaffolds.

The effect of degradation products of polymers on their biological environment is important in determining the biocompatibility of promising biomaterials. In this work, the well-known MTT assay was used to quantify the short-term effects of the degradation products of the nanocomposite fibers following EtO and LTP treatments on the viability of L929 fibroblasts. Results showed that the extracts from LTP- and EtO-

treated fibers had no effect on cell viability, which suggests the biocompatibility of the extracts. As no cytotoxic effects of the nanocomposite fiber eluates were discovered, it can be said that the LTP and EtO sterilization methods did not induce any degradation of the nanocomposite fibers into potentially toxic or putative particles.

The indirect cytotoxicity contact tests were complemented with direct contact tests to evaluate the effects of EtO and LTP chemical modifications on the cell behavior. Surprisingly, the fibroblasts viability following direct contact incubation with sterilized fiber scaffolds was unaffected by the type of sterilization used. As literature suggests cells should profit by surfaces exhibiting more oxygen and more specifically hydroxyl groups[111], an increased cellular viability was expected following incubation of fibroblasts on LTP-sterilized scaffolds. As discussed previously, LTP treatment resulted in significant increase of hydroxyl functional groups, which was expected to have an outcome on the cellular viability. In our study, the fibroblastic response depended mainly on the type of scaffold used and not the sterilization treatments. The high fibroblastic viability and absence of negative effects on the cell viability with LTP-treated fibers suggest that the free radicals normally produced by plasma exposure at and below the polymer surface probably reacted with atmospheric oxygen and water vapor.

As the ultimate application of the PET/HA fibers would be in orthopedics, the inflammatory responses due to degradation products was also quantified by looking at the release of TNF-α by Raw 264.7 macrophages. The present experiments demonstrated that after 24 h macrophages incubation, EtO-sterilized fiber extracts demonstrated a significantly higher TNF-α release than LTP. The trend of stronger

macrophage stimulation by the EtO extracts can be explained by the previously discussed alkylation reaction detected by XPS following EtO treatment. As the EtO residues remain reactive, they then freely react with various components of the biological media which increases macrophages activation. This elevated TNF-α production disappeared after 24 h as the levels of TNF-α release by LTP and EtO extracts poised at similar thresholds at 48 h. It should be noted that the extracts have not been chemically analyzed and the exact composition of the alkylating particles should be determined in future works.

Similarly to the indirect contact, EtO- and LTP-treated PET0 fiber scaffolds co-cultured with Raw 264.7 macrophages demonstrated a higher TNF-α release level following EtO treatment at 24 h and 48 h. However, the fiber scaffold charged with 10% HA demonstrated similar macrophage activation levels following both EtO and LTP treatments. As XPS analysis demonstrated a higher alkylation of PET0 than other nanocomposite fibers, the trend of higher macrophage stimulation to a potentially larger quantity of toxic residues is justified. As other investigators have shown, EtO and its byproducts (ethylene glycol and ethylene chlorohydin) are differently retained on the various polymers based on their surface chemistry[107]. Other studies comparing the effects of sterilization on *in vivo* inflammation found strong cellular infiltration in the tissues surrounding EtO-sterilized allografts that was not found in non-sterilized grafts[112]. They also found that macrophage-like cells infiltrated tissues surrounding fresh bone grafts and not the fresh EtO-sterilized grafts, presumably due to a toxic effect of EtO on macrophages[112]. The importance of the TNF-α release in an *in vivo* environment

comes from its crucial role in provoking the inflammatory response, which as demonstrated by Merkel *et al.* has often resulted in osteolysis around hip implant[113]. As the novel materials are ultimately developed for load bearing bones replacements, the TNF-α release levels and consequently the inflammation reaction become crucial parameters. This idea is further supported by the macrophages plated directly on EtO-sterilized PET0 as well as the macrophages incubated with EtO-treated fiber extracts always leading to a higher TNF-α concentration than that of the LTP-sterilized fibers.

5.6 CONCLUSION

This study was carried out to compare LTP and EtO sterilization in terms of chemical modifications and resulting cellular biocompatibility *in vitro*. This was important as in some cases an inadequate choice of the sterilizing method can cause irreversible damage to the morphological, physical, chemical and consequently biological characteristics of polymeric biomaterials that can reduce and/or induce wrong interpretations about the overall performance of the biomaterial. Following LTP treatment, material modifications were found to be limited to surface layer oxidation, whereas EtO induced alkylation. Considering the *in vitro* biocompatibility results shown in this article, none of the sterilization methods (EtO and LTP) are completely unsuitable for use on the novel nanocomposite fibers. However the plasma treatment have proved particularly effective for L929 growth and low TNF-α release by RAW 264.7; whereas the EtO treatment resulted in an increased TNF-α release levels particularly on the pure PET fibers.

Multiple physical and chemical parameters contribute to an optimized interaction between the material surface and the biosystem, and the surface chemistry alone is not sufficient to explain the biological improvements that occurred on the LTP-treated PET/HA nanocomposite fiber surfaces.

5.7 ACKNOWLEDGMENTS

The authors gratefully acknowledge Natural Sciences and Engineering Research Council of Canada (NSERC) for their financial support and Dr. Caroline Bernard and Dr. Kenneth Cole for his time and help.

5.8 REFERENCES

See general references in the Bibliography section.

Chapter 6: General Discussion

This master thesis deals with the biocompatibility, surface chemistry and sterilization method characterization of a newly developed biomimetic nanocomposite compounded from synthetic HA nanoparticles and PET polymer in the form of fibers.

The interest in this new biomimetic, non-degradable, orthopedic biomaterial lies in the lack of commercially available biomaterials adaptable for load-bearing bone applications not based on titanium and its alloys. The lack of comparative performance data in clinical studies, relevant animal models or *in vitro* systems among the non-load bearing bone applications commercially available biomaterials leaves the biomedical community without a clear consensus on the ideal proprieties of a biomaterial targeted for bone applications.

The novel PET/HA nanocomposite fibers were synthesized at IMI-CNRC in 2005 using a proprietary process. Their biological, chemical and mechanical characterization had not been carried out or published before. Consequentially, based on an extensive literature review of the AAMI standardized *in vitro* systems relevant for bone applications, this thesis assessed the potential biomedical interest in novel PET/HA nanocomposite fibers targeted for load-bearing bone applications.

Anticipating that the PET fibers charged with 10% HA (the highest amount of HA nanoparticles added) are superior candidates for bone replacements applications, we characterized the fabricated PET/HA fibers with 2, 4, 6, 8 and 10 wt% HA nanoparticles in order to evaluate the true effects of the progressive HA addition. The PET fibers

without HA addition were treated in the same fashion as all other fibers, and were used as an additional negative control throughout all chemical and biological experiments. Having fibers with no HA allowed us to asses the general trends imposed on the novel PET/HA fibers by the HA addition.

The thesis was separated in three subparts, each of which comprises a study in its own evolving from previously raised uncertainties. In the first part we studied the biological responses towards the PET/HA fibers extracts as well as the PET/HA 3D scaffolds. The true aim of the first part was the general evaluation of the fibers biocompatibility, which is precisely what dictates the general interest in the fibers thereafter. In the second part of this thesis, we elucidated the chemical modifications induced by the addition of the HA nanoparticles in the PET/HA fibers, in order to better understand the biological responses obtained previously. Following the surface characterization, we sterilized the fibers with the two leading low temperature sterilization methods EtO and LTP. The fibers were characterized once more to determine the appropriate sterilization method in terms of chemical and biological modifications induced. Lastly, we characterized the HA effects on the PET/HA fibers mechanical properties and included the results under annex 1 as the mechanical properties were not the core aim of this study but more of a satellite interest.

6.1 Biocompatibility study

In this first part, we confirmed our hypothesis that PET/HA nanocomposites with 10% bioactive HA addition would demonstrate acceptable *in vitro* biocompatibility and superior surface properties for cell proliferation. We evaluated the *in vitro* cellular response to variously charged HA fiber scaffolds and their degradation products and looked at biological response variation in terms of HA content in PET/HA nanocomposites fibers being evaluated.

As the ultimate applications of the PET/HA nanocomposites fibers is load-bearing bone replacements, their chemical stability under a physiological *in vivo* environment is a fundamental parameter. Although, the load-bearing *in vivo* environment with mechanical constraint could not be replicated in our laboratory, the highest allowed AAMI agitation parameter under physiological conditions (incubated in complete cellular growth medium at 37°C) was applied to the fibers to assess their chemical stability. Results showed that the extracts from the polymer fibers without HA and the polymer fibers with HA had no effect on the cell viability, which suggests biocompatibility of the extracts.

The indirect cytotoxicity contact tests were complemented with direct contact tests of the 3D fibers scaffolds. The direct contact test served to evaluate the cell-material contact arrangements as they are dictated by material surface features and properties, which may lead to differences in cytotoxicity. As it is well known, the initial interaction between biomaterials and cells is mediated by a previously absorbed layer of proteins resultant from cell culture medium *in vitro*[114]. In the present study, a new

variable factor is introduced in the outer layer of the PET composite fiber formed of HA aggregated nanocrystals. In this context, based on the surface modifications induced by the addition of HA, we expected the scaffold-cells interaction to be superior for the scaffolds charged with the highest amount of HA. As expected, metabolic activity of fibroblasts increased proportionally with the amount of HA present in the nanocomposite fibers. This trend of cell viability increase, relative to the HA amount, may be due to:

- surface roughness of the composite fibers that is increased at higher HA concentrations, as the HA nanocrystals tend to aggregate on the surface of the fibers;
- changes induced on the surface chemistry by the HA nanocrystals addition (which is analyzed in the second part of the thesis);
- or the above mentioned factors combined.

However in terms of biological responses a conclusive mechanism of cell adhesion is not yet established, leaving the chemistry, shape and surface texture of implants as equally important factors in the determination of cell-material contact and cell proliferation[4].

A heated debate throughout this research has been the use of L929 fibroblastic cell line for cellular adhesion studies, while the composites are intended for orthopedic use. Undoubtedly, bone specific biocompatibility can only be evaluated through an osteoblastic cell line. In that context, fibroblasts can be used to evaluate the materials general toxicity properties. The choice of a fibroblastic cell line was founded in their

model properties that can reliably determine the general biocompatibility of novel materials and screen them for future *in vitro* and *in vivo* experiments[58], as the general biocompatibility of the PET/HA nanocomposite fibers had never been previously assessed. Furthermore, as fibroblasts and osteoblasts are both anchorage dependent cells they possess similar affinities for biomaterial surface characteristics in terms of attachment spreading and growth[115], allowing the possibility of osteoblastic activity parallel trend to the fibroblastic one.

The choice of the negative control used in this study, TCP, is based on its ability to provide excellent conditions for the attachment and proliferation of cells *in vitro*. Hence it is considered as the ideal surface for cell growth and commonly used as negative control by researchers as an easily replicable and comparable inter-laboratory standard. Compared to TCP and all other fibers scaffolds, PET10 fiber scaffolds stimulated a higher cell adhesion, growth and proliferation. This improved cellular response supported by PET10 fiber scaffolds was seen through quantitative Alamar Blue cellular viability assay and confirmed by qualitative FEG-SEM imaging. The results are coherent with studies demonstrating that small modifications in the composition and texture of the surfaces of materials can have major impacts on the subsequent host-implant interactions. However, further studies with cell lines that have the potential to differentiate into the osteoblast phenotype are necessary in order to evaluate PET10 nanocomposite fibers potential as bioactive scaffolds.

As the ultimate application of the fibers used in the present study would be a hip prosthesis or a portion thereof, the inflammatory responses due to degradation products

as well as the 3D fiber scaffolds was also quantified by looking at the release of inflammatory cytokine TNF-α by Raw 264.7 macrophages. The choice of Raw 264.7 macrophages was due to macrophages role as the principal cells of cytokine formation, found in the pseudo-membranous tissue formed around hip implants at revision surgery[59]. Although the level of stimulation of the extracts was higher than the negative control, it was comparable to that observed with ceramic particles[116] and with metal ions[81] of orthopedic interest. Considering the high concentration of the extracts (undiluted), as well as the high agitation speed induced on the fibers to generate the extracts, the stimulation level can be deemed acceptable. The interesting results in terms of inflammation potential of the fibers were seen following the assessment of the inflammatory responses due to the initial interactions between the macrophages and 3D PET/HA fiber scaffolds. Raw 264.7 macrophages demonstrated a significant reduction of TNF-α release when incubated with PET10 3D scaffolds, indicating that the addition of HA resulted in a significant reduction of inflammatory cytokines by macrophages *in vitro.*

In conclusion, the effects of HA nanocrystals dosage in PET fibers were investigated on L929 fibroblasts and Raw 264.7 macrophages. L929 fibroblasts proliferation on the PET10 fibers scaffolds, demonstrated increased growth kinetics when compared to all other PET/HA fiber scaffolds. This variation in the monolayer culture growth kinetics is expected to have a final outcome on the stimulation of new tissue formation at the interface. As previously mentioned, the second part of the thesis examines more closely the surface modifications induced upon the fibers by the HA

nanoparticles addition in order to elucidate the reasons for the increased cellular proliferation on the PET10 fibers scaffolds. It was also possible to prove that PET10 3D fiber scaffold has low inflammation potential on Raw 264.7 macrophages (extracts and 3D form) and the addition of HA nanoparticles in the fibers are at least partially responsible for the lowered macrophages activation. Overall these results strongly support the interesting biocompatibility of the PET10 nanocomposite fibers.

6.2 Surface chemistry variations in PET/HA nanocomposites

Following the interesting results of increased cellular viability with increased HA content in the fibers, in this second part we tried to understand the solicited biological response. However, understanding biological response of a biomaterial is a complicated matter, as a conclusive mechanism of cell adhesion, response and proliferation is not yet established. Despite the ambiguities surrounding the biomaterial-cell biocompatibility field, it is widely believed that the biomaterial-cell interactions mainly depend of the materials surface chemistry and topography. Therefore in the second part of the thesis, the surface chemistry of the nanocomposites was determined by XPS analysis. To fully grasp the surface modifications trends arising at higher HA percentages, the nanocomposites fibers surface chemistry was analyzed independently and comparatively. The interest in the surface chemistry of the novel nanocomposites was twofold:

- as just described, in a first place the fibers surface chemistry elucidation allows a clearer understanding of the possible causes inflicting the previously described cellular response modifications at higher HA percentages;
- at a second place the surface chemistry fingerprints of the untreated nanocomposite fibers could be used as reference to identify the surface modifications induced on the fibers by the sterilization method.

As demonstrated by surface sensitive XPS analysis, the predominant chemical surface modifications induced on the novel PET/HA fibers by the increased HA addition, was the reduced overall carbon surface content in favor of increased oxygen content via the formation of new hydroxyl groups. XPS analysis didn't detect any surface exposed HA.

On the other hand, as detected by SEM-EDX the surface roughness increase with HA increase, induced by the HA nanoparticles and large HA aggregates, was the main surface topography modification at higher HA contents. The area specific chemical analysis performed through SEM-EDX also demonstrated that:

- the HA nanoparticles large aggregates in the fibers were covered by a thin layer of PET at all times;
- nano- and micron-sized HA particles were exposed on the PET10 fibers surface. However as HA is undetected by XPS analysis the total content of surface exposed HA is below 3%.

The surface analysis results were surprising as surface exposed HA was expected at high concentrations, mainly due to the visible texture/surface changes occurring with increased HA additions. In addition, the surface chemistry results detecting less than 3% surface exposed HA was surprising, as the previously characterized biological response at higher HA contents suggested bioactivity typically acquired from surface exposed HA. Although more conclusive results are needed, this preliminary research suggests that at higher HA contents the increased biological activity was acquired through increased hydroxyl (C-OH) content conjointly to increased surface roughness of the fibers rather than a direct *in vitro* cellular -HA nanocrystals interaction.

6.3 Sterilization effects on surface chemistry

The sterilization method becomes important when considering the practical applications of the novel nanocomposite fibers as implantable material. In other words as the nanocomposite fibers are expected to have an ultimate commercialized implantable function, their sterility in terms of a microbiological as well as functional aspect becomes important. As shown in Figure 6.1 below, unsterilized PET10 fibers quickly developed a bacterial colony in our laboratory.

Figure 6.1 Bacterial contamination expressed in our laboratory at the Hearth Institute of Montreal on un-sterilized nanocomposite fibers.

EtO and LTP sterilization methods, evaluated by XPS analysis revealed the following chemical modifications onto the PET/HA nanocomposite fibers: EtO treatment induced slight alkylation and LTP treatment induced an increase in the hydrogen bonds and overall O% increase. Despite the surface chemical modifications in terms of biologic response both treatments appear suitable.

The surface modifications seen by XPS were than reassessed by FTIR. The FTIR analysis reconfirmed the XPS detected modifications, and to avoid redundant information the FTIR results are included as Appendix 2 and not an integral part of the thesis.

Chapter 7 : Conclusion

This work has been an exploration of a novel biomaterial designed for orthopedic applications. This biomaterial has been designed through an interdisciplinary approach bridging elements of biology, chemistry and mechanics. As a first evaluation of their potential application in the biomedical industry all of the above mentioned aspects were only scanned.

As anticipated the overall biocompatibility of the PET/HA nanocomposite fibers was strongly supported. More interestingly, it was seen that the HA nanocrystals dosage in the PET fibers resulted in a beneficial general biologic response on L929 fibroblasts and Raw 264.7 macrophages, which is expected to have a final outcome on the support of new tissue formation at the interface.

However in terms of biologic evaluation of 3D structures for bone replacement the short-comings are obvious. Mainly the 3D fiber scaffolds bone specific biocompatibility needs to be evaluated through an osteoblastic cell line. Furthermore their ability to support osteoblastic differentiation and ECM formation would also be an important factor to determine. As mentioned in the introduction, 3D scaffolds need to also allow cell migration within the structure for bone regeneration. The cellular infiltration, viability and proliferation within the scaffold should also be assayed. Lastly, in terms of a biological perspective if the 3D scaffolds still present interesting *in vitro* results comparative to relevant literature they should than be evaluated *in vivo* on a relevant animal model. Evidently, the complete biocompatibility and bioactivity

characterization of the novel nanocomposites was not performed in this research, as this it was designed to screen the general biocompatibility of the PET/HA nanocomposite fibers for future *in vitro* and *in vivo* experiments[58].

The second aspect that clearly has to be optimized in this research are the 3D scaffolds themselves. They were fabricated to possess large pore sizes and 90% porosity mimicking that of bone. However, the ideal pore size from 100 to 350 μm has not been optimized to allow maximal tissue ingrowth, and should be done as a fundamental parameter for further usage of the scaffolds.

In terms of surface chemistry characterization, the XPS analysis elucidated the increased oxygen and hydroxyl groups ratio at higher HA dosages explaining the improved cellular response. SEM-EDX detected a) trace amounts of HA exposed to the surface in nano- and micro-aggregates form and b) surface topography variations. Although it helps us understand the improved biological response, multiple physical and chemical parameters contribute to an optimized interaction between the material surface and the biosystem, and the surface chemistry alone is not sufficient to explain the biological improvements. For a clearer understanding the contact angle variation proportionally to the HA dosage should be evaluated, as well as the surface topography trough a more precise technique such as atomic force microscopy. These last parameters are also pertinent as they may unravel unexpected results about the very popular HA ceramic and its effects on biomaterials surfaces and *in vitro* interactions.

In terms of sterilization an inadequate choice of the sterilizing method can in some cases cause irreversible damage to the morphological, physical, chemical and

consequently biological characteristics of polymeric biomaterials that can reduce and/or induce wrong interpretations about the overall performance of the biomaterial. The comparison of both commonly used low temperature sterilization techniques showed some chemical changes but they seemed to be limited to surface layer oxidation for LTP, and alkylation for EtO. Considering the *in vitro* biocompatibility results, none of the sterilization methods are completely unsuitable for use on the novel nanocomposite fibers.

Lastly, further work on the dispersion of HA into PET fibers is necessary to obtain the mechanical properties that will make possible the use of these fibers into load-bearing orthopedic applications. However, the mechanical properties and their present shortcomings are simply introduced in this thesis.

Bibliography

1. Williams D.F. The Williams Dictionary of Biomaterials; 1999.
2. Chung T.W., Liu D.Z., Wang S.Y., Wang S.S. Enhancement of the growth of human endothelial cells by surface roughness at nanometer scale. Biomaterials 2003(24):4655-4661.
3. Chen C.S., Mrksich M. Huang S., Whitesides G.M., Ingber D.E. Geometric control of cell life and death. Science, 1997(276):1425-1428.
4. Marques A, Cruz H, Coutinho O, Reis R. Effect of starch-based biomaterials on the *in vitro* proliferation and viability of osteoblast-like cells. J Mat Scien: Mats Medicine 2005;16(9):833-842.
5. Meredith Jr. J.E., Fazeli B., Schwartz M.A. The Extracellular Matrix as a Cell Survival Factor. Molecular Biology of the Cell 1993(4):953-961.
6. Culp L.A. Biochemical Determinants of Cell Adhesion. . Current Topics in Membranes and Transport 1978;2:327-396.
7. Agrawal C.M., Athanasiou K.A., Heckman J.D. Biodegradable PLA-PGA polymers for tissue engineering in orthopaedics. Mater Sci For 1997(250):115-28.
8. Maquet V., Jerome R. Design of macroporous biodegradable polymer scaffolds for cell transplantation. Porous Mater Tissue Eng 1997(250):15-42.
9. Thompson R., Wake M.C., Yaszemski M., Mikos A.G. Biodegradable polymer scaffolds to regenerate organs. Adv Polym Sci 1995(122):247-74.
10. Saad B., Ciardelli G., Matter S., Welti M., Uhlschmid G.K., Neuenschwander P., Suter U.W. Degradable and highly porous polyesterurethane foam as biomaterial: Effects and phagocytosis of degradation products in osteoblasts. J Biomed Mater Res 1998(39):594-602.
11. Langer R.S., Vacanti J.P. Tissue engineering: the challenges ahead. Scientific American 1999;280:86-9.
12. Anselme K., Bigerelle M., Noel B., Dufresne E., Judas D., Iost A., Hardouin P. Qualitative and quantitative study of human osteoblast adhesion on materials with various surface roughnesses. J Biomed Mater Res 2000(49):155-66.
13. Dubois J.C., Souchier C., Couble M.L., Exbrayat P., Lissac M. An image analysis method for the study of cell adhesion to biomaterials. Biomaterials 1999(20):1841-9.
14. Dobkowski J., Kolos R., Kaminski J., Kowalczynska H.M. Cell adhesion to polymeric surfaces: Experimental study and simple theoretical approach. J Biomed Mater Res 1999(47):234-42.
15. Ikada Y., Surface Modification of Polymers for Medical Applications. Biomaterials 1994(15):725-36.
16. Tziampazis E., Kohn J., Moghe P.V. PEG-variant biomaterials as selectively adhesive protein templates: model surfaces for controlled cell adhesion and migration. Biomaterials 2000(21):511-20.

17. Freed L.E., Vunjak-Novakovic G. Culture of organized cell communities. Adv Drug Deliver Rev 1998(33):15-30.
18. Lu L., Mikos A.G. The importance of new processing techniques in tissue engineering. MRS Bull, 1996(21):28-32.
19. Middleton J.C.,Tipton A.J. Synthetic biodegradable polymers as orthopedic devices. Biomaterials 2000 (21):2335-46.
20. Shapiro L., Cohen S. Novel alginate sponges for cell culture and transplantation. Biomaterials 1997(18):583-90.
21. Thomson R.C., Yaszemski M.J., Powers J.M., Mikos A.G. Fabrication of biodegradable polymer scaffolds to engineer trabecular bone. J Biomater Sci Polym Ed 1995(7):23.
22. Middleton J.C., Tipton A.J., Synthetic biodegradable polymers as orthopedic devices. Biomaterials 2000 (21:):2335-46.
23. Ratner B.D. New ideas in biomaterials science- a path to engineered biomaterials. J. Biomed. Mat. Res. 1993(27):837-850.
24. Whang K., Healy K.E., Elenz D.R., Nam E.K., Tsai D.C., Thomas C.H., Nuber G.W., Glorieux F.H., Travers R., Sprague S.M. Engineering bone regeneration with bioabsorbable scaffolds with novel microarchitecture. Tissue Engineering 1999(5):35-51.
25. Tuzlakoglu K., Bolgen N., Salgado A. J., Gomes M. E., Piskin E., Reis R. L. Nano- and micro-fiber combined scaffolds: A new architecture for bone tissue engineering. J Mat Science: Materials in Medicine 2005;V16(12):1099-1104.
26. Li W.J., Jiang Y.J., Tuan R.S. Chondrocyte Phenotype in Engineered Fibrous Matrix Is Regulated by Fiber Size. Tissue Engineering 2006;12(7):1775-1785.
27. Santos M.I., Fuchs S., Gomes M.E., Unger R.E., Reis R.L., Kirkpatrick C.J. Response of micro- and macrovascular endothelial cells to starch-based fiber meshes for bone tissue engineering. Biomaterials 2007;28(2):240-248.
28. Albrektsson T., Johansson C., Sennerby L. Biological aspects of implant dentistry : osseointegration. Periodontology 2000;2:58-73.
29. Gemmell C.H., Park J.Y. Initial Blood interactions with endosseous implant materials. Bone Engineering 2000:108-117.
30. Osborn J.F., Newesely H. Dynamic aspects of the implant bone interface. Dental implants: materials and systems 1980:111-23.
31. Davies J.E. Understanding Peri-Implant Endosseous Healing. Journal of Dental Education 2003;67(8).
32. Murugan R., Ramakrishna S. Development of nanocomposites for bone grafting. Composites Science and Technology 2005(65): 2385-2406.
33. Ratner B.D, Hoffman A.S., Schoen F.J., Lemons J.E. An introduction to Materials in Medicine. Biomaterials Science 2004(2).
34. Suchanek W., Yashimura M. Processing and properties of hydroxyapatite-based biomaterials for use as hard tissue replacement implants. Journal of Materials Research 1998;13(1):94-117.
35. Puajindanetr S., Best S.M., Bonfield W. Characterization and sintering of precipitated hydroxyapatite. British Ceramic Transactions, 1993;93(3):96-99.

36. Knowles J.C., Talal S. Santo ffects in a glass reinforced hydroxyapatite. Biomaterials 1996(17):1437-1442.
37. Bonfield W., Bowman J.A., Grynpas M.D. Composite material for use in orthopaedics. U.S. Pat. No. 5017627. 1991.
38. Bonfield W., Tanner E. Hydroxyapatite Composite Biomaterials – Evolution and Applications. Materials World 1997;5(1):18-20.
39. Bonfield W., Grynpas M.D., Tully A.E., Bowman J., Abram J. Hydroxyapatite reinforced polyethylene - a mechanically compatible implant material for bone-replacement. Biomaterials 1981;2(3):185-186.
40. Bonfield W. Composites for bone replacement. J. Biomed. Eng. 1988;10(6):522-526.
41. Bonner M., Saunders L.S., Ward I.M., Davies G.W., Wang M., Tanner K.E., Bonfield W. Anisotropic mechanical properties of oriented HAPEXTM. J. Mater. Sci. Mater. Med. 2002;37(2):325-334.
42. Huang M, Feng J, Wang J , Zhang X , Li Y, Yan Y. Synthesis and characterization of nano-HA/PA66 composites. J Mater Sci-Mater Med. 2003;14(7):655-60.
43. Kobayashi M., Nakamura T., Okada Y., Fukumoto A., Furukawa T., Kato H., Kokobu T., Kikutani T. Bioactive bone cement: comparison of apatite and wollastonite containing glass-ceramic, hydroxyapatite, and β-tricalcium phosphate fillers on bone bonding strength. J. Biomed. Mater. Res. 1998;42(2):223-237.
44. Watson K.E., Tenhuisen K.S., Brown P.W. The formation of hydroxyapatite-calcium polyacrylate composites. J. Mater. Sci. Mater. Med. 1999(10):205-213.
45. Greish Y.E., Brown P.W. An evaluation of mechanical property and microstructural development in HAp-Ca polycarboxylate biocomposites prepared by hot pressing. J. Biomed. Mater. Res. (Appl. Biomater.) 2000;53(4):421-429.
46. Harper E.J., Behiri J.C., Bonfield W. Flexural and fatigue properties of a bone cement based upon polyethylmethacrylate and hydroxyapatite. J. Mater. Sci.Mater. Med. 1995;6(12):799-803.
47. Shinzato S., Kobayashi M., Mousa W.F., Kamimura M., Neo M., Kitamura Y., Kokubo T., Nakamura T. Bioactive polymethyl methacrylate-based bone cement: comparison of glass beads, apatite- and wollastonite-containing glass-ceramic, and hydroxyapatite fillers on mechanical and biological properties. J. Biomed. Mater. Res. 2000;51(2):258-272.
48. Abu Bakar M.S., Cheang P., Khor K.A. Mechanical properties of injection molded hydroxyapatite-polyetheretherketone biocomposites. Comp. Sci. Tech 2003;63:421-425.
49. Abu Bakar M.S., Cheang P., Khor K.A. Thermal processing of hydroxyapatite reinforced polyetheretherketone composites. J. Mater. Process. Tech 1999;89:462-466.
50. Abu Bakar M.S., Cheng M.H.W., Tang S.M., Yu S.C., Liao K., Tan C.T., K.A. K, Cheang P. Tensile properties, tension-tension fatigue and biological response of polyetheretherketone-hydroxyapatite composites for loadbearing orthopedic implants. Biomaterials 2003;24(13):2245-2250.

51. Wang M. Developing bioactive composite materials for tissue replacement. Biomaterials 24(13):2133-2151.
52. Metzger A. Polyethylene Terephthalate and the Pillar™ Palatal Implant: Its Historical Usage and Durability in Medical Applications. J Am Pod Assoc 1975;65:1-12.
53. Homsy C.A., McDonald K.E., Akers W.W., Short C., Freeman B.S. Surgical Suture-Canine Tissue Interaction for Six Common Suture Types. J Biomed Mater Res 1968(2):215.
54. Francioni G, Ansaldo V, Magistrelli P, Pari A, Rinaldi P, SaninC, Rafaeli W, Pari G. The use of prosthesis in abdominal and thoracic wall defect, 15 year experience: evaluation of tissue reactions and complications. . Chir Italiana, 1999;51(1):21.
55. Riepe G, Loos J, Imig H, Schröder A, Schneider E, Petermann J, Rogge A, Ludwig M, Schenke A, Nassutt R, Chakfe N, Morlock M.. Long-term in vivo Alterations of Polyester Vascular Grafts in Humans. Eur J Vasc Endovasc Surg 1997(13):540-548.
56. Illingworth B, Tweden K, Schroeder R, Cameron JD. . In Vivo Efficacy of Silver-Coated (Silzone)Infection-Resistant Polyester Fabric Against a Biofilm-Producing Bacteria, Staphylococcus Epidermidis,. J Heart Valve Dis 1998;5(7):524-530.
57. Neumann A, Reske T, Held M, Jahnke K, Ragoay C, Maier HR. Comparative investigation of the biocompatibility of various silicon nitride ceramic qualities in vitro. J Mater Sci: Mater Med 2004;15(10):1135-1140.
58. Timmer MD, Shin H, Horch RA, Ambrose CG, Mikos AG. In Vitro Cytotoxicity of Injectable and Biodegradable Poly(propylene fumarate)-Based Networks: Unreacted Macromers, Cross-Linked Networks, and Degradation Products. Biomacromolecules 2003;4(4):1026-1033.
59. Wan H, Williams RL, Doherty PJ, Williams DF. A study of cell behaviour on the surfaces of multifilament materials. Journal of Materials Science: Materials in Medicine 1997;8(1):45-51.
60. Silvio L.D., Dalby M.J., Bonfield W. Osteoblast behaviour on HAP/PE composite surfaces with different HA volumes. Biomaterials 2002(23):101-107.
61. Di Silvio L, Dalby MJ, Bonfield W. Osteoblast behaviour on HA/PE composite surfaces with different HA volumes. Biomaterials 2002;23(1):101-107.
62. Abu Bakar MS, Cheng MHW, Tang SM, Yu SC, Liao K, Tan CT, Khor KA, Cheang P. Tensile properties, tension-tension fatigue and biological response of polyetheretherketone-hydroxyapatite composites for load-bearing orthopedic implants. Biomaterials 2003;24(13):2245-2250.
63. Cheang P, Khor KA. Effect of particulate morphology on the tensile behaviour of polymer-hydroxyapatite composites. Mater Sci Eng A 2003;345(1-2):47-54.
64. Juhasz JA, Best SM, Brooks R, Kawashita M, Miyata N, Kokubo T, Nakamura T, Bonfield W. Mechanical properties of glass-ceramic A-W-polyethylene composites: effect of filler content and particle size. Biomaterials 2004;25(6):949-955.

65. Liming F, Yang L, Ping G. Processing and mechanical properties of HA/UHMWPE nanocomposites. Biomaterials 2006;27(20):3701-3707.
66. Mathews R.G., Ajji A., Dumoulin MM, Prud'homme RE. The Effects of Roll Drawing on the Structure and Properties of Poly(ethylene terephthalate). Polymer Engineering and Science 1999;39(12):2377-2388.
67. Ajji A., Denault J., Bureau M. N. , Ton-That M.-T., Trudel-Boucher D., Côté D. Polymer Nanocomposites Fibers and Applications. Annual Technical Conference ANTEC, May 7-11 2006, Charlotte (USA) 2006.
68. Limin S, Christopher C. B, Karlis A. G, Ahmet K. Material fundamentals and clinical performance of plasma-sprayed hydroxyapatite coatings: A review. J Biomed Mater Res 2001;58(5):570-592.
69. Wang J, Huang N, Yang P, Leng YX, Sun H, Liu ZY, Chu PK. The effects of amorphous carbon films deposited on polyethylene terephthalate on bacterial adhesion. Biomaterials 2004;25(16):3163-3170.
70. Curran J.M., Gallagher J.A., Hunt J. A. The inflammatory potential of biphasic calcium phosphate granules in osteoblast/macrophage co-culture. Biomaterials 2005;26(26):5313-5320.
71. Moldawer L.L. Biology of proinflammatory cytokines and their antagonists. Crit Care Med 1994;22(7):S3-7.
72. Gonzales J.B., Purdon M.A., Horowitz S.M. In vitro studies on the role of titanium in aseptic loosening. Clin Orthop 1996;330:244-250.
73. Sabokar A., Fujikawa Y., Brett J., Murray D.W., Athanasou N.A. Increased osteoclastic differentiation by PMMA particle associated macrophages. Acta Orthop Scand 1996;6(67):593-598.
74. Jaffe W.L., Scott D.F. Total hip arthroplasty with hydroxyapatitecoated prostheses. J Bone Joint Surg Am 1996;78(12):1918-1934.
75. Morscher E.W., Hefti A., Aebi U. Severe osteolysis after thirdbody wear due to hydroxyapatite particles from acetabular cup coating. J Bone Joint Surg Br 1998;80(2):267-272.
76. Marques A. P. , Reis R. L. , Hunt J. A. . Cytokine secretion from mononuclear cells cultured *in vitro* with starch-based polymers and poly-L-lactide. J Biomed Mater Res A 2004;71A(3):419-429.
77. ANSI/AAMI/ISO , 10993-5. Biological evaluation of medical devices, Part 5: Tests for in vitro cytotoxicity. 1999.
78. Ahmed S.A. , Gogal Jr. , Walsh J.E. . A new Rapid and Simple Non-Radioactive assay to Monitor and Determine the proliferation of Lymphocytes: An Alternative to H3-thymidine incorporation assay. J Immunol Meth 1994(170):211-224.
79. Bandyopadhyay-Ghosh S., Reaney I. M., Brook I. M., Hurrell-Gillingham K., Johnson A., Hatton P. V. *In vitro* biocompatibility of fluorcanasite glass-ceramics for bone tissue repair. J Biomed Mater Res A 2007;80A(1):175-183.
80. Petit A., Catelas I., Antoniou J., Zukor J.D., Huk O.H. Differential apoptotic response of J774 macrophages to alumina and ultra-high-molecular-weight polyethylene particles. J Orthop Res 2002;20(1):9-15.

81. Catelas I, Petit A, Zukor DJ, Antoniou J, Huk OL. TNF-[alpha] secretion and macrophage mortality induced by cobalt and chromium ions in vitro-Qualitative analysis of apoptosis. Biomaterials 2003;24(3):383-391.
82. Bukata S. V. , Gelinas J., Wei X., Rosier R. N. , Puzas J. E., Zhang X., Schwarz E. M. , Song X. R. , Griswold D. E. , O'Keefe R. J. . PGE2 and IL-6 production by fibroblasts in response to titanium wear debris particles is mediated through a Cox-2 dependent pathway. J Orthop Res 2004;22(1):6-12.
83. Ninomiya J. T. , Struve J. A. , Stelloh C. T. , Toth J. M., Crosby K. E. Effects of hydroxyapatite participate debris on the production of cytokines and proteases in human fibroblasts. J Orthop Res 2001;19(4):621-628.
84. Huang J., Best S. M., Bonfield W., Brooks R. A., Rushton N., Jayasinghe S. N., Edirisinghe M. J. *In vitro* assessment of the biological response to nano-sized hydroxyapatite. J Mater Sci: Mater Med 2004;15(4):441-445.
85. Zhang YZ, Venugopal J, Huang ZM, Lim CT, Ramakrishna S. Characterization of the Surface Biocompatibility of the Electrospun PCL-Collagen Nanofibers Using Fibroblasts. Biomacromolecules 2005;6(5):2583-2589.
86. Dalton BA, McFarland CD, Gengenbach TR, Griesser HJ , Steele JG. Polymer surface chemistry and bone cell migration. J Biomater Sci Polym Ed. 1998;9(8):781-99.
87. Salgado AJ, Figueiredo JE, Coutinho OP, Reis RL. Biological response to pre-mineralized starch based scaffolds for bone tissue engineering. J Mater Sci Mater Med 2005;16(3):267-275.
88. Moscato S., Cascone M.G., Lazzeri L, Danti S., Mattii L., Dolfi A., Bernardini N. Morphological features of ovine embryonic lung fibroblasts cultured on different bioactive scaffolds. J. Biomed. Mater. Res., Part A 2005;76A(1):214-221.
89. Dimitrievska S, Petit A, Ajji A, Bureau NM, Yahia L. Biocompatibility of Novel Polymer-Apatite Nanocomposite Fibers, J Biomed Mater Res Part B 2007.
90. Woedtke V, Schlosser T, Urban M, Hartmann G, Julich V, Abel WD, Wilhelm PU. The influence of antimicrobial treatments on the cytocompatibility of polyurethane biosensor membranes. Biosens Bioelectron 2003;19(3):269-276.
91. Eick JD, Kostoryz EL, Rozzi SM, Jacobs DW, Oxman JD, Chappelow CC, Glaros AG, Yourtee DM. In vitro biocompatibility of oxirane/polyol dental composites with promising physical properties. Dent Mater 2002;18(5):413-421.
92. Stitzel J, Liu J, Lee SJ, Komura M, Berry J, Soker S, Lim G, Van Dyke M, Czerw R, Yoo JJ, Atala A. Controlled fabrication of a biological vascular substitute. Biomaterials 2006;27(7):1088-1094.
93. Risbud M, Nabi S, Jog D, Bhonde J, Ramesh L. Preparation, characterization and in vitro biocompatibility evaluation of poly(butylene terephthalate)/wollastonite composites. Biomaterials 2001;22(12):1591-1597.
94. Zhang YZ, Venugopal J, Huang Z, Lim CT, Ramakrishna S. Characterization of the Surface Biocompatibility of the Electrospun PCL-Collagen Nanofibers Using Fibroblasts. Biomacromolecules 2005;6(5):2583-2589.
95. Marreco PR, Luz MP, Candelária GS, Moraes ÂM. Effects of different sterilization methods on the morphology, mechanical properties, and cytotoxicity of chitosan

membranes used as wound dressings. J Biomed Mater Res, Part A 2004;71B(2):268-277.
96. Ma N, Petit A, Huk O, Yahia L, Tabazian M. Safety issue of re-sterilization of polyurethane electrophysiology catheters: a cytotoxicity study. J Biomater. Sci., Polym. Ed. 2003;14(3):214-226.
97. ST27-1988 AA. Guideline for industrial ethylene oxide sterilization of medical devices. New York: American National Standards Institute 1988.
98. Lerouge S, Guignot C, Tabrizian M, Ferrier D, Yagoubi N, Yahia L. Plasma-based sterilization: Effect on surface and bulk properties and hydrolytic stability of reprocessed polyurethane electrophysiology catheters. J Biomed Mater Res 2000;52(4):774-782.
99. Hury V, Desor,Pelletier,Lagarde,. A parametric study of the destruction efficiency of Bacillus spores in low pressure oxygen-based plasmas. Letters in Applied Microbiology 1998;26(6):417-421.
100. Dorothee R, Lendlein A, Schmidt AM, Kelch S, RoehlkeW, Fuhrmann R, Franke RP. In vitro cytotoxicity testing of AB-polymer networks based on oligo(ε-caprolactone) segments after different sterilization techniques. J. Biomed. Mater. Res., Part B 2003;67B(2):722-731.
101. Lerouge S, Tabrizian M, Wertheimer MR, Marchand R, Yahia L. Safety of plasma-based sterilization: Surface modifications of polymeric medical devices induced by Sterrad® and Plazlyte™ processes. J Biomed Mater Res 2002;12:3-13.
102. Bathina MN, Mickelsen S, Brooks C, Jaramillo J, Hepton T, Kusumoto FM. Safety and efficacy of hydrogen peroxide plasma sterilization for repeated use of electrophysiology catheters. J Am Coll Cardiol 1998;32(5):1384-1388.
103. Kazanci M, Cohn D, Marom G, Ben-Bassat H. Surface oxidation of polyethylene fiber reinforced polyolefin biomedical composites and its effect on cell attachment. J Mater Sci- Mater Med 2002;13(5):465-468.
104. Moisan M., Barbeau J., Moreau S., Pelletier J., Tabrizian M., Yahia L'H. Low-temperature sterilization using gas plasmas: a review of the experiments and an analysis of the inactivation mechanisms. Int. J. Pharm. 2001;226(1-2):1-21.
105. Mayer G, Blanchemain N, Dupas-Bruzek C, Miri V, Traisnel M, Gengembre L, Derozier D, Hildebrand HF. Physico-chemical and biological evaluation of excimer laser irradiated polyethylene terephthalate (pet) surfaces. Biomaterials 2006;27(4):553-566.
106. Yang DQ, Martinu L, Sacher E, Sadough-Vanini A. Nitrogen plasma treatment of the dow Cyclotene 3022 surface and its reaction with evaporated copper. Appl Surf Sci 2001;177(1-2):85-95.
107. Kilpadi DV, Johnston MS, Ferguson DE, Estridge TD, Feldman DS. The effect of solvent extraction and sterilization procedure on the tissue response to Dacron(R) velour. Biomaterials 1999;20(2):129-136.
108. Moscato S, Cascone MG, Lazzeri L, Danti S, Mattii L, Dolfi A, Bernardini N. Morphological features of ovine embryonic lung fibroblasts cultured on different

bioactive scaffolds. J Biomed Materials Research Part A 2005;Volume 76A, (Issue 1):214-221.
109. Wilson DJ, Rhodes NP, Williams RL. Surface modification of a segmented polyetherurethane using a low-powered gas plasma and its influence on the activation of the coagulation system. Biomaterials 2003;24(28):5069-5081.
110. Lucas AD, Merritt K, Hitchins VM, Woods TO, McNamee SG, Lyle DB, Brown SA. Residual ethylene oxide in medical devices and device material. J Biomed Mater Res, Part B 2003;66B(2):548-552.
111. Mayer G, Blanchemain N, Dupas-Bruzek C, Miri V, Traisnel M, Gengembre L, Derozier D, Hildebrand HF. Physico-chemical and biological evaluation of excimer laser irradiated polyethylene terephthalate (pet) surfaces. Biomaterials 2006;27(4):553-566.
112. Tshamala M, Cox E, De Cock H, Goddeeris BM, Mattheeuws D. Antigenicity of cortical bone allografts in dogs and effect of ethylene oxide-sterilization. Vet. Immunol. Immunopathol. 1999;69(1):47-59.
113. Merkel KD, Erdmann JM, McHugh KP, Abu-Amer Y, Ross FP, Teitelbaum SL. Tumor Necrosis Factor-alpha Mediates Orthopedic Implant Osteolysis. Am J Pathol 1999;154(1):203-210.
114. Steele J.G. DBA, Thomas C.H., Healy K.E., Gengenbach T.R., Mcfarland C.D. In Bone Engineering 1999:225.
115. Kunzler T.P., Drobek T., Schuler M., Spencer N.D. Systematic study of osteoblast and fibroblast response to roughness by means of surface-morphology gradients. Biomaterials 2007;28(13):2175-2182.
116. Alain Petit ICJADJZOLH. Differential apoptotic response of J774 macrophages to alumina and ultra-high-molecular-weight polyethylene particles. Journal of Orthopaedic Research 2002;20(1):9-15.

Appendix 1

HA effects on the PET/HA fibers mechanical properties

Although their biocompatibility and bioactivity remain a central issue, the success of load-bearing biomaterials is also dictated by their mechanical properties. This importance comes from the major, and extremely important, role of the biomaterial in providing mechanical strength and support to the tissue being replaced. Therefore when tissue is grown outside its native environment, a mechanical support mimicking that found in such environments has to be provided.

It is difficult to find a material that meets all desired characteristics for a particular application. For example, polymers with ideal biocompatibility properties often present insufficient mechanical properties (polymers for hip stems or bone grafts). The opposite can also be true. Polymers with ideal mechanical properties might not present the biocompatibility required (PTFE or Acetal for acetabular cups). A way to address this problem in an effective manner and tune the material properties to satisfy the application requirements is to synthesize a bioactive composite material with properties that can be tailored for specific applications. The mechanical properties of the fibers were evaluated in terms of HA percentage added to the fiber.

The modulus of elasticity and yield stress results for all fibers studied are shown in Figure 7.1 and Figure 7.2 respectively. The PET/HA fibers show a trend of decreased modulus of elasticity and yield stress upon HA addition in the fibers; the highest mechanical properties are exhibited by the fibers with no added HA. This behavior of

the nanocomposites fibers was not expected. Indeed, a previous study had shown that mechanical properties of similar nanocomposite fibers were improved by the presence of HA[67]. This behavior was attributed to the mechanical reinforcement of the well-dispersed, strong(er) HA particles present in the fibers and to their preferred orientation along the fibers length.

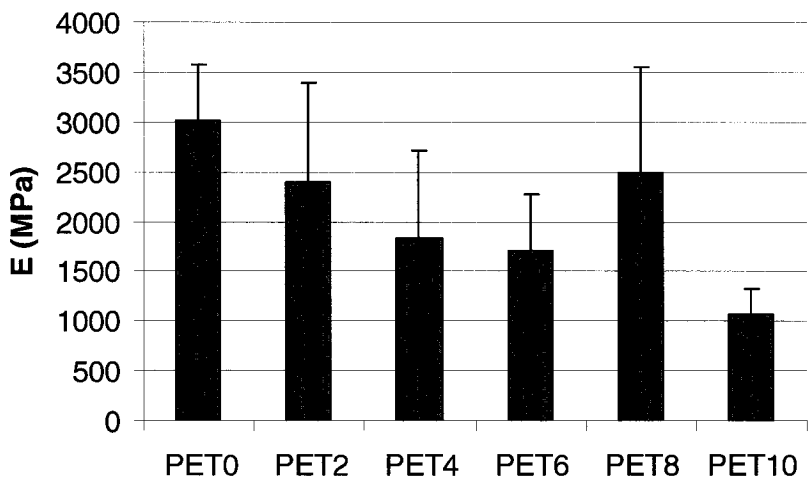

Figure 7.1 Modulus of elasticity of PET/HA nanocomposites in terms of HA percentage in fibers.

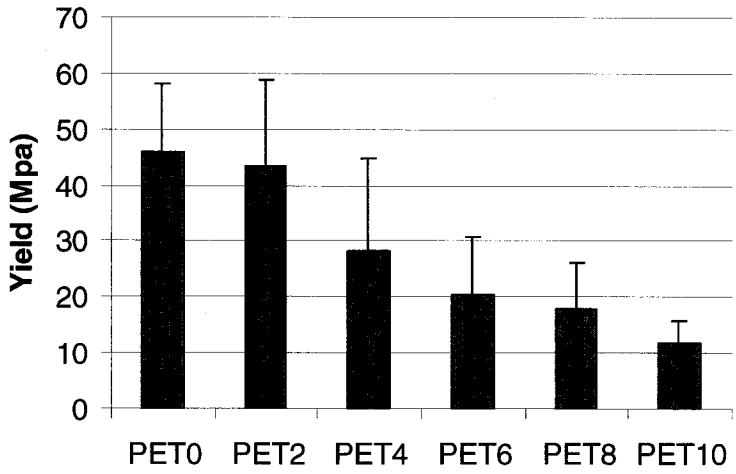

Figure 7.2 Yield stress of PET/HA nanocomposites in terms of HA percentage in fibers.

The morphology of the PET/HA fibers was therefore observed in order to find an explanation to this unexpected behavior. From the optical micrographs presented in Figure 7.3 below and the SEM micrographs in Chapter 4, it is clear that at higher HA concentrations the added nanoparticles agglomerated into large aggregates in the fibers. These aggregates, sometimes as large as the fibers themselves, acted as mechanical defects. The composite fibers could be compared as short sections of PET fibers and HA aggregates organized in series, a case for which mechanical stresses transfer expected between the matrix (PET) and the mechanical reinforcement (HA) cannot occur. In such a case, mechanical reinforcement effects prevented the expected mechanical improvements to occur.

Figure 7.3 Optical micrographs of PET0, PET4 and PET10 fibers for simple reference to fibers morphology

It is needless to say that further work on the dispersion of HA into PET fibers is necessary to obtain the properties that will make possible the use of these fibers into load-bearing orthopedic applications. However, although being important issues, the mechanical properties and their present shortcomings were simply introduced in this thesis as an aspect that requires further research, and not as the focus of this thesis.

Appendix 2

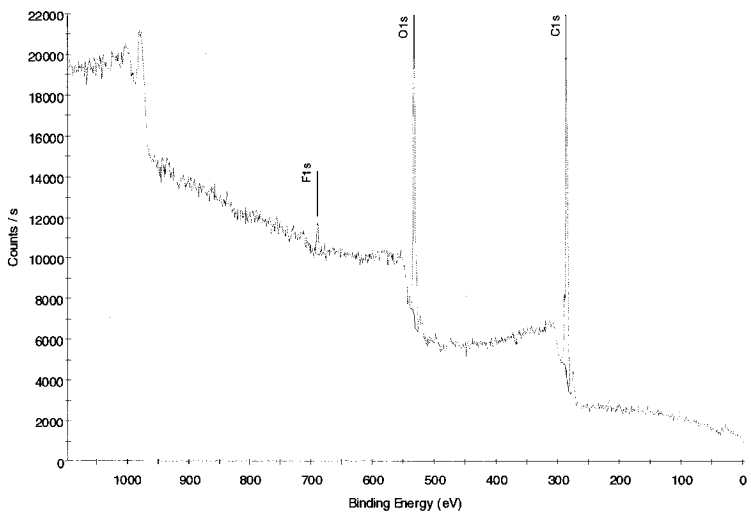

Survey (low resolution) XPS scans of untreated PET10 fibers

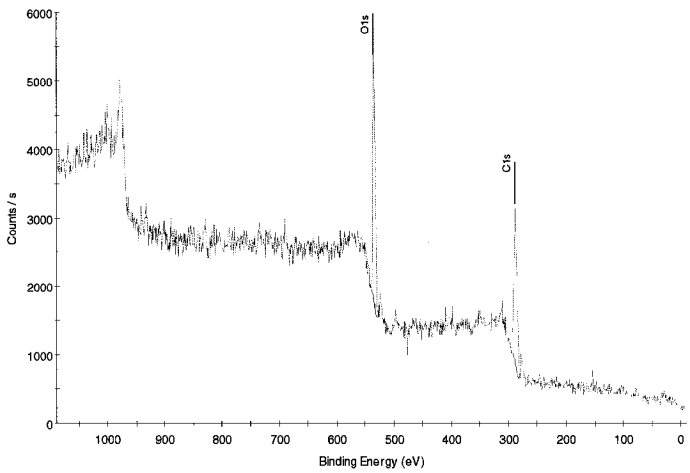

Survey (low resolution) XPS scans of Plasma treated PET10 fibers

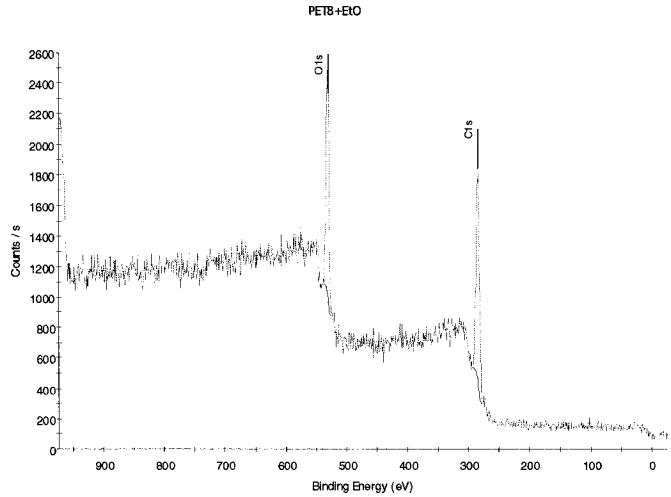

Survey (low resolution) XPS scans of EtO treated PET10 fibers

Appendix 3

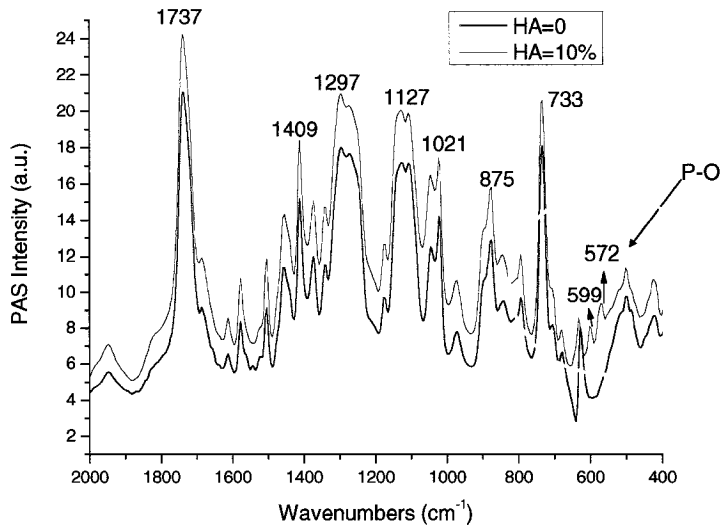

ATR-FTIR spectra of PET0 (red line) and PET10 (black line). The yellow circle is concentrated on the modified region of the nanocomposite .

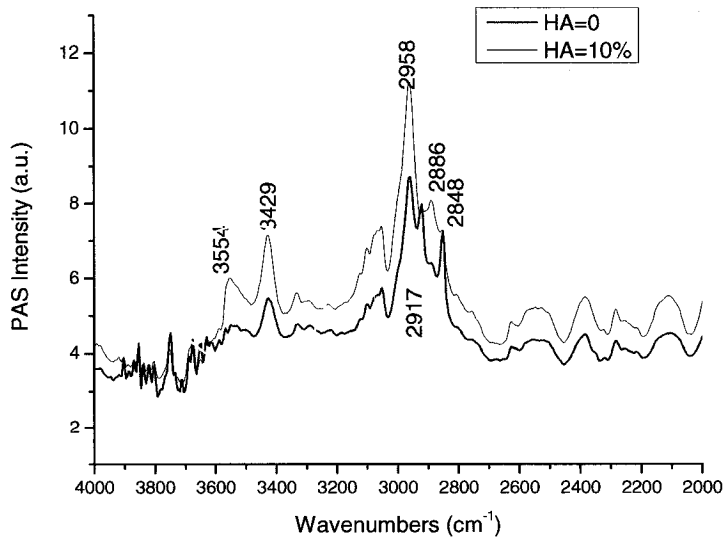

ATR-FTIR spectra of PET0 (red line) and PET10 (black line). The yellow circle represents the modified region of the nanocomposite .

Appendix 4

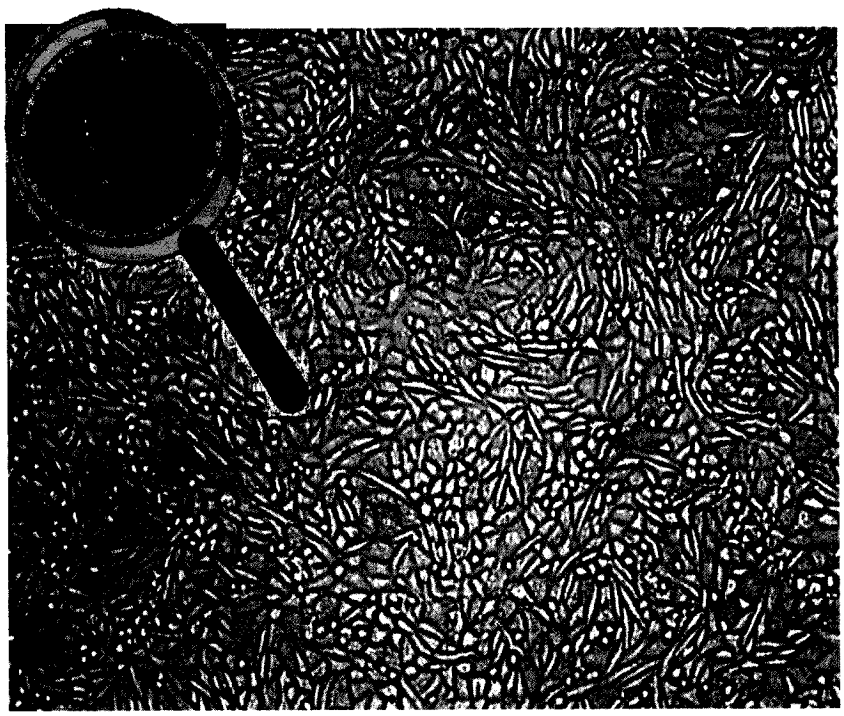

High magnification optical micrograph of L929 culture at 3 days with PET10 extracts. The picture is chosen as a representative one of all fibroblastic cultures with the nanocompostes extracts due to their similar viability.